

WASHINGTON UNIVERSITY IN ST. LOUIS
Division of Biology and Biomedical Sciences
Immunology

Dissertation Examination Committee:

Kenneth M. Murphy, Chair
Deepta Bhattacharya
Marco Colonna
Takeshi Egawa
Thaddeus S. Stappenbeck

Classical Dendritic Cell Development Excludes Alternative Myeloid Cell Fates
Characterized by Distinct Transcription Factors
by
Xiaodi Wu

A dissertation presented to the
Graduate School of Arts and Sciences
of Washington University
in partial fulfilment of the
requirements for the degree
of Doctor of Philosophy

May 2018
St. Louis, Missouri

TABLE OF CONTENTS

List of Figures and Tables.....	iii
List of Abbreviations	v
Acknowledgments	vii
Abstract	viii
Chapter 1: Introduction	2
Classical and Plasmacytoid DCs	3
Macrophages and Monocyte Progeny	6
Chapter 2: <i>Bcl11a</i> Is Required for Plasmacytoid Dendritic Cell Development	11
Results	12
Discussion	19
Methods.....	29
Chapter 3: <i>Zeb2</i> Is Required for Plasmacytoid Dendritic Cell and Monocyte Development	33
Results	35
Discussion	40
Methods.....	54
Chapter 4: <i>Mafb</i> Lineage Tracing Distinguishes Macrophages From Other Lineages	60
Results and Discussion	61
Methods.....	76
References	87
Appendix A: Code Listing.....	110

LIST OF FIGURES AND TABLES

Figure 1: DC development proceeds through progressively-restricted progenitor stages	10
Figure 2: Variations in gene expression among DC and macrophage subsets	10
Figure 3: Bcl11a is required for development of lymphoid and DC progenitors in the fetus	22
Figure 4: Bcl11a is required for development of lymphoid and DC progenitors in the adult....	23
Figure 5: Bcl11a regulates expression of <i>Flt3</i> and <i>Il7r</i>	24
Figure 6: Bcl11a is required <i>in vivo</i> for development of pDCs but not cDCs.....	25
Figure 7: Bcl11a deficiency <i>in vivo</i> impairs lymphoid and myeloid development.....	26
Figure 8: Bcl11a is required <i>in vitro</i> for FLT3L-derived DCs but not GM-CSF-derived DCs ...	27
Figure 9: Cytokine signalling in DC development and regulation by Bcl11a	28
Figure 10: Zeb2 is required for pDC development <i>in vivo</i>	44
Figure 11: Plasmacytoid DCs require Zeb2 in a dose-dependent and cell-intrinsic manner.....	46
Figure 12: Type I interferon diverts Zeb2-deficient progenitors to the CD24 ⁺ cDC lineage.....	47
Figure 13: Zeb2-deficient Sirp- α^+ cDCs express more abundant <i>Id2</i> mRNA.....	48
Figure 14: Overexpression of Ifi-204 or SMAD7 does not promote development of pDCs	49
Figure 15: Zeb2 is required for monocyte development <i>in vivo</i>	50
Figure 16: Zeb2-deficient Ly-6C ^{hi} monocytes express neutrophil-associated genes.....	52
Figure 17: <i>Mafb</i> expression distinguishes macrophages from DCs	68
Figure 18: Monocyte progeny are marked by <i>Mafb</i> -driven lineage tracing.....	69
Figure 19: <i>Mafb</i> -driven lineage tracing distinguishes macrophages from populations of similar immunophenotype in the BM and lung	71
Figure 20: <i>Mafb</i> -driven lineage tracing distinguishes peritoneal macrophages from DCs	72

Figure 21: Steady state LCs are marked by <i>Mafb</i> -driven lineage tracing but express <i>Zbtb46</i>	73
Figure 22: Ly-6C ⁺ monocyte-derived cells mature in the inflamed lung but lack <i>Zbtb46</i>	75
Figure 23: Primer sequences used for the generation of a MafB overexpression vector	77
Figure 24: Primer sequences used for the generation of a <i>Mafb</i> targeting plasmid.....	79

LIST OF ABBREVIATIONS

4-OHT	4-Hydroxytamoxifen
BM	Bone marrow
BMP	Bone morphogenetic protein
BSA	Bovine serum albumin
cDC	Classical dendritic cell
CDP	Common dendritic cell progenitor
ChIP	Chromatin immunoprecipitation
cMoP	Committed monocyte progenitor
CLP	Common lymphoid progenitor
CMP	Common myeloid progenitor
DC	Dendritic cell
DTR	Diphtheria toxin receptor
EAE	Experimental autoimmune encephalomyelitis
EDTA	Ethylenediaminetetraacetic acid
GFP	Green fluorescent protein
GMP	Granulocyte–macrophage progenitor
HDM	House dust mite
HSC	Hematopoietic stem cell
IL	Interleukin
LC	Langerhans cell

LCMV	Lymphocytic choriomeningitis virus
Lin	Lineage
LN	Lymph node
LPM	Large peritoneal macrophage
MDP	Macrophage–dendritic cell progenitor
MEP	Megakaryocyte–erythrocyte progenitor
MHC	Major histocompatibility complex
MHC-I	Major histocompatibility complex class I
MHC-II	Major histocompatibility complex class II
moDC	Monocyte-derived dendritic cell
MPP	Multipotent progenitor
mRNA	Messenger RNA
NK	Natural killer
PCR	Polymerase chain reaction
pDC	Plasmacytoid dendritic cell
qPCR	Quantitative polymerase chain reaction
RT	Reverse transcription
SPM	Small peritoneal macrophage
TGF	Transforming growth factor
WT	Wild-type
YFP	Yellow fluorescent protein

ACKNOWLEDGMENTS

My collaborators and I thank the Immunological Genome Project Consortium; J. Michael White and the technical staff of the Transgenic Knockout Micro-Injection Core (Department of Pathology and Immunology); and the Genome Technology Access Center (Department of Genetics).

This work was made possible by constant and generous support from Ken Murphy, whose able mentoring has been utterly transformative; by patient help from Theresa Murphy, whose breadth of knowledge has been indispensable; and by the advice and encouragement of committee members past and present: Deepta Bhattacharya, Marco Colonna, Takeshi Egawa, Thad Stappenbeck, and Barry Sleckman.

Members of the Murphy lab have made invaluable contributions to this work, and I am deeply in their debt. Special thanks in particular to Wumesh KC, Ansu Satpathy, Carlos Briseño, Vivek Durai, Gary Grajales, and Nicole Kretzer; and to Jörn Albring, Malay Haldar, and Ari Iwata. I would also like to acknowledge my classmates in the Medical Scientist Training Program and to thank Brian Sullivan, Christy Durbin, Liz Bayer, and Linda Perniciaro for their tireless efforts in supporting all of us in the Program. Finally, to friends near and far, and to my mother, father, and sister, my deepest gratitude.

Xiaodi Wu

Washington University in St. Louis

May 2018

ABSTRACT OF THE DISSERTATION

Classical Dendritic Cell Development Excludes Alternative Myeloid Cell Fates

Characterized by Distinct Transcription Factors

by

Xiaodi Wu

Doctor of Philosophy in Biology and Biomedical Sciences

Immunology

Washington University in St. Louis, 2018

Kenneth M. Murphy, Chair

Dendritic cells (DCs) play key roles in the interface between innate and adaptive immunity. They are capable of detecting a wide range of pathogens and other stimuli; they internalize, process, and present antigens; and they modulate the activity of other immune cells. Recent advances have demonstrated that distinct subsets of DCs play unique roles at steady state and under inflammatory conditions. We found that the transcription factors Bcl11a and Zeb2 are each essential for development of plasmacytoid DCs but dispensable for development of classical DCs *in vivo*. Zeb2-deficient bone marrow cells are also deficient in replenishment of monocytes, which along with their macrophage progeny represent a hematopoietic lineage closely related to that of DCs. Finally, we developed a lineage-tracing mouse strain using Cre recombinase under the control of the transcription factor-encoding locus *Mafb*; with that model, we determined that Langerhans cells in the skin are unique in displaying certain characteristics of both macrophages and DCs.

And having heard, or more probably read somewhere, in the days when I thought I would be well advised to educate myself, or amuse myself, or stupefy myself, or kill time, that when a man in a forest thinks he is going forward in a straight line, in reality he is going in a circle, I did my best to go in a circle, hoping in this way to go in a straight line.... And if I did not go in a rigorously straight line, with my system of going in a circle, at least I did not go in a circle, and that was something. And by going on doing this, day after day, and night after night, I looked forward to getting out of the forest, some day.

—Samuel Beckett, *Molloy*

CHAPTER 1: INTRODUCTION

Portions of this chapter are adapted from a review co-authored in collaboration with Ansuman T Satpathy, Jörn C. Albring, and Kenneth M. Murphy, which was published in Nature Immunology 13(12): 1145–1154. Personal contributions to that review included data analysis, drafting of selected parts of the text and figures, and revisions to all parts of the text and figures.

Portions of this chapter are adapted from text published or submitted for publication in association with work presented in succeeding chapters. Personal contributions to those works are outlined in the corresponding chapters.

Dendritic cells (DCs) were first distinguished from other adherent splenocytes based on their distinct morphology: a large, contorted, and refractile nucleus with small nucleoli; a cytoplasm arranged in pseudopods of varying shapes and rich in spherical mitochondria; and—unlike macrophages—no features of active endocytosis such as membrane ruffling (Steinman and Cohn, 1973). First in mixed lymphocyte reactions and then in transplanted organs, DCs were shown to be the principal population that can stimulate allogeneic T cell responses (Lechler and Batchelor, 1982; Steinman and Witmer, 1978). Since then, DCs have been found sparsely populating tissues throughout the body, and they are now known to perform critical functions in innate and adaptive immune responses; moreover, these cells can be grouped into several lineages, which include the classical DCs (cDCs), plasmacytoid DCs (pDCs), monocyte-derived DCs (moDCs), and Langerhans cells (LCs) (Satpathy et al., 2012b).

Classical and Plasmacytoid DCs

Classical DCs act as ‘sentinels’ that capture antigen in peripheral tissues; when activated by microbial or inflammatory signals, these cells increase surface expression of major histocompatibility complex (MHC) proteins and costimulatory molecules and migrate to lymphoid organs to initiate adaptive immune responses (Steinman, 2012). Divergent responses are orchestrated by two subsets of cDCs that are distinguished by several phenotypic markers in the mouse. CD8⁺ CD24⁺ CD205 (DEC-205)⁺ cDCs in lymphoid tissues (Crowley et al., 1989; Vremec and Shortman, 1997; Vremec et al., 1992) and equivalent cells identified by expression of CD103 in other tissues (Edelson et al., 2010; Ginhoux et al., 2009) are unified by their expression of the chemokine receptor XCR1 (Bachem et al., 2012; Crozat et al., 2011). This subset is thought to be more efficient at cross-presentation of exogenous antigens using MHC class I (MHC-I) (den Haan et al., 2000; Kamphorst et al., 2010), a critical source of interleukin (IL)-12 during infection by *Toxoplasma gondii* (Mashayekhi et al., 2011), an obligate entry point during early dissemination of *Listeria monocytogenes* (Edelson et al., 2011a; Neuenhahn et al., 2006), and an essential component for CD8⁺ T cell priming during infection by West Nile virus (Hildner et al., 2008), mouse cytomegalovirus (Torti et al., 2011), or herpes simplex virus (Zelenay et al., 2012). CD11b⁺ CD172a (Sirp-α)⁺ cDCs, which in some lymphoid tissues show heterogeneous surface expression of CD4 (Vremec et al., 2000), are thought to be more efficient at antigen presentation using MHC class II (MHC-II) (Dudziak et al., 2007; Kamphorst et al., 2010), an essential component for the initiation of T helper 2 responses that are hallmarks of allergy (Gao et al., 2013; Williams et al., 2013), and a promoter of T helper 17

responses through production of cytokines such as IL-23 (Schlitzer et al., 2013), for which they are an obligate source during infection by the attaching-and-effacing bacterium *Citrobacter rodentium* (Satpathy et al., 2013).

Plasmacytoid DCs have a plasma cell-like morphology and are specialized in the massive secretion of type I interferon (Cella et al., 1999; Siegal et al., 1999). In the mouse, these cells express low levels of MHC-II and CD11c but can be identified by surface expression of CD45R (B220), Siglec-H, and bone marrow stromal antigen 2 (Bst2) (Asselin-Paturel et al., 2001; Björck, 2001; Blasius et al., 2006a; Blasius et al., 2006b; Blasius et al., 2004; Nakano et al., 2001; Zhang et al., 2006). Upon activation, pDCs acquire several characteristics of cDCs, including dendritic morphology and increased expression of MHC and costimulatory molecules; however, their capacity for antigen presentation and T cell priming remain incompletely characterized (Reizis et al., 2011b; Villadangos and Young, 2008). An essential role for pDCs has been demonstrated in the context of infection by mouse hepatitis virus (Cervantes-Barragan et al., 2007) or chronic lymphocytic choriomeningitis virus (LCMV) (Blasius et al., 2012; Cervantes-Barragan et al., 2012); moreover, adoptive transfer experiments have suggested that pDCs may limit airway hyperreactivity (Lombardi et al., 2012), while antibody-based depletion experiments have produced conflicting results regarding the role of pDCs during experimental autoimmune encephalomyelitis (EAE) (Bailey-Bucktrout et al., 2008; Ioannou et al., 2013; Isaksson et al., 2009).

Studies have described a succession of progressively restricted progenitors that give rise to cDCs and pDCs (Figure 1). In the lineage (Lin)⁻ Kit⁺ Sca-1⁻ IL-7 receptor subunit α (IL-

$7Ra^-$ fraction of mouse bone marrow (BM), Fc γ RII/III lo CD34 $^+$ common myeloid progenitors (CMPs) give rise to all myeloid lineages via Fc γ RII/III hi CD34 $^+$ granulocyte-macrophage progenitors (GMPs) or Fc γ RII/III lo CD34 $^-$ megakaryocyte-erythrocyte progenitors (MEPs) (Akashi et al., 2000). Macrophage-DC progenitors (MDPs) can be distinguished from GMPs by lower expression of Kit and higher expression of the chemokine receptor CX $_3$ CR1 (Fogg et al., 2006). These cells, which express both macrophage colony-stimulating factor 1 receptor (M-CSFR, CD115) and the cytokine receptor FLT3, give rise to Kit int M-CSFR $^+$ FLT3 $^+$ common DC progenitors (CDPs) and Kit $^+$ M-CSFR $^+$ FLT3 $^-$ Ly-6C $^+$ committed monocyte progenitors (cMoPs) (Auffray et al., 2009; Hettinger et al., 2013; Naik et al., 2007; Onai et al., 2007). Loss of either FLT3 or FLT3 ligand (FLT3L) decreases abundance of cDCs and pDCs, and supraphysiological quantities of FLT3L dramatically increases abundance of those subsets (Kingston et al., 2009; Manfra et al., 2003; Maraskovsky et al., 1996; McKenna et al., 2000; Waskow et al., 2008).

From the CDP, pDCs develop in the BM via Kit int M-CSFR $^-$ IL-7Ra $^-$ FLT3 $^+$ progenitors with prominent pDC developmental potential (Onai et al., 2013). Immature committed progenitors of cDCs (pre-cDCs), which also develop in the BM from the CDP, were thought to circulate hematogenously to peripheral tissues before completing their development (Diao et al., 2006; Liu et al., 2009; Naik et al., 2006). However, committed progenitors of CD8 $^+$ /CD103 $^+$ cDCs and committed progenitors of CD4 $^+$ /CD11b $^+$ cDCs have been identified in the BM (Grajales-Reyes et al., 2015; Schlitzer et al., 2015).

Several transcription factors are specifically required for the development or survival of DCs. These include interferon regulatory factor 8 (Irf8) (Schiavoni et al., 2002) for CD8⁺/CD103⁺ cDCs and pDCs; ID-2 (Hacker et al., 2003; Jackson et al., 2011), basic leucine zipper transcription factor ATF-like 3 (Batf3) (Edelson et al., 2010; Hildner et al., 2008), and nuclear factor IL-3-regulated protein (Nfil3) (Kashiwada et al., 2011) for CD8⁺/CD103⁺ cDCs; interferon regulatory factor 4 (Irf4) (Suzuki et al., 2004) and neurogenic locus notch homologue protein 2 (Notch2) (Caton et al., 2007; Lewis et al., 2011) for CD4⁺/CD11b⁺ cDCs; and transcription factor 4 (Tcf4, E2-2) (Cisse et al., 2008) for pDCs. Some findings, however, demand a more nuanced interpretation of transcription factor activity. For example, in the context of competitive BM reconstitution, Irf8 is also required for normal CD4⁺/CD11b⁺ cDC development (Becker et al., 2012); Batf3, ID-2, and Nfil3 are not absolutely required for CD8⁺/CD103⁺ cDC development (Seillet et al., 2013; Tussiwand et al., 2012); Irf4-deficient mice retain CD11b⁺ cDCs in most tissues (Bajaña et al., 2012); and Notch2 participates to some extent in the terminal differentiation of all cDCs (Satpathy et al., 2013).

Macrophages and Monocyte Progeny

Unlike DCs, macrophages are non-migratory, tissue-resident cells generally inefficient at antigen presentation; instead, they possess high proteolytic and catabolic activity, which contributes to their capacity for scavenging pathogens, dead cells, and cellular debris (Murray and Wynn, 2011). Macrophages are considered to play an anti-inflammatory role at steady state, maintaining organ homeostasis in part by producing regulatory cytokines such as IL-10 (Denning et al., 2007; Rivollier et al., 2012). However, they can become ‘classically activated’

under inflammatory conditions, taking on pro-inflammatory functions (Mosser and Edwards, 2008). At steady state, the majority of tissue-resident macrophages derive from cells that maintain themselves in the tissue independently of BM progenitors after they have been seeded prenatally; other macrophages develop postnatally from circulating monocytes that infiltrate the tissue (Ginhoux et al., 2010; Hashimoto et al., 2013; Schulz et al., 2012; Yona et al., 2013). Although distinct gene expression and epigenetic profiles can be identified for macrophages that reside in different organs (Gautier et al., 2012; Gosselin et al., 2014; Lavin et al., 2014; van de Laar et al., 2016), nearly all subsets depend on M-CSFR and the transcription factor PU.1 for their development (Schulz et al., 2012; Wynn et al., 2013).

Difficulties in distinguishing DCs from macrophages based on the expression of surface markers have prompted alternative approaches to elucidate lineage relationships. By principal component analysis of global gene expression profiles, DC populations can be segregated on the basis of subset independently of tissue location (Elpek et al., 2011; Miller et al., 2012). When several DC and macrophage samples were included in such an analysis, the lineage-segregating principal component revealed a ‘continuum’ of transcriptional programs along which CD8⁺/CD103⁺ cDCs were furthest segregated from macrophages (Figure 2A) (Satpathy et al., 2012b). In cDC and macrophage populations, *Zbtb46* expression correlated strongly with score in that principal component (Figure 2B), consistent with findings that *Zbtb46* expression distinguishes cDCs from other lineages in a green fluorescent protein (GFP) reporter model (Satpathy et al., 2012a) and in a diphtheria toxin receptor (DTR) depletion model (Meredith et al., 2012). These models have been used to clarify the composition of heterogeneous

populations, confirming that CD11c⁺ CD103⁻ CD11b⁺ cells in the intestinal lamina propria include non-cDCs. Further work using a *Clec9a*-driven lineage-tracing model to mark the progeny of committed DC progenitors has also confirmed that CD11c⁺ CD103⁻ CD11b⁺ cells in the intestinal lamina propria do include CDP-derived cells (Schraml et al., 2013).

Besides differentiating into macrophages, monocytes isolated from the mouse can also differentiate into moDCs upon treatment with granulocyte macrophage colony-stimulating factor (GM-CSF) and IL-4 (Inaba et al., 1992; Sallusto and Lanzavecchia, 1994), and they acquire *Zbtb46* expression under such conditions (Satpathy et al., 2012a). These cells are a heterogeneous population comprising both macrophage-like and DC-like fractions (Helft et al., 2015), although it is unclear whether human moDCs *in vitro* are similarly heterogeneous. In the context of inflammation, cells that express the surface markers MHC-II, CD11c, and Ly-6C have been identified as *in vivo* moDCs (Langlet et al., 2012; Merad et al., 2013; Plantinga et al., 2013). Further, depletion of Ly-6C^{hi} monocytes using an anti-CCR2 antibody decreases the frequency of Ly-6C^{lo} *Zbtb46*-GFP⁺ cells in the inflamed gut (Zigmond et al., 2012). Thus, moDCs may lose expression of Ly-6C and acquire expression of *Zbtb46* upon differentiation from monocytes (Zigmond et al., 2012); alternatively, Ly-6C^{hi} monocytes may help to recruit *Zbtb46*-expressing DCs. Indeed, some have suggested that Ly-6C⁺ moDCs might be indistinguishable from monocyte-derived macrophages and myeloid-derived suppressor cells (Chow et al., 2016; Guilliams et al., 2014), or even from relatively undifferentiated monocytes (Jakubzick et al., 2013).

Finally, LCs are branched, unpigmented, and slowly dividing cells resident in the epidermis with an unresolved relationship to other myeloid subsets (Guilliams et al., 2014; Satpathy et al., 2012b). They develop from embryonic monocytes and are replenished under inflammatory conditions by progenitors in the blood or BM (Ginhoux et al., 2006; Hoeffel et al., 2012; Merad et al., 2002; Seré et al., 2012). Like microglia, LCs are unaffected by loss of FLT3 or FLT3L; instead, they require IL-34 signalling through M-CSFR (Ginhoux et al., 2009; Ginhoux et al., 2006; Greter et al., 2012b; Kingston et al., 2009; Wang et al., 2012). However, like cDCs and unlike macrophages, activated LCs increase migration to the draining lymph node (LN) (Silberberg-Sinakin et al., 1976), where they upregulate expression of genes such as *Flt3* and *Zbtb46* (Miller et al., 2012; Satpathy et al., 2012b). LCs that migrate out of human skin explants also express abundant *ZBTB46* messenger RNA (mRNA) (Artyomov et al., 2015), and depletion of *Zbtb46*-expressing cells decreases the frequency of LCs among cells that migrate out of mouse skin explants and among cells within mouse draining LNs (Mollah et al., 2014).

In the following chapters, a series of experiments are presented that aim to address two questions concerning the development and function of DCs. First, how are B-cell lymphoma/leukemia 11A (*Bcl11a*) and zinc finger E-box-binding homeobox 2 (*Zeb2*), two transcription factors widely expressed in the hematopoietic system, involved in specification or commitment of specific myeloid lineages? Second, where and when (if ever) do DCs emerge from monocyte progenitors, and how are self-renewing peripheral myeloid lineages such as LCs related to such populations?

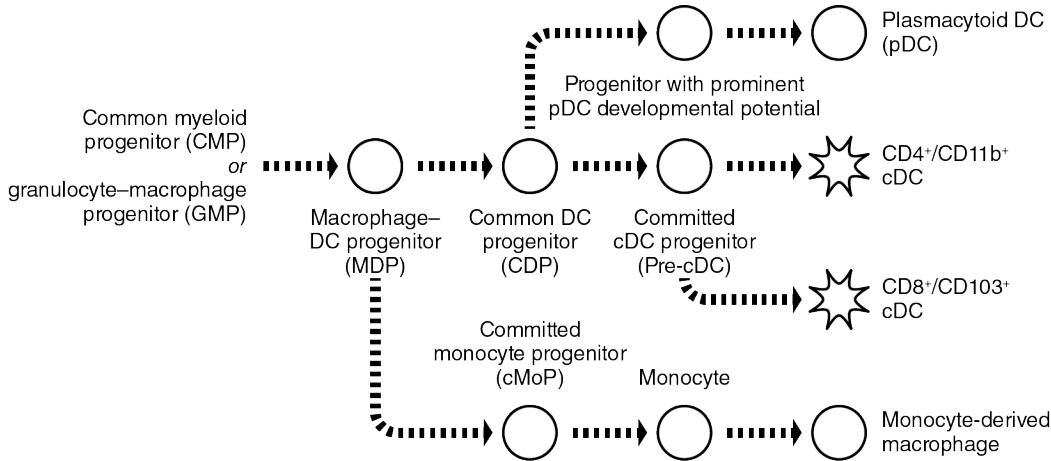


Figure 1: DC development proceeds through progressively-restricted progenitor stages

In the bone marrow (BM), macrophage–dendritic cell progenitors (MDPs) give rise to common DC progenitors (CDPs) and committed monocyte progenitors (cMoPs). Both cDCs and pDCs arise from CDPs after transiting intermediate committed or biased progenitor stages, while monocytes and their macrophage progeny arise from cMoPs.

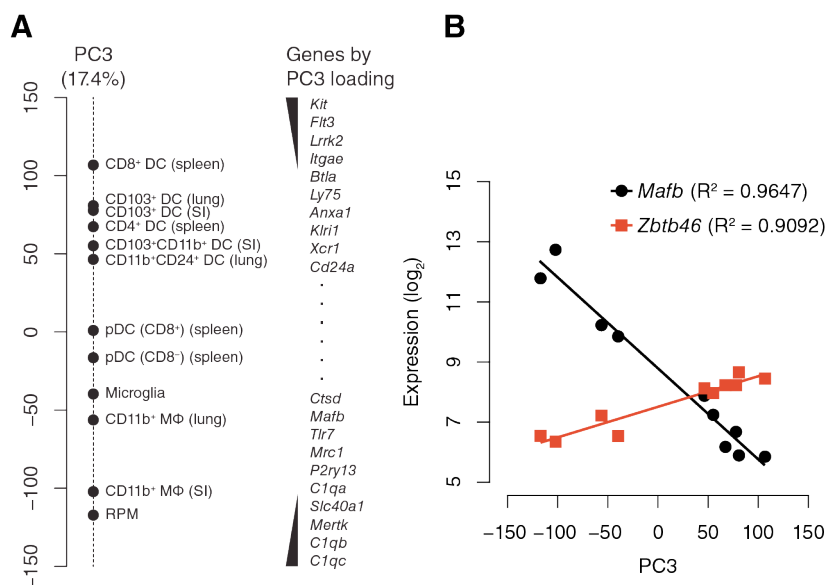


Figure 2: Variations in gene expression among DC and macrophage subsets

(A) Principal component analysis of gene expression in DCs and macrophages (MΦ) yields a principal component (PC3) that segregates populations by lineage. Genes known to distinguish populations by lineage are ‘heavily weighted’ on PC3. RPM, red pulp macrophage; SI, small intestine. (B) Among cDC and MΦ populations, *Zbtb46* mRNA abundance is correlated with PC3 score and *Mafb* mRNA abundance is anticorrelated with PC3 score. (See also page 110.)

CHAPTER 2: *Bcl11a* IS REQUIRED FOR
PLASMACYTOID DENDRITIC CELL DEVELOPMENT

This work was performed in collaboration with Ansuman T Satpathy, Wumesh KC, Pentao Liu, Theresa L. Murphy, and Kenneth M. Murphy and was published in PLOS ONE 8(5): e64800. Personal contributions included the design and carrying out of selected experiments; data analysis; and writing of the paper.

A bioinformatic analysis of global gene expression patterns has identified groups of transcription factors that may be involved in fate decisions along the DC lineage (Miller et al., 2012). Among genes that increase in expression from the MDP to the CDP, those that do not increase in expression from the MDP to the monocyte were labelled in that analysis as possible promoters of DC commitment. Transcription factors identified by these criteria include some previously associated only with pDC development, including E2-2 and Spi-B (Ghosh et al., 2010; Schotte et al., 2004), and some previously associated only with cDCs, including Zbtb46 (Meredith et al., 2012; Satpathy et al., 2012a). Other factors identified in this analysis include Irf8, Bcl11a, and Runx2. It has been demonstrated in the setting of competitive BM reconstitution that Irf8 promotes the development of all DC subsets (Becker et al., 2012), even though *Irf8^{-/-}* mice in other settings do not show defects in CD4⁺ cDC development (Tamura et al., 2005; Tsujimura et al., 2003). We wondered, therefore, whether a similar early role in DC development could be identified for another factor such as Bcl11a.

Bcl11a was first described as a gene located at a common proviral integration site in BXH2 myeloid leukemias, and its human orthologue was found to be a recurrent target of translocations in B cell malignancies (Nakamura et al., 2000; Satterwhite et al., 2001). This gene encodes a Krüppel-like zinc finger transcription factor expressed in neural and lymphoid tissues that is essential for the development of B cells and for thymocyte maturation (Liu et al., 2003). In the human erythroid lineage, BCL11A acts *in trans* to silence the fetal hemoglobin locus in cooperation with the transcription factor SOX6 (Sankaran et al., 2009; Xu et al., 2010). Indeed, differences in stage-specific expression between human BCL11A and mouse *Bcl11a* account at least in part for interspecies differences in fetal hemoglobin expression patterns (Sankaran et al., 2009).

Although *Bcl11a* has been recognized as a useful marker of pDCs (Pelayo et al., 2005; Pulford et al., 2006), its actual role in DC development remains unreported. Thus, we sought to examine DC development in the setting of *Bcl11a* deficiency *in vivo* and *in vitro*. We found that *Bcl11a* was required for normal expression of IL-7 receptor (IL-7R) as well as FLT3 in early hematopoietic progenitors. In addition, we observed a strict requirement for *Bcl11a* in pDC development and found evidence for a *Bcl11a*-independent pathway of cDC development *in vivo*.

Results

***Bcl11a* is required for development of CLPs and CDPs**

During hematopoiesis, *Bcl11a* is expressed at similar levels in the hematopoietic stem cell (HSC), multipotent progenitor (MPP), common lymphoid progenitor (CLP), CMP, and

MEP (Miller et al., 2012). To study the function of *Bcl11a* in hematopoietic progenitors, we used mice targeted for deletion of the first exon of *Bcl11a* (Liu et al., 2003). Since *Bcl11a*^{-/-} mice die *in utero* or perinatally, we compared hematopoietic progenitor populations present in wild-type (WT) and *Bcl11a*^{-/-} fetal livers at embryonic day 14.5. First, we analysed development of Lin⁻ Sca-1⁺ Kit⁺ (LSK), CLP, GMP, MEP, and CDP populations (Figure 3). WT and *Bcl11a*^{-/-} fetal livers showed comparable frequencies of GMPs and MEPs. However, *Bcl11a*^{-/-} fetal livers showed a greater than twofold decrease in the frequency of LSK cells and more marked decreases in frequencies of IL-7R⁺ CLPs and FLT3⁺ CDPs relative to WT fetal livers (Figure 3A, B); within the LSK fraction, *Bcl11a*^{-/-} fetal livers showed defects in both CD150 (Slamf1)⁺ and Slamf1⁻ populations (Figure 3C). One study has demonstrated that a Sca-1^{lo} Kit⁺ FLT3⁺ Slamf1⁻ population with granulocyte and macrophage potential (SL-GMP) can be identified which excludes mast cell potential (Franco et al., 2010); GMPs in the *Bcl11a*^{-/-} fetal liver, however, lacked FLT3 expression (data not shown) and no SL-GMP population could be identified (Figure 3D).

Next, we analysed hematopoietic development in chimeras produced by transferring WT or *Bcl11a*^{-/-} fetal liver cells into lethally irradiated congenic recipient mice (Figure 4). Four to six weeks after transfer, donor-derived *Bcl11a*^{-/-} BM showed decreased frequencies of LSK cells, CLPs, and CDPs but comparable frequencies of GMPs and MEPs relative to donor-derived WT BM (Figure 4A, B); within the LSK fraction, donor-derived *Bcl11a*^{-/-} BM showed a greater proportion of Slamf1⁺ cells than did donor-derived WT BM, corresponding to a decrease in the overall frequency of the more differentiated Slamf1⁻ population (Figure 4C). As

in *Bcl11a*^{-/-} fetal livers, no SL-GMP population could be identified in donor-derived *Bcl11a*^{-/-} BM (Figure 4D). In summary, the loss of Bcl11a in hematopoietic progenitors resulted in impaired development of LSK cells as well as a selective loss of CLPs and CDPs; these effects were observed both in the fetal stage and in the adult chimera, demonstrating that this factor is required in fetal and adult hematopoiesis.

Conceivably, the absence of IL-7R⁺ CLPs and FLT3⁺ CDPs in *Bcl11a*^{-/-} fetal livers and BM could result from a requirement for Bcl11a in the development of the CLP and CDP or from a more restricted requirement for Bcl11a in the expression of IL-7R and FLT3, the surface markers that identify these populations. In either case, however, the loss of Bcl11a should result in DC defects because FLT3L signalling is essential for DC development in the steady state (Laouar et al., 2003; McKenna et al., 2000; Onai et al., 2006).

Bcl11a regulates expression of Il7r and Flt3

To identify Bcl11a target genes that explain its role in hematopoietic progenitors, we compared global gene expression by microarray for donor-derived WT and *Bcl11a*^{-/-} populations isolated from chimeric BM (Figure 5). Since we observed that IL-7R- and FLT3-expressing populations were affected by the loss of Bcl11a, we avoided the use of these surface markers in order to allow for comparison of equivalent populations across genotypes. Thus, we isolated MPPs as identified by the lack of Slamf1 expression within the LSK fraction (Kiel et al., 2005; Ogawa et al., 1991; Spangrude et al., 1988). We also isolated GMPs from the same BM, since the size of this population was unaffected by loss of Bcl11a.

We found that WT and *Bcl11a*^{-/-} GMPs were more similar to each other in gene expression than WT and *Bcl11a*^{-/-} MPPs were to each other (Figure 5A). One hundred and thirty-four probe sets showed a greater than twofold change in expression between WT and *Bcl11a*^{-/-} GMPs. In contrast, 1020 probe sets showed a greater than twofold change in expression between WT and *Bcl11a*^{-/-} MPPs; of these, only 38 also showed a greater than twofold change between WT and *Bcl11a*^{-/-} GMPs (Figure 5B). These data suggest that GMP population size is unaffected by loss of Bcl11a because this transcription factor regulates relatively few genes in GMPs.

Since the loss of Bcl11a impaired development of CDPs but not GMPs, we examined Bcl11a target genes which showed expression patterns that distinguish DCs from monocytes and macrophages. Thus, we compared the ratio of gene expression in CDPs relative to monocytes against the ratio of gene expression in *Bcl11a*^{-/-} MPPs relative to WT MPPs (Figure 5C). Of genes most highly expressed in CDPs relative to monocytes, those most affected by loss of Bcl11a included *Flt3*, *Cnn3* (encoding calponin 3), *Dntt* (encoding the template-independent DNA polymerase TdT), *Il7r*, and *Blnk* (encoding B-cell linker protein, which links components of B-cell receptor signalling). We also compared changes in gene expression between WT and *Bcl11a*^{-/-} MPPs for members of the core cDC transcriptional signature identified in a published bioinformatic analysis (Miller et al., 2012) (Figure 5D). Within this core signature, we found only three genes—*Ass1*, *Amica1*, and *Flt3*—that showed a greater than twofold decrease in expression in *Bcl11a*^{-/-} MPPs relative to WT MPPs. Taken together, the decreased expression

of *Flt3* and *Il7r* in *Bcl11a*^{-/-} MPPs suggests that Bcl11a may be specifically required for the expression of these genes.

Bcl11a is required for pDC but not cDC development in vivo

Next, we examined the development of mature hematopoietic subsets in WT and *Bcl11a*^{-/-} fetal liver chimeras (Figure 6). In accordance with previous reports (Liu et al., 2003), we observed atrophic thymi in *Bcl11a*^{-/-} chimeras (data not shown). In the BM, the size of the donor-derived compartment was comparable in WT and *Bcl11a*^{-/-} chimeras; in the spleen and skin-draining LNs, *Bcl11a*^{-/-} cells were somewhat impaired in their competition against the residual host population (Figure 6A). Within the donor-derived compartment of the spleen, a profound defect in pDC development was apparent in *Bcl11a*^{-/-} chimeras relative to WT chimeras (Figure 6B). In contrast, donor-derived cDCs were present in *Bcl11a*^{-/-} chimeras with no significant decrease relative to WT chimeras (Figure 6C).

Among lymphoid subsets, donor-derived B cells, CD4 T cells, CD8 T cells, and $\gamma\delta$ T cells were decreased in frequency by at least tenfold in the spleens of *Bcl11a*^{-/-} chimeras as compared to WT chimeras, consistent with previous reports (Liu et al., 2003), while NK cells were decreased by slightly more than threefold (Figure 7A). Among myeloid subsets other than pDCs, donor-derived CD8⁻ cDCs showed a modest threefold decrease in the spleens of *Bcl11a*^{-/-} chimeras as compared to WT chimeras; other myeloid populations examined, including CD8⁺ cDCs, were not decreased in frequency (Figure 7B). Thus, Bcl11a was strictly required for the development of pDCs but not cDCs *in vivo*.

FLT3-dependent, but not GM-CSF-dependent, DC development requires *Bcl11a* in vitro

We compared the development of WT and *Bcl11a*^{-/-} cells *in vitro* in response to treatment with FLT3L or granulocyte macrophage colony-stimulating factor (GM-CSF) (Figure 8). The observation that *Flt3*^{-/-} mice retain DC development (Waskow et al., 2008) suggests an alternative receptor for FLT3L or a FLT3L-independent pathway for DC development. Thus, we supplied excess FLT3L or GM-CSF to distinguish between these possibilities in the context of *Bcl11a* deficiency. As expected, pDCs developed from WT fetal liver cells (Figure 8A) and from the donor-derived BM cells of WT chimeras (Figure 8B) in response to FLT3L treatment. In contrast, pDCs developed in markedly decreased numbers from *Bcl11a*^{-/-} fetal liver cells and completely failed to develop from the donor-derived BM cells of *Bcl11a*^{-/-} chimeras under these conditions (Figure 8A, B), demonstrating that *Bcl11a* is required for pDC development in response to FLT3L both *in vivo* and *in vitro*. We also examined cDC development from WT and *Bcl11a*^{-/-} fetal liver cells *in vitro* in response to treatment with FLT3L or GM-CSF. FLT3L-derived cDCs were markedly decreased in cultures of *Bcl11a*^{-/-} fetal liver cells relative to cultures of WT fetal liver cells (Figure 8C, E). However, GM-CSF-derived DCs developed in normal numbers from cultures of *Bcl11a*^{-/-} fetal liver cells relative to cultures of WT fetal liver cells (Figure 8D, F). These results suggest that FLT3L cannot signal through an alternative receptor to rescue cDC development in *Bcl11a*^{-/-} cells, but that an alternative pathway of DC development may be mediated by GM-CSF.

Loss of FLT3L results in lineage-specific defects in pDC development

Next, we examined the development of splenic pDCs in the context of IL-7R or FLT3L deficiency. A previous study has demonstrated that splenic pDCs in *Il7r^{-/-}* mice or *Il7^{-/-}* mice are decreased in absolute number when compared to WT controls (Vogt et al., 2009). We found that splenic pDCs in *Il7r^{-/-}* mice were not decreased in proportion to total splenocytes when compared to WT controls matched for strain, age, and sex (Figure 9A). This result suggests that the hematopoietic defects in these mice may have relatively few lineage-specific consequences for pDC development.

Previously, it has been found that *Flt3^{-/-}* mice and *Flt3l^{-/-}* mice show defects in the development of pDCs (Kingston et al., 2009; Waskow et al., 2008). Accordingly, and in contrast to our observations in *Il7r^{-/-}* mice, we found that *Flt3l^{-/-}* mice showed a greater than fourfold reduction in splenic pDC frequency as compared to WT littermate controls (Figure 9B), in addition to reductions in absolute spleen size (data not shown).

Bcl11a is required for FLT3 expression in cDCs and binds the Flt3 genomic locus

Because we observed cDC development in *Bcl11a^{-/-}* chimeras, we assessed whether these cells might express FLT3 in a Bcl11a-independent manner; however, unlike WT cDCs in the BM, *Bcl11a^{-/-}* cDCs in the same compartment showed no discernible FLT3 expression by flow cytometry (Figure 9C), again suggesting that a FLT3-independent pathway is instead responsible for their development. Finally, to assay Bcl11a binding at the *Flt3* locus, we performed chromatin immunoprecipitation (ChIP) using mouse pro-B cells. By quantitative polymerase chain reaction (qPCR), we detected an approximately threefold enrichment at a

region in the first intron of the *Flt3* locus in DNA precipitated using anti-Bcl11a antibody as compared to isotype control (Figure 9D).

In summary, our results document a strict requirement for Bcl11a in pDC development both *in vivo* and *in vitro*; further, the requirement for Bcl11a in cDC development may differ based on the cytokine stimulus to which progenitors are exposed. The actions of Bcl11a include regulation of FLT3 expression by direct binding to the *Flt3* locus, and Bcl11a is required for FLT3 expression in DCs and their progenitors.

Discussion

This study extends the known actions of *Bcl11a* in immune lineage development and provides a mechanism for its effects. Although *Bcl11a* has been recognized as a factor required for normal lymphoid development (Liu et al., 2003), the basis for this requirement has been unclear. It has been shown that Bcl11a acts upstream of the early B-cell factor COE1 (Ebf1) and the B-cell-specific factor Pax-5, and that *Il7r* mRNA is not expressed in *Bcl11a*^{-/-} fetal livers (Liu et al., 2003). Here, we demonstrate that Bcl11a is required for normal expression of IL-7R as early as the CLP and we add the novel observation that Bcl11a promotes the development of FLT3-dependent lineages. Together, these actions provide a more complete account for previously observed defects in lymphocyte development in *Bcl11a*^{-/-} mice, since T cell potential is preserved in IL-7-deficient CLPs in a FLT3L-dependent manner (Moore et al., 1996; Sitnicka et al., 2007). The mechanisms by which Bcl11a deficiency impairs T and B cell development, however, still remain incompletely explored. Consistent with a previous report (Liu et al., 2003), we confirmed the presence of residual T and B cells in the spleen of chimeras

reconstituted with *Bcl11a*^{-/-} fetal liver cells. By contrast, tamoxifen-induced deletion of *Bcl11a* in chimeras that have been reconstituted with *Gt(ROSA)26Sor-Cre-ER*^{T2}; *Bcl11a*^{fl/fl} BM cells results in a more profound loss of T and B cells (Yu et al., 2012). Thus, synchronous deletion of *Bcl11a* within a previously intact hematopoietic compartment produces a different outcome than does sustained deficiency throughout hematopoiesis. These results may point to a crucial lymphopoietic role for cells in which *Bcl11a* is dispensable for survival but necessary for development or maturation, or vice versa; these cells could include HSCs, mature T and B cells, or even residual CLPs undetectable due to a lack of IL-7R and FLT3 expression.

In line with a previous finding that E2-2 regulates *Bcl11a* expression (Ghosh et al., 2010), we also document a strict requirement for *Bcl11a* in the development of pDCs. The development of pDCs *in vivo* was lost in *Bcl11a*^{-/-} fetal liver chimeras. In agreement, FLT3L cultures of BM derived from these *Bcl11a*^{-/-} chimeras showed a complete loss of pDC development *in vitro*. Because mature pDCs are short-lived, non-proliferative, and continuously replenished from progenitor populations (Liu et al., 2007; Merad and Manz, 2009), the nearly complete loss of this population is most attributable to a developmental defect and not merely to cell survival defects in mature pDCs. This interpretation would be consistent with a finding that rescue of *Bcl11a*-deficient progenitors from increased apoptosis by p53 deficiency is unable to restore lymphoid potential (Yu et al., 2012).

Notably, however, *in vitro* development of cDCs was eliminated in FLT3L cultures of *Bcl11a*^{-/-} fetal liver cells but was maintained in GM-CSF cultures of *Bcl11a*^{-/-} fetal liver cells. FLT3L and GM-CSF have distinct, non-redundant actions in supporting cDC development

(Edelson et al., 2011b; Greter et al., 2012a). The combined loss of FLT3L and GM-CSF causes a more severe cDC deficiency than loss of FLT3L alone; indeed, FLT3L-deficient mice retain an appreciable population of FLT3-expressing progenitors (Kingston et al., 2009). The maintenance of cDCs in *Bcl11a*^{-/-} fetal liver chimeras suggests that these cells may rely on a Bcl11a- and FLT3-independent pathway for their development, survival, or expansion. Conditional knockout models would clarify which of these alternatives underlie the observed phenotype in *Bcl11a*^{-/-} mice. Since DCs developed normally *in vitro* from *Bcl11a*^{-/-} progenitors treated with GM-CSF, it is possible that *Bcl11a*^{-/-} cDCs *in vivo* indeed represent development from GM-CSF-dependent progenitors, related perhaps to moDC lineages (Satpathy et al., 2011).

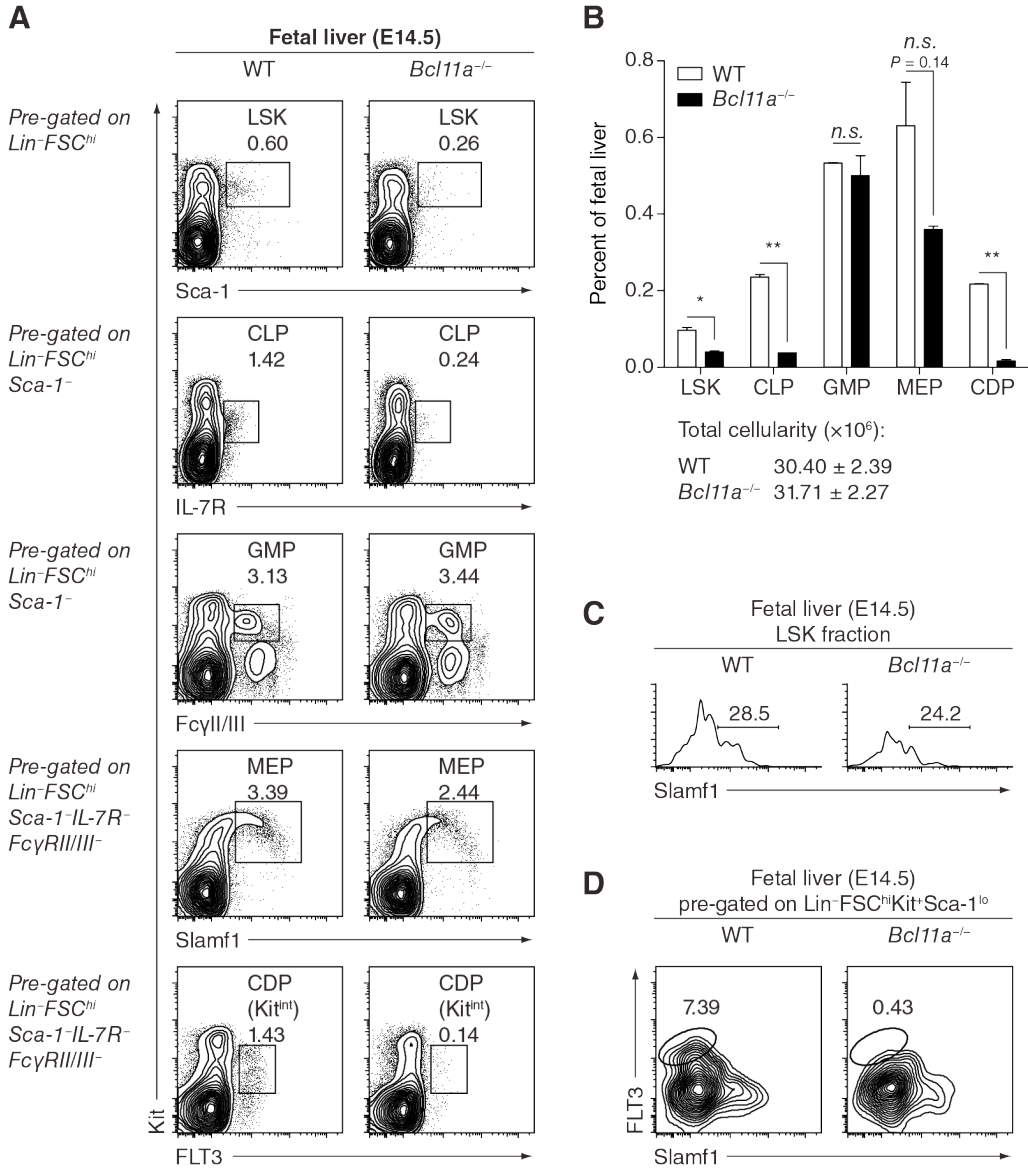


Figure 3: Bcl11a is required for development of lymphoid and DC progenitors in the fetus

(A) Flow cytometry analysis of progenitor populations in WT and *Bcl11a*^{-/-} fetal livers dissected at embryonic day 14.5 (E14.5). Populations are gated as indicated; numbers represent the percentage of cells within the histogram that lie in the indicated gate. Data are representative of two mice per group. (B) Progenitor populations in WT and *Bcl11a*^{-/-} fetal livers at E14.5, analysed by flow cytometry as in (A) and presented as a percentage of total fetal liver cells. Bars represent the mean (\pm SEM) of two mice per group. (C) CD150 (Slamf1) expression within the LSK fraction in WT and *Bcl11a*^{-/-} fetal livers at E14.5. (D) SL-GMPs in WT and *Bcl11a*^{-/-} fetal livers at E14.5.

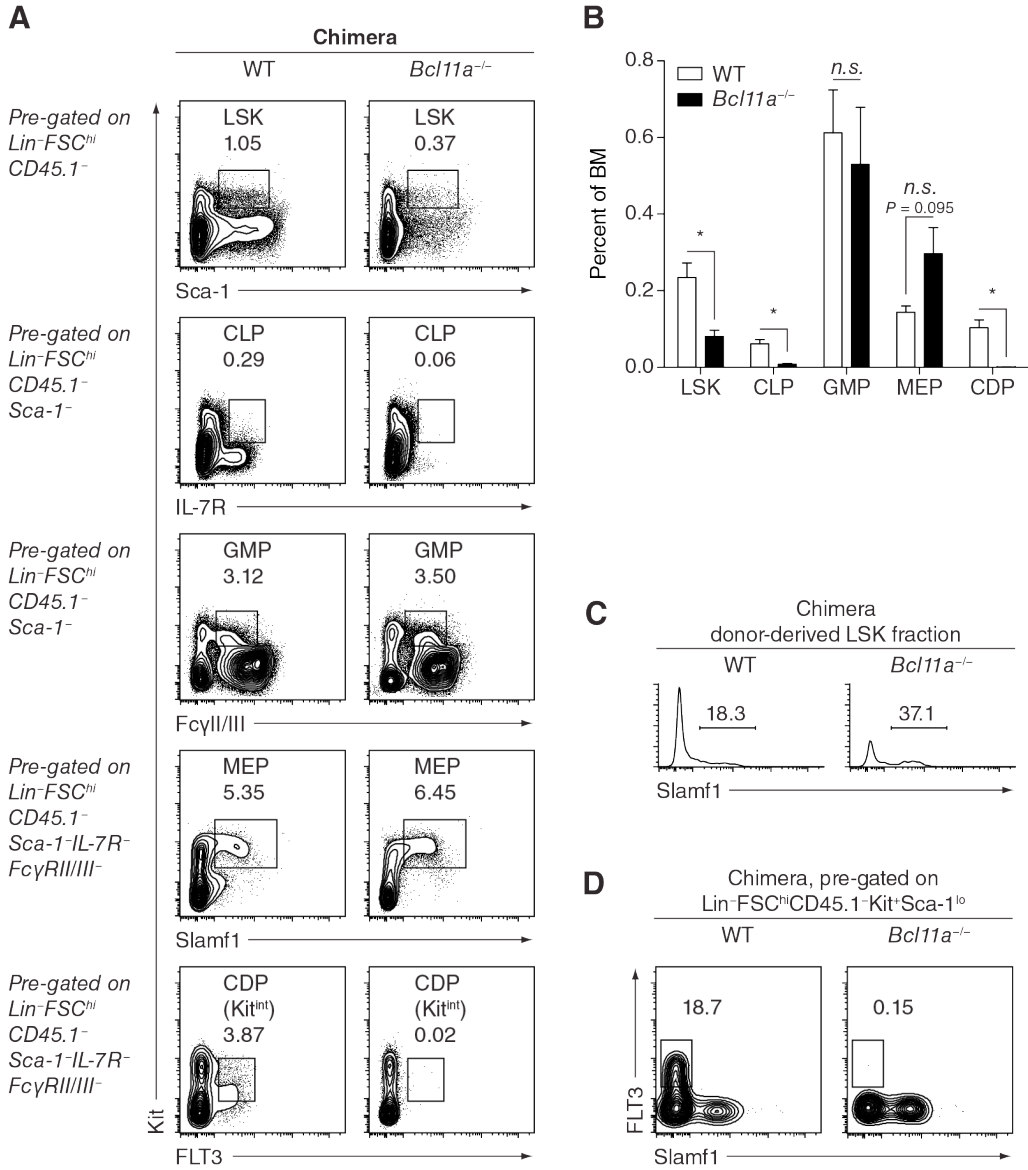


Figure 4: *Bcl11a* is required for development of lymphoid and DC progenitors in the adult

(A) Flow cytometry analysis of progenitor populations in lethally irradiated congenic mice reconstituted with WT or *Bcl11a*^{-/-} fetal liver cells, analysed four weeks after transplant. Data are representative of three mice per group. (B) Progenitor populations in WT and *Bcl11a*^{-/-} fetal liver chimeras at four weeks after transplant, analysed by flow cytometry as in (A) and presented as a percentage of total BM cells. Bars represent the mean (\pm SEM) of three mice per group. (C) CD150 (Slamf1) expression within the donor-derived LSK fraction in WT and *Bcl11a*^{-/-} fetal liver chimeras at four weeks after transplant. (D) SL-GMPs in WT and *Bcl11a*^{-/-} fetal liver chimeras at four weeks after transplant.

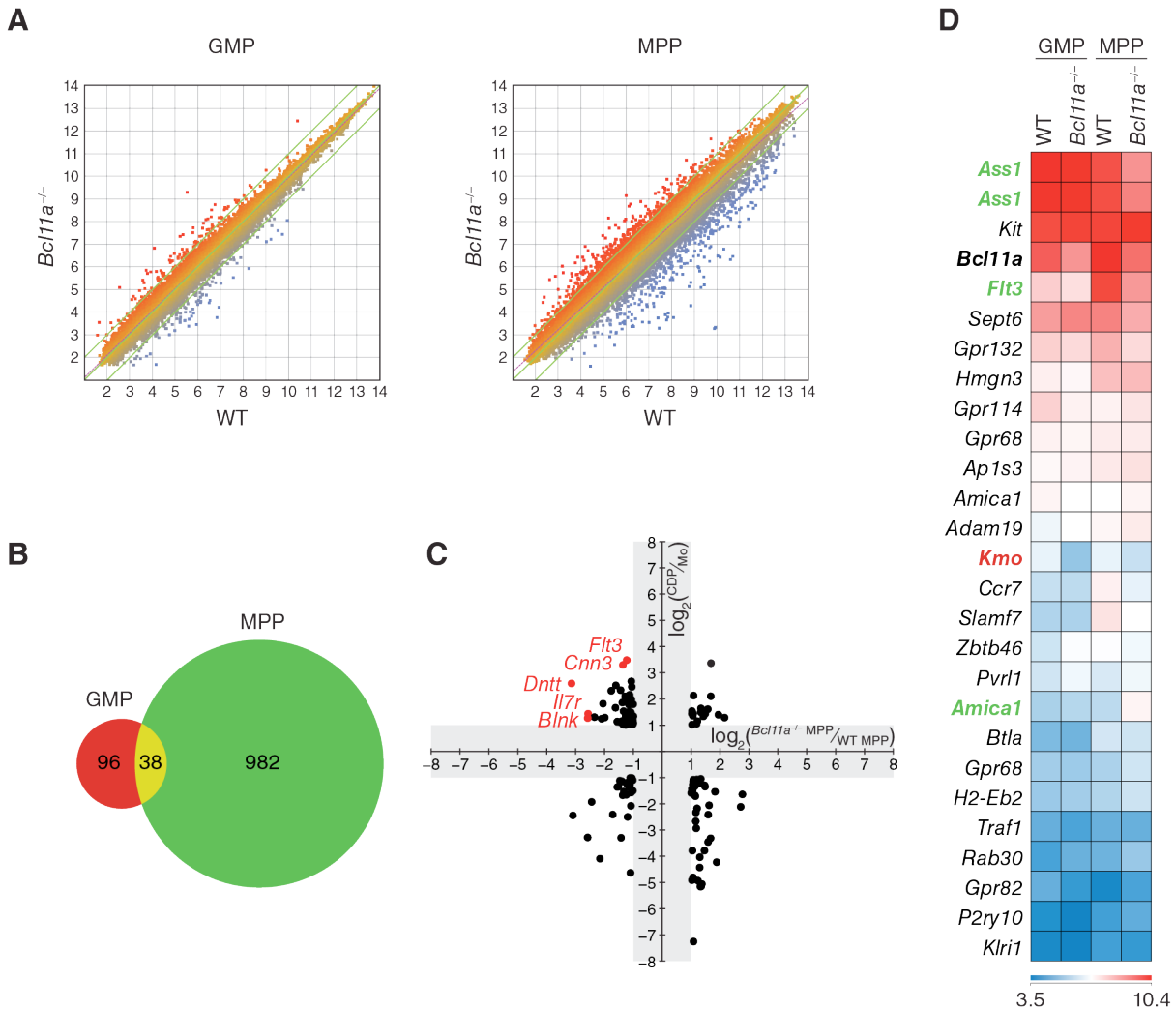


Figure 5: *Bcl11a* regulates expression of *Flt3* and *Il7r*

(A) Microarray analysis of sorted GMPs (left) and MPPs (right) from WT and *Bcl11a*^{-/-} fetal liver chimeras. (B) Shown is a Venn diagram of probe sets (excluding normalization controls) with a greater than twofold change in expression between WT and *Bcl11a*^{-/-} MPPs. (C) Shown are log₂-transformed ratios of gene expression in *Bcl11a*^{-/-} MPPs relative to WT MPPs (*x*-axis) plotted against log₂-transformed ratios of gene expression in WT CDPs relative to WT monocytes (data from ImmGen; *y*-axis). For clarity, probe sets with less than twofold changes in expression (log₂-transformed ratios between -1 and 1) along either dimension are omitted (grey). (D) Shown is a heat map of log₂-transformed gene expression in WT and *Bcl11a*^{-/-} GMPs and MPPs for probe sets that constitute an ImmGen core cDC signature. Highlighted are genes that show a greater than twofold change in expression between WT and *Bcl11a*^{-/-} GMPs (red) or between WT and *Bcl11a*^{-/-} MPPs (green).

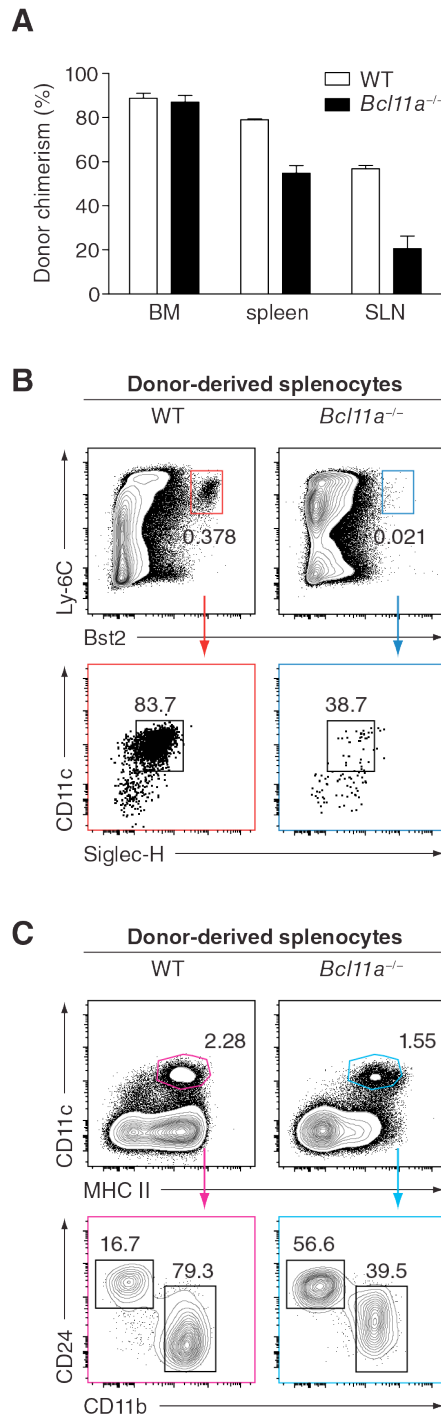


Figure 6: Bcl11a is required *in vivo* for development of pDCs but not cDCs

(A) Donor-derived (CD45.2⁺) chimerism in the BM, spleen, and skin-draining LN (SLN) of WT and *Bcl11a^{-/-}* fetal liver chimeras. Bars represent the mean (\pm SEM) of three mice per group. (B) Flow cytometry analysis of donor-derived pDCs in the spleen. Data are representative of three mice per group. (C) Flow cytometry analysis of donor-derived cDCs in the spleen. Data are representative of three mice per group.

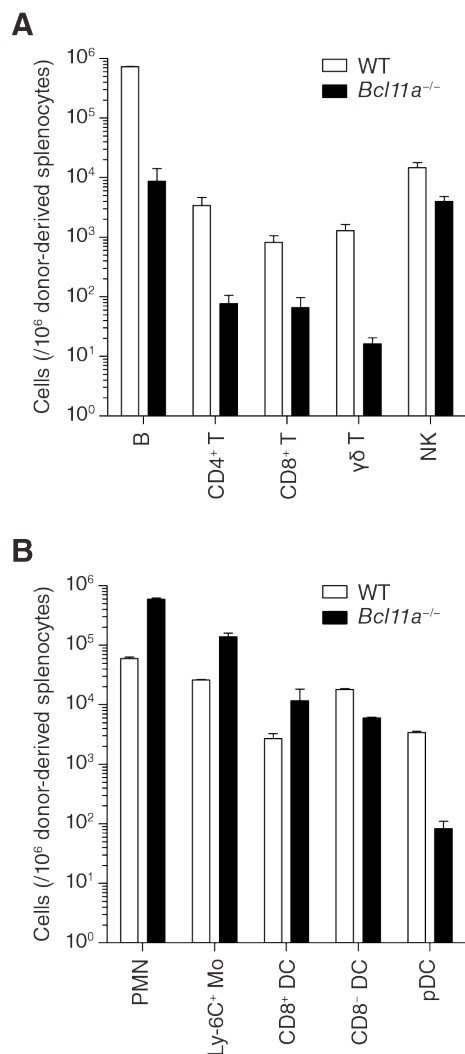


Figure 7: *Bcl11a* deficiency *in vivo* impairs lymphoid and myeloid development

(A) Donor-derived lymphoid populations in the spleen of WT and $Bcl11a^{-/-}$ fetal liver chimeras, analysed by flow cytometry. Bars represent the mean (\pm SEM) of three mice per group. (B) Donor-derived myeloid populations in the spleen of WT and $Bcl11a^{-/-}$ fetal liver chimeras, analysed by flow cytometry as in Figure 6. Bars represent the mean (\pm SEM) of three mice per group.

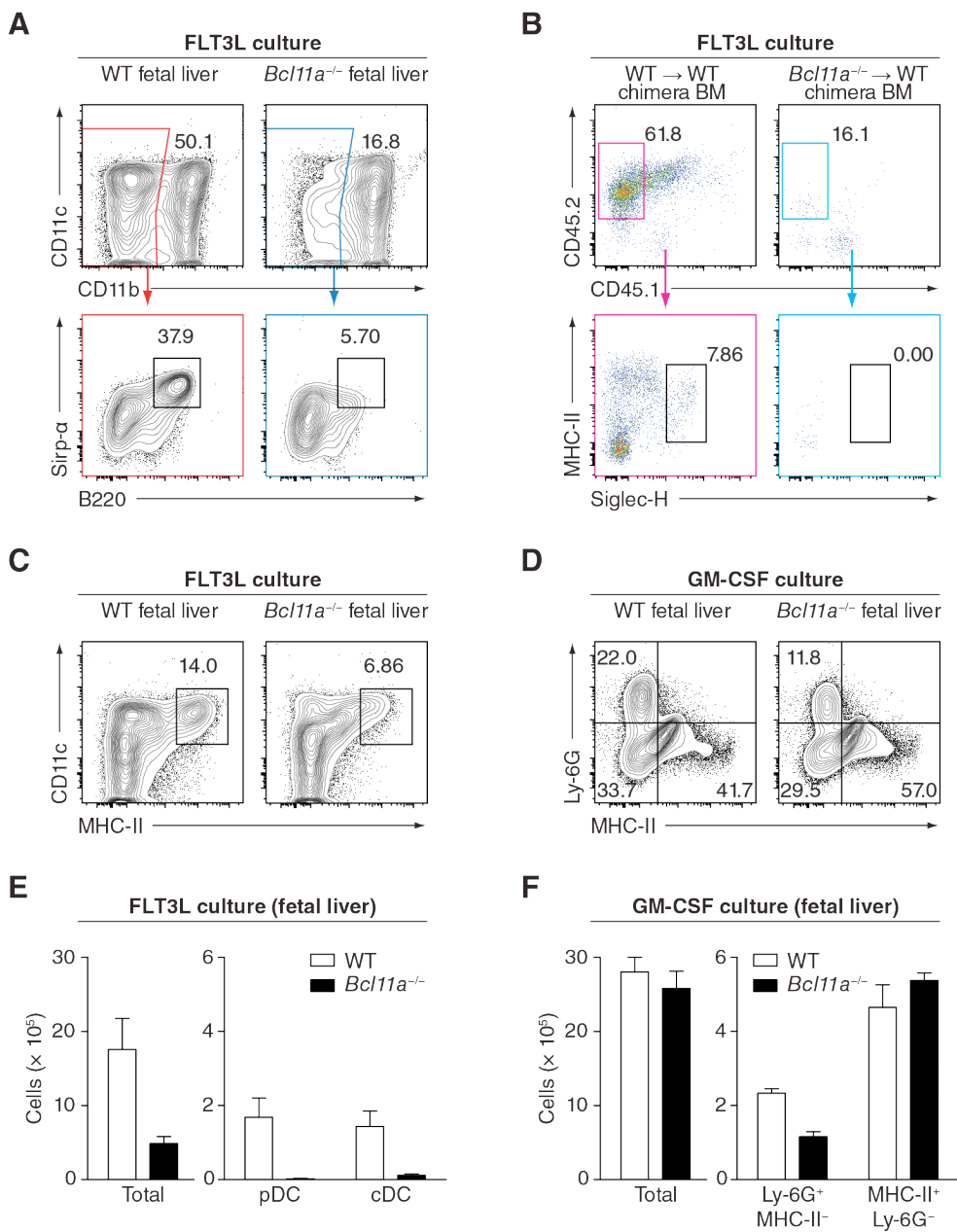


Figure 8: Bcl11a is required *in vitro* for FLT3L-derived DCs but not GM-CSF–derived DCs

(A) Flow cytometry analysis of pDCs in FLT3L cultures of fetal liver cells. Data are representative of 3–4 replicates over two experiments. (B) Flow cytometry analysis of pDCs in FLT3L cultures of BM cells derived from fetal liver chimeras. Data are representative of three replicates. (C, D) Flow cytometry analysis of FLT3L -derived cDCs (C) or GM-CSF-derived DCs (D) in cultures of fetal liver cells. Data are representative of 3–4 replicates over two experiments. (E, F) Counts of total cells and indicated subsets in FLT3L cultures (E) or GM-CSF cultures (F) of fetal liver cells, analysed by flow cytometry as in (C) or (D), respectively. Bars represent the mean (\pm SEM) of 3–4 replicates per group pooled from two experiments.

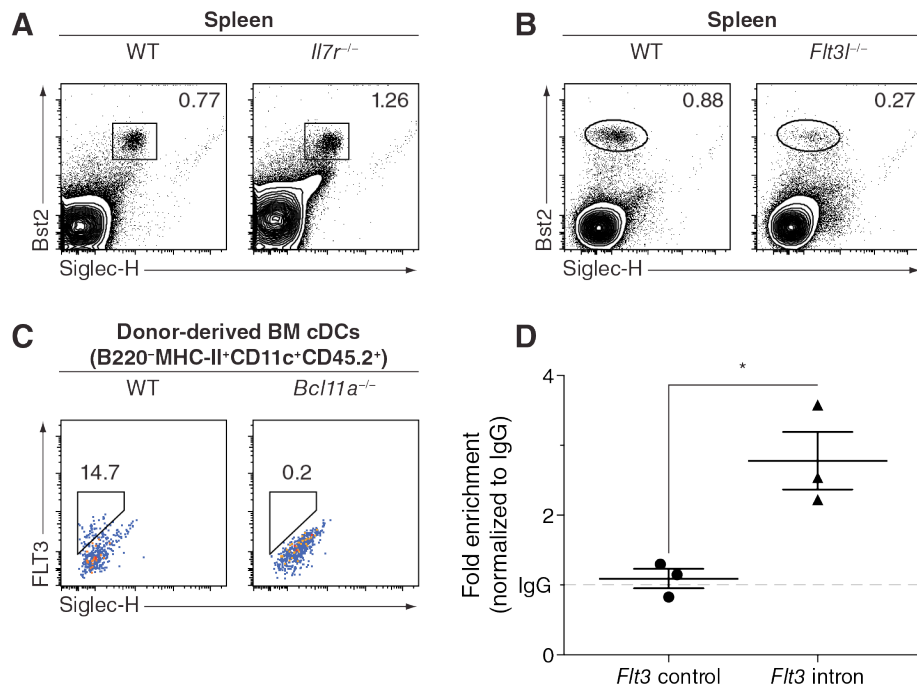


Figure 9: Cytokine signalling in DC development and regulation by Bcl11a

(A) Flow cytometry analysis of pDCs in WT and *Il7r*^{-/-} spleens. Data are representative of four mice per group over two experiments. (B) Flow cytometry analysis of pDCs in WT and *Flt3l*^{-/-} spleens. Data are representative of three mice per group over two experiments. (C) Flow cytometry analysis of donor-derived cDCs in the spleen of WT and *Bcl11a*^{-/-} fetal liver chimeras, analysed by flow cytometry as in Figure 6. Data are representative of three mice per group. (D) Bcl11a binding in the *Flt3* genomic locus assayed by ChIP-qPCR. Data are represented as fold enrichment as compared to isotype control.

Methods

Mice

C57BL/6, B6.SJL, *Il7^{-/-}*, and *Il7r^{-/-}* mice were purchased from The Jackson Laboratory. *Flt3l^{-/-}* and *Rag2^{-/-}* mice were purchased from Taconic Farms. *Flt3l^{-/-}* mice were subsequently crossed to *Zbtb46^{gfp/gfp}* mice generated previously (Satpathy et al., 2012a); F2 offspring were studied, with *Zbtb46^{+/gfp};Flt3l^{+/+}* or *Zbtb46^{gfp/gfp};Flt3l^{+/+}* mice used as WT littermate controls. *Bcl11a^{-/-}* mice were obtained from Dr. Pentao Liu (Liu et al., 2003).

Mice were bred and maintained in a specific pathogen–free animal facility. Mice were euthanized by CO₂ overdose followed by cervical dislocation.

Single-cell suspensions of fetal liver

At embryonic day 14.5, fetal livers were mechanically dissociated with a syringe plunger and sterile 70-µm cell strainer (Fisher) into I10F (Iscove’s modified Dulbecco’s medium + 10% (v/v) fetal bovine serum). For subsequent cell culture or flow cytometry, red blood cells were lysed in ACK lysing buffer before counting by Vi-CELL (Beckman Coulter).

Antibodies

The following antibodies were purchased from BD Biosciences: FITC anti-CD3e (145-2C11), APC anti-CD4 (RM4-5), V450 anti-CD4 (RM4-5), PerCP-Cy5.5 anti-CD8a (53-6.7), PerCP-Cy5.5 anti-CD11b (M1/70), APC anti-CD11c (HL3), APC anti-CD19 (1D3), PE-Cy7 anti-CD24 (M1/69), APC anti-CD25 (PC61), FITC anti-CD45 (30-F11), APC anti-CD45.2 (104), APC-Cy7 anti-CD45.2 (104), PE anti-CD135 (A2F10.1), APC anti-CD172a (P84), FITC anti-B220 (RA3-6B2), V500 anti-B220 (RA3-6B2), PE anti-Gr-1 (RB6-8C5), V450 anti-Gr-1

(RB6-8C5), PerCP-Cy5.5 anti-IgM (R6-60.2), PE-Cy7 anti-Ly-6A/E (Sca-1) (D7), FITC anti-Ly-6C (AL-21), V450 anti-Ly-6C (AL-21), PE anti-Ly-6G (1A8), PE anti-MHC II (I-A/I-E) (M5/114.15.2), PE anti-TCR γ δ (GL3). The following antibodies were purchased from eBioscience: APC-eFluor 780 anti-CD11c (N418), eFluor 450 anti-CD11c (N418), PerCP-Cy5.5 anti-CD16/32 (93), APC-eFluor 780 anti-CD44 (IM7), biotin anti-CD45.1 (A20), PerCP-Cy5.5 anti-CD45.1 (A20), Alexa Fluor 700 anti-CD45.2 (104), PE-Cy7 anti-CD49b (DX5), PE anti-CD103 (2E7), APC-eFluor 780 anti-CD117 (ACK2), PE-Cy7 anti-CD117 (2B8), FITC anti-CD127 (A7R34), APC anti-CD150 (mShad150), eFluor 450 anti-B220 (RA3-6B2), PE-Cy7 anti-B220 (RA3-6B2), APC anti-Bst2 (eBio927), eFluor 450 anti-Bst2 (eBio927), FITC anti-F4/80 (BM8), PE anti-IgD (41239), eFluor 450 anti-MHC-II (I-A/I-E) (M5/114.15.2), eFluor 450 anti-NKp46 (29A1.4), FITC anti-Siglec-H (eBio440C). The following antibodies were purchased from Caltag: FITC anti-CD8a (5H10), PE anti-B220 (RA3-6B2). Qdot 605 streptavidin was purchased from Invitrogen and V500 streptavidin was purchased from BD Biosciences.

Flow cytometry and sorting

Staining was performed at 4 °C in the presence of Fc Block (clone 2.4G2, BD Biosciences or BioXCell) in MACS buffer (Dulbecco's phosphate-buffered saline + 0.5% bovine serum albumin (BSA) + 2 mM ethylenediaminetetraacetic acid (EDTA)). Cells were analysed using a FACSCanto II (BD Biosciences) or sorted using a FACSaria (BD Biosciences); data were visualized using FlowJo software (TreeStar).

Cell cultures

Cells were diluted to 2×10^6 cells/ml in I10F + 20 ng/ml FLT3L or GM-CSF, cultured in 12-well plates for 10 days (FLT3L) or 7 days (GM-CSF), then analysed by flow cytometry.

Chimeras

B6.SJL mice were lethally irradiated (1200 rad) and injected intraorbitally with 4×10^6 fetal liver cells isolated from WT or *Bcl11a*^{-/-} fetuses. After 4 or 6 weeks, BM was isolated by grinding and Histopaque-1119 (Sigma-Aldrich) centrifugation and either sorted by flow cytometry or cultured. From these mice, thymi were minced and digested in 250 µg/ml collagenase B (Roche) and 30 U/ml DNase I (Sigma-Aldrich) and analysed by flow cytometry.

Microarray analysis

MPP and GMP populations were sorted from fetal liver chimeras and pooled by donor genotype. RNA was isolated using an RNAAqueous-Micro Kit (Ambion) and submitted for amplification, labelling and hybridization. Expression values were analysed after RMA quantile normalization using ArrayStar software (DNASTAR). Data were deposited in the Gene Expression Omnibus repository under accession number GSE46270.

ChIP-qPCR

Pro-B cell cultures were established using *Rag2*^{-/-} BM isolated by flushing and resuspended in I10F + 5 ng/ml IL-7. Chromatin was prepared from 1×10^7 cultured pro-B cells sonicated using a Bioruptor (Diagenode), immunoprecipitation was performed with a rabbit polyclonal anti-Bcl11a antibody (NB600-261, Novus Biologicals) or control rabbit IgG, and qPCR analysis was carried out using SYBR Green-based detection and the following previously

published primers (Carotta et al., 2010): *Flt3* control forward, 5'-TTTGCACTCGTAGCAAATGG-3'; *Flt3* control reverse, 5'-GTTCAAGCTGCCAAAGAGAGG-3'; *Flt3* promoter forward, 5'-GTTCAAGCTGCCAAAGAGAGG-3'; *Flt3* promoter reverse, 5'-CGTCACTGACCACAGATTCC-3'; *Flt3* intron forward, 5'-AAAAGAGGAACATTGGTATTCG-3'; *Flt3* intron reverse, 5'-TGACAGTAGTGAAACACACACACA-3'.

Statistics

Statistical differences were identified using Prism 6 (GraphPad) by multiple unpaired Student's *t* tests, controlling the false discovery rate (Q) by the method of Benjamini and Hochberg. *, Q=0.05; **, Q=0.01.

CHAPTER 3: *Zeb2* IS REQUIRED FOR
PLASMACYTOID DENDRITIC CELL AND MONOCYTE DEVELOPMENT

This work was performed in collaboration with Carlos G. Briseño, Gary E. Grajales-Reyes, Malay Haldar, Arifumi Iwata, Nicole M. Kretzer, Wumesh KC, Roxane Tussiwand, Yuijiro Higashi, Theresa L. Murphy, and Kenneth M. Murphy. Personal contributions included the initial conception of the project, the design and carrying out of experiments; data analysis; and writing of the paper.

Zeb2 (Sip1, Zfhx1b) is a transcription factor first identified by its interaction with activated members of the SMAD family of signal transducers (Verschueren et al., 1999). The protein contains an N-terminal cluster and a C-terminal cluster of zinc finger domains, a centrally located homeodomain, a SMAD-binding domain, and a C-terminal-binding protein (CtBP)-interaction domain (Vandewalle et al., 2009). It exerts multiple actions during epithelial–mesenchymal transition, including downregulation of E-cadherin and other components of cell junctions (Comijn et al., 2001; Vandewalle et al., 2005). Loss of Zeb2 is associated with severe defects during mouse embryogenesis that culminate in embryonic lethality (Higashi et al., 2002; Van de Putte et al., 2003). In humans, heterozygous defects in this protein are associated with Hirschprung’s disease and with Mowat–Wilson syndrome, and dysregulated expression is found in several types of human cancer (Vandewalle et al., 2009).

Zeb2 controls myelination in the central nervous system by modulating the activity of SMAD proteins activated by bone morphogenetic proteins (BMPs), members of the transforming growth factor (TGF)- β superfamily (Weng et al., 2012). In the oligodendrocyte precursor cell, which expresses low amounts of Zeb2, activated SMAD proteins bind the coactivator histone acetyltransferase p300 to activate negative regulatory genes such as *Id2* and *Hes1*; in the differentiating oligodendrocyte, oligodendrocyte transcription factor 1 (Olig1) and oligodendrocyte transcription factor 2 (Olig2) upregulate expression of Zeb2, which then binds SMAD-p300 complexes to antagonize activity at the *Id2* and *Hes1* loci and which also promotes expression of the inhibitory SMAD family member SMAD7 (Weng et al., 2012).

In the hematopoietic system, Zeb2 is required for terminal maturation of natural killer (NK) cells and for terminal differentiation of CD8 $^{+}$ T cells (Dominguez et al., 2015; Omilusik et al., 2015; van Helden et al., 2015). Previously, we and others identified Zeb2 as a transcription factor downregulated during commitment to the CD8 $^{+}$ /CD103 $^{+}$ cDC lineage in the BM (Grajales-Reyes et al., 2015; Schlitzer et al., 2015). *Zeb2* transcript is found in the CDP and maintained in CD4 $^{+}$ /CD11b $^{+}$ cDCs and in pDCs; however, it is substantially downregulated in CD8 $^{+}$ /CD103 $^{+}$ cDCs (Miller et al., 2012). It is also known that *Id2* expression is induced by TGF- β and is required for the development of CD8 $^{+}$ /CD103 $^{+}$ cDCs (Ginhoux et al., 2009; Hacker et al., 2003) and that the ratio between ID-2 and its target E2-2 determines the balance between CD8 $^{+}$ /CD103 $^{+}$ cDC development and pDC development (Cisse et al., 2008; Ghosh et al., 2014; Ghosh et al., 2010). Moreover, administration of exogenous TGF- β to BM progenitors accelerates their differentiation to cDCs rather than pDCs (Felker et al., 2010).

Mice selectively lacking Zeb2 in CD11c⁺ cells show modest but often statistically significant defects in pDC and CD4⁺/CD11b⁺ cDC development; those results have been interpreted as evidence that Zeb2 must regulate commitment to both of those lineages (Scott et al., 2016). However, upregulation of CD11c during development of cDCs occurs in tandem with lineage specification (Grajales-Reyes et al., 2015). Consequently, earlier and more robust models of inducible deletion are necessary to address whether Zeb2 mediates lineage diversification. In this study, we confirmed that Zeb2 regulated expression of *Id2* in DCs and that it was required for the development of pDCs. However, synchronized deletion of Zeb2 at early progenitor stages produced modest perturbations in CD4⁺/CD11b⁺ cDC development. Thus, we demonstrate a stringent requirement for Zeb2 during pDC development not shared by CD4⁺/CD11b⁺ cDCs. Furthermore, we found that loss of Zeb2 impaired both expression of M-CSFR and development of Ly-6C^{hi} monocytes, implicating Zeb2 activity in the diversification of multiple hematopoietic lineages.

Results

We generated mice in which Zeb2 is conditionally deleted in cells expressing Cre recombinase driven by the *Itgax* promoter (CD11c-Cre) (Caton et al., 2007). Comparing Zeb2-sufficient (*Zeb2*^{f/f}) mice to CD11c-Cre–driven Zeb2-deficient (*Zeb2*^{fl/fl};CD11c-Cre(tg)) mice, pDC frequency was substantially decreased in the spleen and skin-draining LN, but not in the BM, of CD11c-Cre–driven Zeb2-deficient mice (Figure 10A). Within the cDC compartment, Zeb2-deficient mice showed an increased ratio of CD24⁺ : Sirp- α ⁺ cDCs in the spleen and an increased ratio of equivalent cell types in other organs examined (Figure 10B, C and data not

shown). Using an inducible model of Zeb2 deficiency driven by the type I interferon–inducible *Mx1*-Cre, we observed nearly complete ablation of pDCs *in vivo* 7–9 days after two administrations of poly(I:C) (Figure 10D). That phenotype persisted at least one year after induction of Zeb2 deletion (Figure 10E). By contrast, the ratio of CD24⁺ : Sirp- α ⁺ cDCs was perturbed only slightly in that system (Figure 10F).

Next, we mixed CD45.1⁺ CD45.2⁺ *Zeb2*^{+/−} BM cells with CD45.1⁺ CD45.2[−] WT BM cells and cultured them *in vitro* in the presence of FLT3L. In that setting, we observed that Zeb2 haploinsufficiency produced a partial defect in the development of pDCs, while we observed no defect in Sirp- α ⁺ DC development from Zeb2-haploinsufficient BM (Figure 11A). To study Zeb2 deficiency *in vitro* without the confounding effects of type I interferon, we used a second inducible model of Zeb2 deficiency driven by the 4-hydroxytamoxifen (4-OHT)–inducible *Gt(ROSA)26Sor-Cre-ER*^{T2} (*R26-iCre*). Administration of 4-OHT almost completely eliminated pDCs in cultures of *Zeb2*^{fl/fl}; *R26*^{iCre/iCre} BM, whereas the same conditions did not perturb pDC development in cultures of WT BM (Figure 11B). Since multiple cell types are found in BM, we depleted CD19⁺ B cells and Ly-6G⁺ neutrophils and sorted a population of Kit^{hi} FLT3⁺ progenitors to culture in the presence of FLT3L and 4-OHT. We mixed CD45.2⁺ *Zeb2*^{fl/fl}; *R26*^{iCre/iCre} cells with congenically marked CD45.1⁺ Zeb2-sufficient cells (B6.SJL) and observed that Zeb2-deficient cells could not support substantial pDC development; by contrast, CD24⁺ cDCs and Sirp- α ⁺ cDCs developed from both the Zeb2-sufficient and Zeb2-deficient fractions (Figure 11C).

Despite conflicting reports (Swiecki et al., 2011), some evidence exists to suggest that type I interferon may promote pDC development (Chen et al., 2013; Li et al., 2011). Thus, we cultured Zeb2-sufficient CD19⁻ Ly-6G⁻ Kit^{hi} FLT3⁺ progenitors *in vitro* in the presence of FLT3L and in the presence or absence of interferon- α . We observed a strong skewing away from CD24⁺ cDC development and towards pDC development (Figure 12A). In parallel, we cultured *Zeb2*^{fl/fl}; *Mx1*-Cre(tg) progenitors under the same conditions; in those cultures, administration of interferon- α (and therefore conditional deletion of Zeb2) instead skewed almost completely towards CD24⁺ cDC development (Figure 12A). Finally, we mixed sorted Zeb2-sufficient and *Zeb2*^{fl/fl}; *Mx1*-Cre(tg) progenitors. We observed that Zeb2-sufficient cells made up the entire complement of pDCs and the majority of Sirp- α ⁺ cDCs, while Zeb2-deficient cells were predominant among CD24⁺ cDCs (Figure 12B).

Because splenic Sirp- α ⁺ cDCs were not eliminated in Zeb2-deficient mice and maintain expression of *Zeb2* transcript in WT mice, we examined targets of Zeb2 regulated during DC development by gene expression microarray analysis of WT and CD11c-Cre–driven Zeb2-deficient splenic Sirp- α ⁺ cDCs (Figure 13). In that assay, fewer than ten genes showed more than a threefold change between groups; among those were *Itgad* (encoding CD11d and part of the CD11c-Cre transgenic integration (Caton et al., 2007)) and *Ms4a1* (encoding CD20) (Figure 13A). However, expression of *Lyz2* (encoding lysozyme) and *Csf1r* (encoding M-CSFR) was more than halved in Zeb2-deficient Sirp- α ⁺ cDCs as compared to WT (Figure 13A, B). Of transcription factor–encoding genes, *Irf7*, *Ifi203*, and *Id2* were each increased in expression less than twofold in Zeb2-deficient Sirp- α ⁺ cDCs as compared to WT (Figure 13C).

Again using WT and CD11c-Cre–driven Zeb2-deficient Sirp- α^+ cDCs, we confirmed that *Id2* expression nearly doubled in the latter population as compared to the former by two-step reverse transcription (RT)-qPCR (Figure 13D). Published results using a commercially available polyclonal anti-Zeb2 antibody show Zeb2 binding to the *Id2* promoter by ChIP-qPCR (Weng et al., 2012). We attempted to reproduce that finding; our initial results were consistent with published results (Figure 13E), but subsequent replicate experiments did not reliably yield the same observation (data not shown).

We noted that expression of *Ifi203* was altered in Zeb2-deficient Sirp- α^+ cDCs as compared to WT (Figure 13C). Because the paralogous gene *Ifi204* encodes a protein known to antagonize the function of ID-2 by cytoplasmic translocation (Liu et al., 2005; Luan et al., 2008), we overexpressed either Ifi-204 or Ifi-203 in BM cultured in the presence of FLT3L. However, we observed no substantial change in the frequency of pDCs upon such overexpression (Figure 14A and data not shown). Finally, because Zeb2 promotes transcription of *Smad7* in the central nervous system (Weng et al., 2012), we overexpressed SMAD7 in BM cultured in the presence of FLT3L. Again, however, we observed no substantial change in the relative frequency of DC subsets (Figure 14B).

In the *Mx1*-Cre–driven model of Zeb2 deficiency, we observed substantial perturbations in other myeloid lineages. In the blood, administration of poly(I:C) to induce *Mx1*-Cre activity resulted in acute loss of Ly-6C^{hi} monocytes in both *Zeb2^{f/f};Mx1-Cre(tg)* mice and in *Zeb2^{f/f}* control mice; these monocytes were replenished within three days in control mice but not in Zeb2-deficient mice (Figure 15A). Similar defects in monocyte frequency were

observed in the BM and spleen one week after two administrations of poly(I:C) (Figure 15B). One year after induction of Zeb2 deletion, Ly-6C^{hi} monocytes continued to be deficient in the blood of Zeb2-deficient mice (Figure 15C). We also noted that surface expression of M-CSFR was almost completely abolished in the BM of *Mx1*-Cre–driven Zeb2-deficient mice one week after two administrations of poly(I:C); by contrast, the frequency of GMPs was not decreased in the BM of *Mx1*-Cre–driven Zeb2-deficient mice as compared to Zeb2-sufficient control mice (Figure 15D).

To determine if commitment to the monocyte lineage was impaired by loss of Zeb2, we used gene expression microarrays to compare neutrophils and Ly-6C^{hi} monocytes sorted from *Zeb2*^{fl/fl} control mice to neutrophils and residual Ly-6C^{hi} monocytes sorted from poly(I:C)-treated *Zeb2*^{fl/fl}; *Mx1*-Cre(tg) mice. Zeb2-deficient neutrophils were not distinguishable from their Zeb2-sufficient counterparts on the basis of this assay; Ly-6C^{hi} monocytes from Zeb2-deficient mice also resembled their Zeb2-sufficient counterparts but showed increased expression of some genes characteristic of neutrophils (Figure 16A, B). Those genes included *Ltf* (encoding lactotransferrin), *Mmp9* (encoding matrix metallopeptidase 9) and *Camp* (encoding cathelicidin antimicrobial peptide). Zeb2-deficient Ly-6C^{hi} monocytes also showed increased expression of genes characteristic of the GMP (Paul et al., 2015) not highly expressed in neutrophils, such as *Mpo* (encoding myeloperoxidase), *Elane* (encoding neutrophil-expressed elastase; the transcript is not highly expressed in neutrophils), and *Prtn3* (encoding proteinase 3) (Figure 16C, D).

Among transcription factor–encoding genes, *Id2*, *Myc*, and *Cdk6* each doubled or nearly doubled in expression in Zeb2-deficient Ly-6C^{hi} monocytes as compared to their Zeb2-sufficient counterparts, whereas those genes were not more highly expressed in neutrophils as compared to Ly-6C^{hi} monocytes (Figure 16E). Other transcription factor–encoding genes such as *Cebpe* and *Zeb1* also showed higher expression in Zeb2-deficient Ly-6C^{hi} monocytes as compared to Zeb2-sufficient counterparts, but those genes were also more highly expressed in neutrophils than in Zeb2-sufficient Ly-6C^{hi} monocytes. Several transcription factor–encoding genes were expressed less abundantly in Zeb2-deficient Ly-6C^{hi} monocytes than in Zeb2-sufficient Ly-6C^{hi} monocytes, including *Tcf4* (encoding E2-2), *Prdm1* (also known as *Blimp1*), *Klf4* (a target of *Irf8* essential for monocyte development (Alder et al., 2008; Feinberg et al., 2007; Kurotaki et al., 2013)), *Jun*, *Irf4*, *Fosb*, and *Atf3* (Figure 16F).

Discussion

Comparisons of gene expression among hematopoietic lineages first showed that *Zeb2* expression is abrogated in CD8⁺/CD103⁺ cDCs but not in other DCs (Miller et al., 2012). We hypothesized, therefore, that Zeb2 represses commitment to the CD8⁺/CD103⁺ cDC lineage in favour of alternative cell fates. In this study, we used multiple models of gene deletion to provide the first full account of DCs that develop in the absence of that transcription factor. We observed that early deletion of Zeb2 nearly eliminated all pDCs and that *in vitro* overexpression of the protein substantially increased pDC frequency. Taken together, the evidence suggests that Zeb2 activity promotes commitment not to the CD4⁺/CD11b⁺ cDC lineage but to the pDC lineage.

Our results suggest that the role of Zeb2 during pDC development is cell-intrinsic and dose-dependent. Using inducible models of gene deletion, however, we expected that cells escaping deletion would preferentially repopulate niches vacated by Zeb2-deficient hematopoietic progenitors. Instead, loss of pDCs proved to be a durable phenotype in *Zeb2^{fl/fl};Mx1-Cre(tg)* mice, suggesting that progenitors depleted of Zeb2 may be long-lived, as their WT counterparts are known to be (Sun et al., 2014).

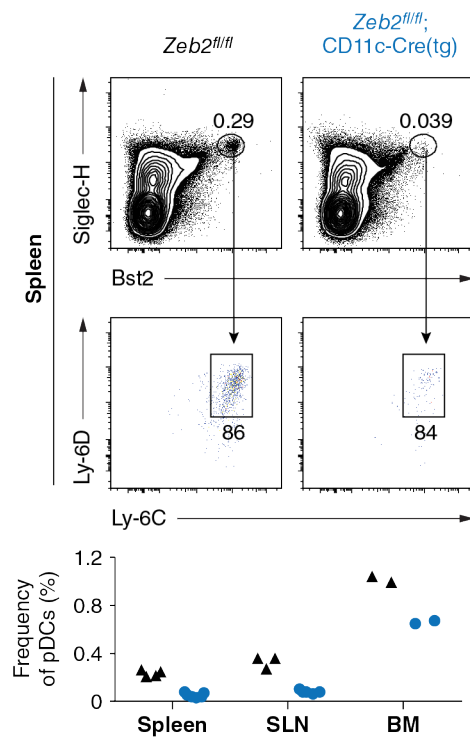
Addition of type I interferon substantially increased the pDC output of WT Kit^{hi} progenitors *in vitro*. This observation raises the possibility that a developmental feed-forward loop could promote pDC development in the context of viral infection; such a mechanism would potentiate the well-studied molecular feed-forward loop that promotes type I interferon production (Hall and Rosen, 2010; Sato et al., 1998). Meanwhile, addition of type I interferon severely perturbed the DC output of Zeb2-deficient Kit^{hi} progenitors *in vitro* in a different manner. In that setting, no pDCs were recovered, while Sirp- α^+ cDC frequency was also diminished as nearly all progeny of Zeb2-deficient Kit^{hi} progenitors appeared to be diverted to the CD24⁺ cDC fate. That result could not be explained as an artefact of disproportionately greater lethality in other subsets, since mixed cultures revealed Zeb2-deficient progenitors to be greatly outcompeting their WT counterparts in giving rise to CD24⁺ cDCs. Thus, pDC development requires Zeb2 in a cell-intrinsic manner not compensated by type I interferon signalling; instead, Zeb2 has an essential role in suppressing overwhelming diversion to the CD24⁺ cDC lineage under such inflammatory conditions.

We found—as have others (Scott et al., 2016; Weng et al., 2012)—that Zeb2 negatively regulates expression of *Id2*. Indeed, the decreased frequency of pDCs and increased frequency of CD8⁺/CD103⁺ cDCs observed in Zeb2-deficient mice is consistent with a decreased frequency of pDCs observed upon ectopic overexpression of ID-2 (Spits et al., 2000) and a decreased frequency of CD8⁺/CD103⁺ cDCs observed in ID-2-deficient mice (Hacker et al., 2003). Furthermore, we found that CD4⁺/CD11b⁺ cDCs continued to develop in the absence of Zeb2 *in vitro* and *in vivo*, consistent with observations that ID-2 regulates the balance between CD8⁺/CD103⁺ cDCs and pDCs (Cisse et al., 2008; Ghosh et al., 2014; Ghosh et al., 2010). It is worth clarifying that descriptions about inhibition of ‘pre-DC2’ development upon overexpression of ID-2 (Spits et al., 2000) make use of an alternative name for pDCs (Reizis et al., 2011a) and do not refer to the committed progenitor of CD4⁺/CD11b⁺ cDCs (Grajales-Reyes et al., 2015; Schlitzer et al., 2015), which now bear the moniker of ‘cDC2s’ (Guilliams et al., 2014).

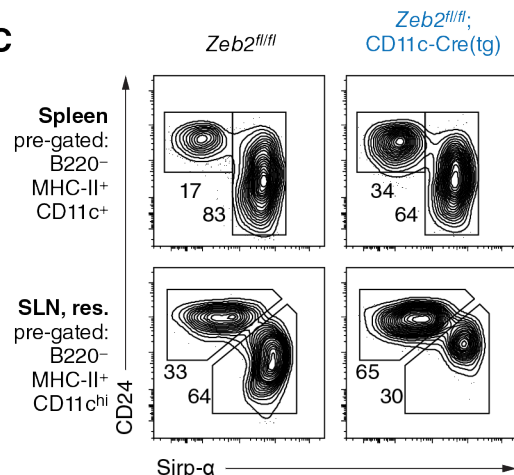
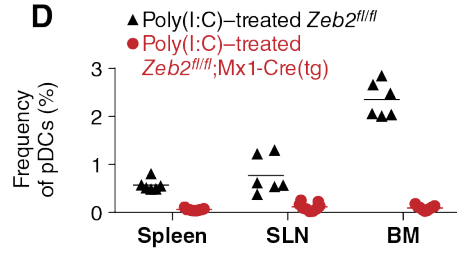
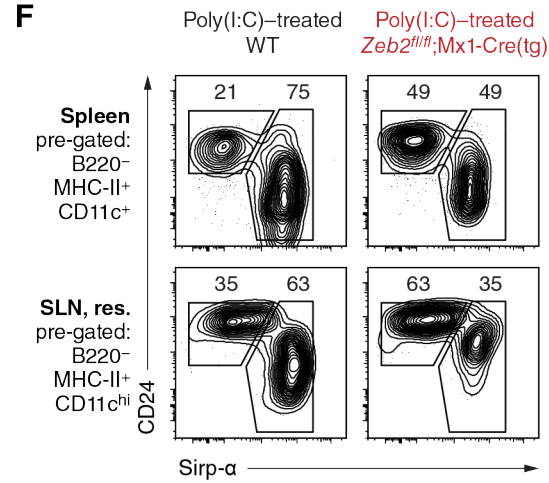
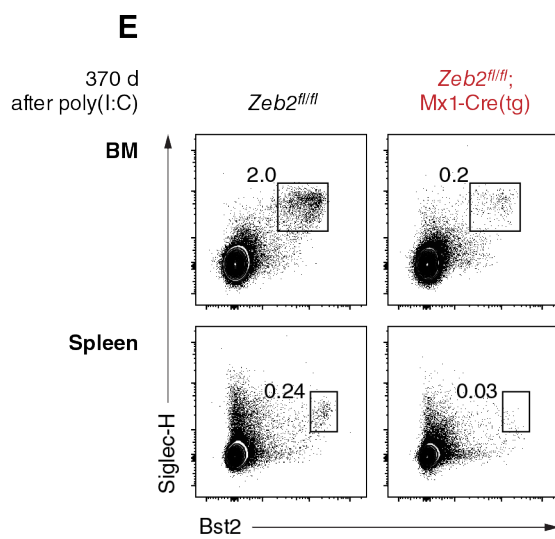
ID-2 can also repress PU.1-mediated induction of *Csf1r* in a dose-dependent manner (Ji et al., 2008), and it is well established that M-CSFR-deficient *op/op* mice show a severely decreased abundance of blood monocytes (Wiktor-Jedrzejczak et al., 1982). Thus, we hypothesized that inducible deletion of Zeb2 would produce a defect in monocyte development. We found exactly such a phenotype in the blood and in other tissues, along with near-total ablation of M-CSFR expression in the BM. Moreover, loss of monocyte development persisted for at least one year after deletion was induced.

Compared to their WT counterparts, Zeb2-deficient Ly-6C^{hi} blood monocytes upregulated *Id2* and characteristic neutrophil genes, although we cannot exclude the possibility that the latter observation might arise from an increased proportion of contaminating neutrophils. However, we also observed aberrantly upregulated expression of genes characteristic of the GMP not highly expressed in neutrophils. These data support the interpretation that Zeb2 deficiency in the GMP results in failed commitment to the monocyte lineage with aberrant maintenance of progenitor gene expression modules and upregulation of neutrophil gene expression modules.

Inducible models of gene deletion make possible an examination of defects that arise from the early and robust loss of Zeb2 during hematopoiesis. We observed that *Id2* mRNA expression was upregulated both in Zeb2-deficient Sirp- α^+ cDCs and in residual Zeb2-deficient Ly-6C^{hi} monocytes as compared to their WT counterparts. These findings suggest that Zeb2 activity may engage similar mechanisms to suppress alternative fates in multiple developing lineages. As lymphoid progenitors not presented here are also known to express Zeb2, those cells and their progeny represent further avenues to explore whether the activities of that transcription factor are similarly required for development of other immune lineages.

A**B**

	<i>Zeb2^{fl/fl}</i>	<i>Zeb2^{fl/fl}; CD11c-Cre(tg)</i>
Spleen	1.28 ± 0.20 [n = 4]	1.33 ± 0.32 [n = 6]
SLN, res.	0.33 ± 0.10 [n = 3]	0.29 ± 0.08 [n = 5]

C**D****E****Figure 10: Zeb2 is required for pDC development *in vivo***

← Continued from previous page

(A) Samples prepared from the spleen, skin-draining LN (SLN), and BM, harvested from mice of the indicated genotypes, are compared for frequency of pDCs. Shown are representative two-colour histograms comparing splenic populations (top) and a plot displaying frequency of pDCs as a proportion of all singlet lymphocytes (bottom). Numbers at top indicate percentage of cells within the indicated gate; dots at bottom each represent a distinct biological replicate and are representative of multiple independent experiments. (B, C) Samples prepared in (A) are compared for frequency of cDCs as a proportion of all singlet lymphocytes (B) and for frequency of CD24⁺ cDCs and Sirp- α ⁺ cDCs as a proportion of cDCs (C). Shown is a table (B) and representative two-colour histograms (C). Numbers in (C) indicate percentage of cells within the indicated gate. (D) Samples prepared from the indicated organs, harvested from mice of the indicated genotypes 7–9 days after administration of poly(I:C), are compared for frequency of pDCs. Shown is a plot displaying frequency of pDCs as a proportion of all singlet lymphocytes. Dots each represent a distinct biological replicate and are representative of multiple independent experiments. (E) Samples prepared from the indicated organs, harvested from mice of the indicated genotypes one year after administration of poly(I:C), are compared for frequency of pDCs. Shown are representative two-colour histograms ($n = 3$ mice per group pooled over two independent, consecutive experiments). Numbers indicate percentage of cells within the indicated gate. (F) Samples prepared in (D) are compared for frequency of cDCs as in (C). Res., resident.

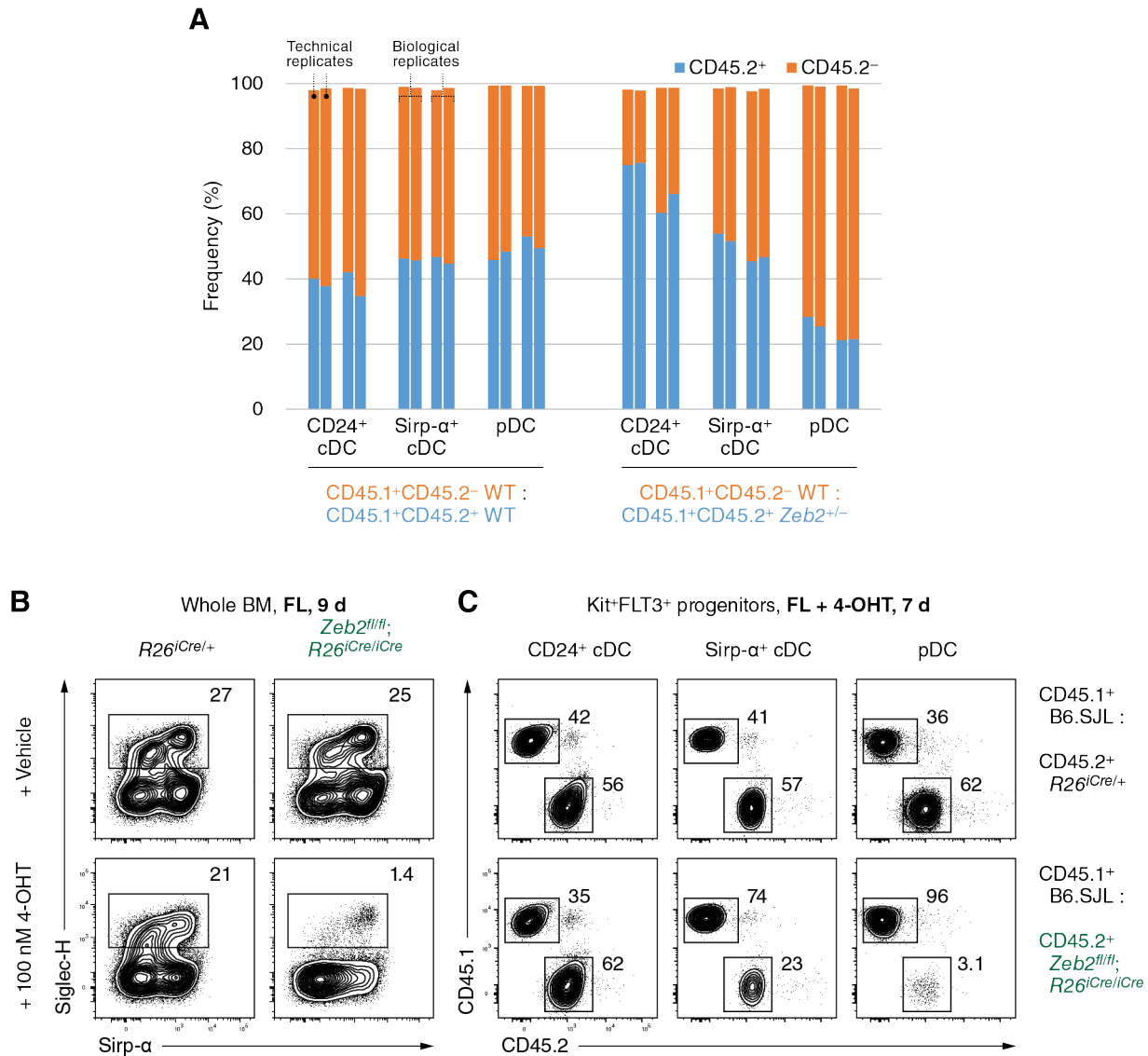


Figure 11: Plasmacytoid DCs require Zeb2 in a dose-dependent and cell-intrinsic manner

(A) Single-cell suspensions of whole BM isolated from WT or *Zeb2*^{+/-} mice were mixed with congenically marked (CD45.1⁺ CD45.2⁻) single-cell suspensions of whole BM isolated from WT B6.SJL mice and cultured in the presence of FLT3L. Shown is the proportion of cells expressing CD45.2 (blue) or not expressing CD45.2 (orange) among progeny within the indicated subsets. (B) Single-cell suspensions of whole BM isolated from mice of the indicated genotypes were cultured in the presence of FLT3L (FL) and either 100 nM 4-OHT dissolved in ethanol or ethanol alone (vehicle). Shown are representative two-colour histograms comparing proportion of Siglec-H⁺ pDCs among progeny after 9 days of culture ($n > 2$ biological replicates per group over at least two independent experiments). (C) BM Kit^{hi} FLT3⁺ progenitors isolated from *R26^{iCre/+}* mice or *Zeb2*^{fl/fl}; *R26^{iCre/iCre}* mice were mixed with congenically marked (CD45.1⁺) BM Kit^{hi} FLT3⁺ progenitors isolated from WT B6.SJL mice and cultured in the presence of FLT3L and 4-OHT. Shown are two-colour histograms comparing the proportion of cells within the indicated subsets expressing CD45.1 or CD45.2.

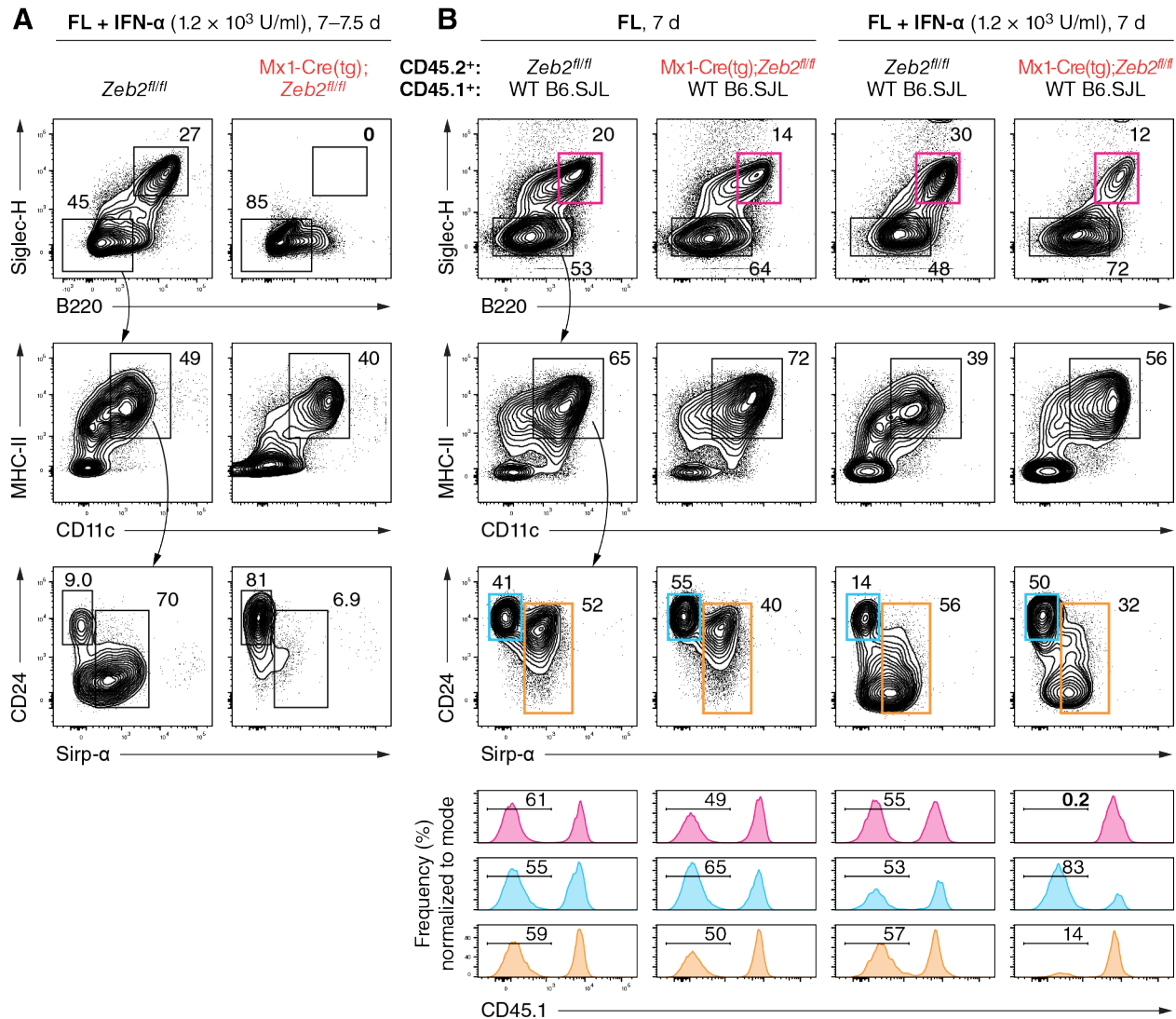


Figure 12: Type I interferon diverts Zeb2-deficient progenitors to the CD24 $^+$ cDC lineage

(A) BM Kit $^{\text{hi}}$ FLT3 $^+$ progenitors isolated from mice of the indicated genotypes were cultured in the presence of FLT3L (FL) and interferon- α (IFN- α). Shown are representative two-colour histograms comparing their progeny as analysed after 7–7.5 days of culture ($n \geq 3$ biological replicates per group over two independent experiments). (B) BM Kit $^{\text{hi}}$ FLT3 $^+$ progenitors isolated as in (A) were mixed with congenically marked (CD45.1 $^+$) BM Kit $^{\text{hi}}$ FLT3 $^+$ progenitors isolated from WT B6.SJL mice and cultured as in (A). Shown are representative two-colour histograms comparing their progeny as analysed after 7 days of culture (top), and one-colour histograms indicating the proportion of pDCs (magenta), CD24 $^+$ cDCs (cyan), and Sirp- α^+ cDCs (orange) lacking expression of CD45.1 ($n \geq 3$ biological replicates per group over two independent experiments). In all panels, numbers indicate percentage of cells within the indicated gate.

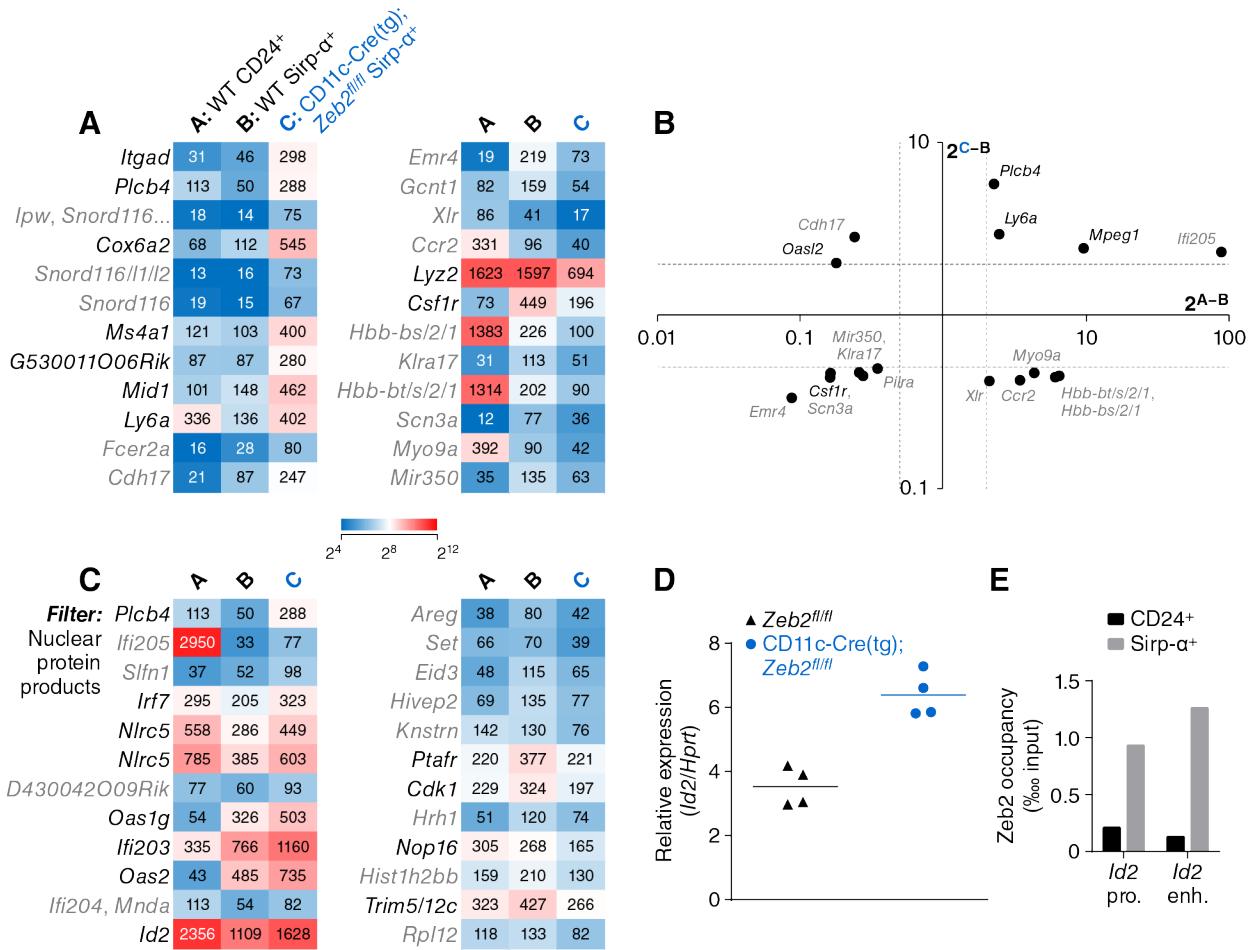


Figure 13: Zeb2-deficient Sirp- α^+ cDCs express more abundant *Id2* mRNA

(A) Heat maps showing relative expression in the indicated populations as determined by gene expression microarray analysis for probe sets with the greatest increase (left) or decrease (right) in expression in Zeb2-deficient Sirp- α^+ cDCs as compared to WT Sirp- α^+ cDCs. (B) Scatterplot comparing changes in gene expression between Zeb2-deficient Sirp- α^+ cDCs and WT Sirp- α^+ cDCs (*y*-axis) to changes in gene expression between WT CD24⁺ cDCs and WT Sirp- α^+ cDCs (*x*-axis). Note that both axes are logarithmic and that probe sets with less than twofold changes in expression along either dimension (dotted lines) are omitted for clarity. (C) Heat maps as in (A) filtered for probe sets assigned to genes encoding nuclear protein products with the greatest increase (left) or decrease (right) in expression in Zeb2-deficient Sirp- α^+ cDCs as compared to WT Sirp- α^+ cDCs. In (A) and (C), gene symbols in grey correspond to probe sets showing scant expression in Zeb2-deficient Sirp- α^+ cDCs (left) or WT Sirp- α^+ cDCs (right). (D) Plot showing relative expression of *Id2* mRNA normalized to *Hprt* mRNA in Sirp- α^+ cDCs isolated from mice of the indicated genotypes as determined by RT-qPCR; each dot represents a biological replicate averaged from technical replicates. (E) Zeb2 occupancy at an *Id2* promoter element (pro.) and *Id2* enhancer element (enh.) assayed by ChIP-qPCR in WT cDCs of the indicated subset. Shown is one replicate not consistently reproduced.

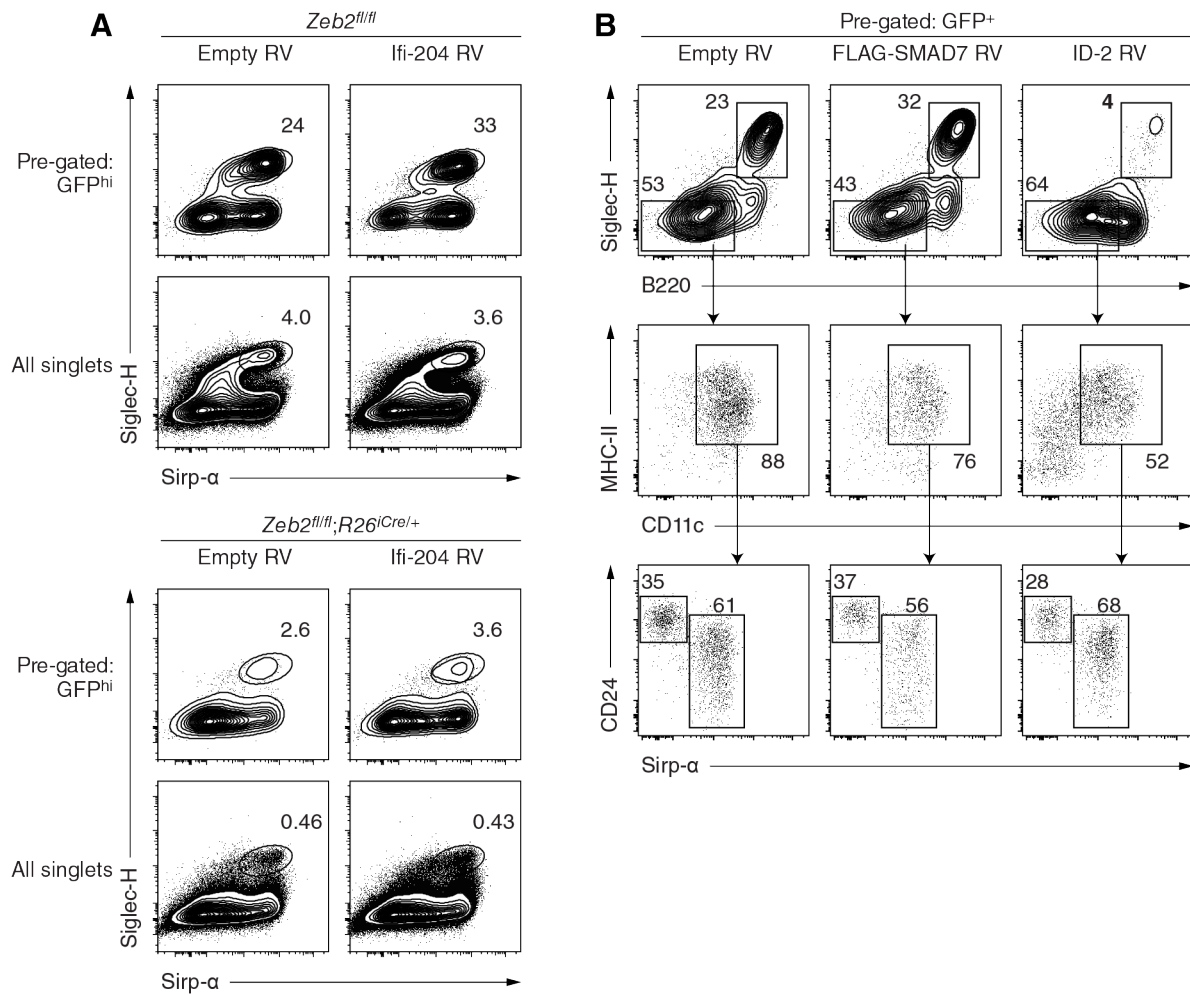


Figure 14: Overexpression of Ifi-204 or SMAD7 does not promote development of pDCs

(A) Single-cell suspensions of whole BM isolated from mice of the indicated genotypes were cultured in the presence of FLT3L and 4-OHT, then retrovirally transduced 2–3 days later to overexpress GFP alone (Empty RV) or Ifi-204 and GFP (Ifi-204 RV). Shown are two-colour histograms comparing pDC frequency among transduced (GFP^{hi}) cells or all cells six days after transduction. (B) Single-cell suspensions of Zeb2-sufficient BM were cultured in the presence of FLT3L, then retrovirally transduced two days later to overexpress GFP alone (Empty RV), N-terminally FLAG-tagged SMAD7 and GFP (FLAG-SMAD7 RV), or ID-2 and GFP (ID-2 RV). Shown are two-colour histograms comparing pDC and cDC frequency among transduced (GFP⁺) cells six days after transduction.

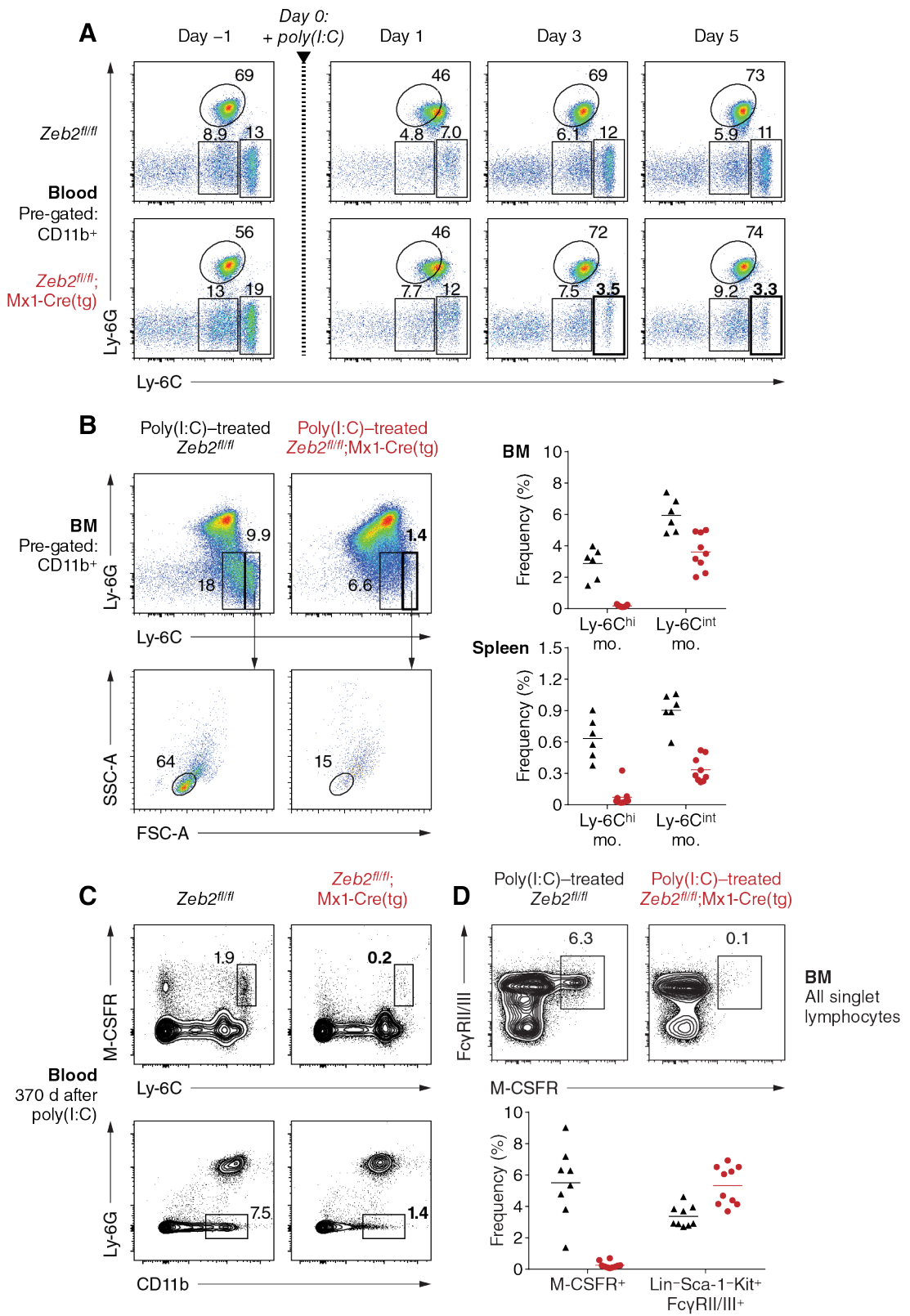


Figure 15: Zeb2 is required for monocyte development *in vivo*

← *Continued from previous page*

(A) Blood from *Zeb2*^{fl/fl} and *Zeb2*^{fl/fl}; *Mx1-Cre*(tg) mice are compared for neutrophil and monocyte frequency before and after administration of poly(I:C). Shown are two-colour histograms analysed on the indicated days. Numbers indicate percentage of cells within the indicated gate. (B) BM and spleen from poly(I:C)-treated mice of the indicated genotypes are compared for monocyte (mo.) frequency 7–9 days after treatment. Shown are two-colour histograms for representative BM samples (left) and plots displaying frequency of the indicated subsets as a proportion of all singlet lymphocytes (right). Numbers at left indicate percentage of cells within the indicated gate; dots at right each represent a distinct biological replicate and are pooled from independent experiments. (C) Blood from poly(I:C)-treated mice of the indicated genotypes are compared using two gating schemes for monocyte frequency one year after administration of poly(I:C). Shown are representative two-colour histograms ($n = 3$ mice per group pooled over two independent, consecutive experiments). Numbers indicate percentage of cells within the indicated gate. (D) BM from poly(I:C)-treated mice are compared for M-CSFR expression and frequency of GMPs (identified as Lin⁻ Sca-1⁻ Kit⁺ FcγRII/III⁺) 7–9 days after treatment. Shown are representative two-colour histograms (top) and a plot displaying frequency of cells identified by the indicated surface markers as a proportion of all singlet lymphocytes (bottom). Numbers at top indicate percentage of cells within the indicated gate; dots at bottom each represent a distinct biological replicate and are pooled from independent experiments.

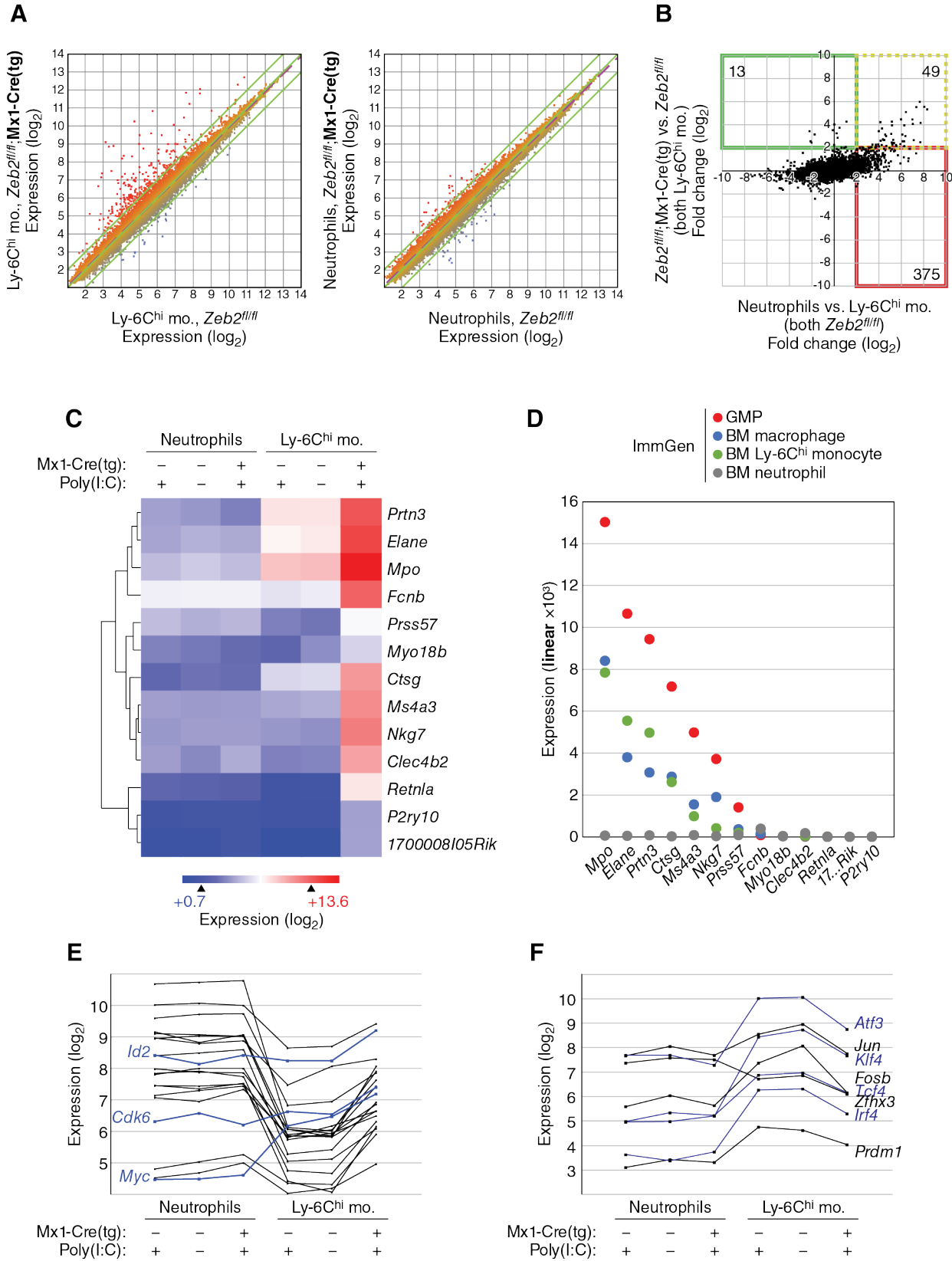


Figure 16: Zeb2-deficient Ly-6 Chi monocytes express neutrophil-associated genes

← *Continued from previous page*

(A) Scatterplots showing global gene expression in Ly-6C^{hi} monocytes (mo.) and neutrophils isolated from poly(I:C)-treated mice of the indicated genotypes. (B) Scatterplot comparing changes in gene expression between Zeb2-deficient Ly-6C^{hi} monocytes and Zeb2-sufficient Ly-6C^{hi} monocytes (*y*-axis) to changes in gene expression between Zeb2-sufficient neutrophils and Zeb2-sufficient Ly-6C^{hi} monocytes (*x*-axis). As compared to their expression in Zeb2-sufficient monocytes, some probe sets are more abundantly expressed in Zeb2-deficient monocytes but not in Zeb2-sufficient neutrophils (solid green), more abundantly expressed in Zeb2-sufficient neutrophils but not in Zeb2-deficient monocytes (solid red), or more abundantly expressed both in Zeb2-deficient monocytes and in Zeb2-sufficient neutrophils (dashed yellow). Numbers in each outlined region indicate absolute probe set count. (C) Heat map showing relative expression of 13 probe sets outlined in (B) (solid green) among the indicated populations. (D) Relative expression of 13 probe sets shown in (C) among the indicated populations in the BM (data from ImmGen). (E, F) Sparklines showing relative expression of transcription factor-encoding genes more (E) or less (F) abundantly expressed in Zeb2-deficient Ly-6C^{hi} monocytes than in Zeb2-sufficient Ly-6C^{hi} monocytes. In all panels, shown are averages of two biological replicates in each group, excepting single-replicate untreated *Zeb2*^{fl/fl} samples.

Methods

Mice

Mice carrying the conditional *Zeb2*^{fl} (B6;129(Cg)-*Zfhx1b*^{tm1.1Yhi}) allele (Higashi et al., 2002) were derived from biological material provided by the RIKEN BioResource Center through the National BioResource Project of the Ministry of Education, Culture, Sports, Science and Technology (MEXT), Japan.

B6.SJL (B6.SJL-*Ptprc*^a *Pepc*^b/BoyJ) mice (Stock No. 002014), CD11c-Cre (B6.Cg-Tg(Itgax-cre)1-1Reiz/J) mice (Stock No. 008068), *Mx1*-Cre (B6.Cg-Tg(*Mx1*-cre)1Cgn/J) mice (Stock No. 003556), and *R26*^{iCre/iCre} (B6.129-*Gt(ROSA)26Sor*^{tm1(cre/ERT2)Tgj}/J) mice (Stock No. 008463) were obtained from The Jackson Laboratory. Mice were bred and maintained in a specific pathogen-free animal facility according to institutional guidelines and under protocols approved by the Animal Studies Committee of Washington University in St. Louis.

Induction of gene deletion

Gene deletion in *Zeb2*^{fl/fl}; *Mx1*-Cre(tg) mice was induced by intraperitoneal injection of 100–150 µg poly(I:C) (Sigma-Aldrich; 1.0 mg/ml stock solution dissolved in saline) either once (Figure 15A) or twice within 36–72 h (all other experiments). Gene deletion in cultures of *Zeb2*^{fl/fl}; *Mx1*-Cre(tg) cells was induced by addition of 1.2 × 10³ U/ml mouse interferon-α (Gibco; 1.82 × 10⁶ U/ml stock solution dissolved in PBS + 0.1% BSA). Gene deletion in cultures of *Zeb2*^{fl/fl}; *R26*^{iCre/iCre} cells was induced by addition of 100–150 nM 4-OHT (50:50 mixture of E/Z enantiomers, Sigma-Aldrich; 100 µM stock solution dissolved in ethanol). Constitutively heterozygous *Zeb2*^{+/−} mice were generated by breeding *Zeb2*^{fl/fl} mice to CMV-

Cre (B6.C-Tg(CMV-cre)1Cgn/J) mice (The Jackson Laboratory, Stock No. 006054), then interbreeding progeny and screening for Cre-negative *Zeb2*^{+/−} mice for further interbreeding or for breeding to WT C57BL/6 or B6.SJL mice.

Cell preparation

Cheek pouch (submandibular) blood samples were collected using Microvette capillaries (Sarstedt) or Microtainer Tubes with EDTA (BD) after venipuncture using a 4-mm Golden Rod Animal Lancet (MEDIpoint) following manufacturer's instructions. Spleen samples were minced and digested in Iscove's modified Dulbecco's medium + 10% FCS (cIMDM) supplemented with 250 µg/ml collagenase B (Roche) and 30 U/ml DNase I (Sigma-Aldrich) for 30 min to 1 h at 37 °C with stirring; LN samples were digested in the same manner without mincing. BM samples were obtained by flushing the femur (or both the femur and the tibia) with MACS buffer (PBS + 0.5% BSA + 2 mM EDTA).

Cell cultures

Single-cell suspensions of whole BM were diluted to a concentration of 2×10^6 cells/ml and cultured in the presence of FLT3L for 9–10 days. Sorted progenitors (fewer than 1×10^5 cells per sample) were cultured in individual wells of a 96-well U-bottom plate in the presence of FLT3L for 7–7.5 days.

For overexpression studies, *Ifi204* coding sequence was amplified from a complementary DNA library synthesized from monocyte mRNA and ligated into the pMSCV IRES-GFP retroviral overexpression vector (Ranganath et al., 1998); frameshift errors in the resulting plasmid were corrected by excision of flanking sequence and ligation of a replacement

synthetic DNA fragment (Integrated DNA Technologies). A sequence encoding FLAG-tagged SMAD7 was amplified from the pBabe Flag Smad7 plasmid (Addgene #14836) and ligated into the pMSCV IRES-GFP retroviral overexpression vector. Purified retroviral overexpression vectors were transfected into Phoenix-E cells using the calcium phosphate method or using Lipofectamine 3000 (Invitrogen) following manufacturer's instructions. Viral supernatants were harvested at two days and three days after transfection, filtered and concentrated by centrifugation, then applied to cell cultures which were subsequently centrifuged at 2000 r.p.m. for 1 h after addition of 2 µg/ml polybrene.

Antibodies and flow cytometry

Samples were stained in MACS buffer at 4 °C and, unless staining for FcγRII/III, also stained in the presence of Fc Block (2.4G2, BD Biosciences). The following antibodies purchased from BD Biosciences, BioLegend, eBioscience, or Tonbo Biosciences were used to detect surface markers by flow cytometry: anti-CD3 (17A2) conjugated to eFluor (eF) 450; anti-CD3e (145-2C11) conjugated to biotin or PE; anti-CD4 (RM4-5) conjugated to PE-Cy7 or PerCP-Cy5.5; anti-CD8a (53-6.7) conjugated to Brilliant Violet (BV) 510, FITC, or V500; anti-CD11b (M1/70) conjugated to biotin, eF450, FITC, PE-Cy7, or PerCP-Cy5.5; anti-CD11c (N418) conjugated to Alexa Fluor (AF) 488, APC-Cy7, APC-eF780, biotin, or PerCP-Cy5.5; anti-FcγRII/III (2.4G2) conjugated to FITC; anti-CD19 (1D3) conjugated to APC-Cy7, biotin, or FITC; anti-CD23 (B3B4) conjugated to PE-Cy7; anti-CD24 (M1/69) conjugated to PE-Cy7; anti-CD25 (PC61) conjugated to APC or PE-Cy7; anti-CD41 (eBioMWReg30) conjugated to PE; anti-CD43 (S7) conjugated to APC or PE; anti-CD44 (IM7) conjugated to APC or APC-

eF780; anti-CD45 (30-F11) conjugated to eF450; anti-CD45.1 (A20) conjugated to BV711 or FITC; anti-CD45.2 (104) conjugated to APC, APC-eF780, PE, or PerCP-Cy5.5; anti-B220 (RA3-6B2) conjugated to BV510, eF450, PE-Cy7, PerCP-Cy5.5, or V500; anti-CD64 (X54-5/7.1) conjugated to AF647; anti-Thy1.1 (OX-7) conjugated to PE; anti-C1qRp (AA4.1) conjugated to APC or PE; anti-CD103 (2E7) conjugated to PE; anti-CD105 (MJ7/18) conjugated to eF450 or PE-Cy7; anti-M-CSFR (AFS98) conjugated to BV711 or PE; anti-Kit (2B8) conjugated to APC-eF780, biotin, Brilliant Ultraviolet 395, or PE-Cy7; anti-Kit (ACK2) conjugated to APC-eF780; anti-IL-7Ra (SB/199) conjugated to BV421; anti-FLT3 (A2F10.1) conjugated to APC or PE-CF594; anti-PDGFR β (APB5) conjugated to APC; anti-CD150 (mShad150) conjugated to APC; anti-CD150 (TC15-12F12.2) conjugated to AF647; anti-NK1.1 (PK136) conjugated to biotin, eF450, FITC, or V450; anti-Sirp- α (P84) conjugated to APC or PerCP-eF710; anti-CD199 (CCR9; CW-1.2) conjugated to PE-Cy7; anti-DEC-205 (NLDC-145) conjugated to AF647 or APC; anti-Bst2 (eBio927) conjugated to APC; anti-F4/80 (BM8) conjugated to APC; anti-Fc ϵ RI (MAR-1) conjugated to PE; anti-IgD (11-26) conjugated to PE; anti-IgM (II/41) conjugated to PerCP-eF710; anti-Ki-67 (B56) conjugated to AF647; anti-Sca-1 (D7) conjugated to biotin, PerCP-Cy5.5, or PE-Cy7; anti-Ly-6C (AL-21) conjugated to AF700, APC, or FITC; anti-Ly-6C (HK1.4) conjugated to AF488 or APC-eF780; anti-Ly-6D (49-H4) conjugated to PE; anti-Ly-6G (1A8) conjugated to FITC, PE, or PerCP-Cy5.5; anti-Gr-1 (RB6-8C5) conjugated to biotin, eF450, or V450; anti-TER-119 conjugated to eF450 or PE-Cy7; anti-MHC-II (M5/114.15.2) conjugated to AF488, BV421, BV510, eF450, Pacific Blue (PB), V500, or violetFluor 450; anti-Siglec-F (E50-2440) conjugated to AF647; anti-Siglec-H

(551) conjugated to PE; anti-Siglec-H (eBio440c) conjugated to PerCP-eF710; and anti-TCR β (H57-597) conjugated to PE. Anti-F4/80 antibody (ref. MF48028) conjugated to APC or PB was purchased from Invitrogen; streptavidin conjugated to eF450 or BV510 was purchased from eBioscience or BD Biosciences, respectively; and 7-AAD viability dye was purchased from BioLegend. Cells were analysed using a FACSCanto II, LSR II, LSR Fortessa, FACSaria II, or FACSaria Fusion flow cytometer (BD) and data were analysed using FlowJo software (FlowJo, LLC). All gating strategies incorporated size and doublet discrimination based on forward and side scatter parameters.

Microarray analysis

CD24 $^+$ cDCs and Sirp- α $^+$ cDCs were sorted from cells harvested from the spleen, and Ly-6C hi monocytes and neutrophils were sorted from cells harvested from the BM. RNA was isolated from sorted cells using an RNAqueous-Micro Kit (Ambion) and submitted for amplification, labelling, and hybridization to Mouse Gene 1.0 ST Arrays (Affymetrix). Expression values were analysed after RMA quantile normalization using ArrayStar 4 or ArrayStar 5 software (DNASTAR).

RT-qPCR

For each biological replicate, 2.5×10^5 Sirp- α $^+$ cDCs were sorted from the spleen of a distinct mouse and RNA was isolated using an EZNA MicroElute Total RNA Kit (Omega Biotek). First-strand cDNA was synthesized using oligo(dT) $_{25}$ primer and SuperScript III Reverse Transcriptase enzyme (Invitrogen). Quantitative analysis was performed using the LightCycler 480 System (Roche) with Luminaris Color HiGreen qPCR Master Mix (Thermo Fisher) and the

following primer pairs: *Id2*, 5'-GCATCCCACTATCGTCAGCC-3' and 5'-AAGGGAATTCAAGATGCCTGC-3'; *Hprt* (PrimerBank ID 7305155a1), 5'-TCAGTCAACGGGGACATAAA-3' and 5'-GGGGCTGTACTGCTTAACCAG-3'.

ChIP-qPCR

BM cells were cultured for 9 days in the presence of FLT3L, then harvested, fixed using paraformaldehyde, and stained for surface marker expression; CD24⁺ cDCs and Sirp-α⁺ cDCs were sorted, then chromatin obtained from each sample was sonicated and immunoprecipitated using rabbit polyclonal anti-Zeb2 antibody (sc-48789, Santa Cruz). Quantitative analysis was performed using the LightCycler 480 System (Roche) with Luminaris Color HiGreen qPCR Master Mix (Thermo Fisher) and the following primer pairs: *Id2* promoter (identified in Weng et al. (2012)), 5'- CGCGGTAATCAGAACAGGTT-3' and 5'- TGCAGAGAACCTTGAGACTC-3'; *Id2* putative enhancer (based on presence of consensus binding motif), 5'- GTGTCAGGGAGAGGAAACAC-3' and 5'- GGGACAAGAGGTACGAGTATGT-3'.

CHAPTER 4: *Mafb* LINEAGE TRACING
DISTINGUISHES MACROPHAGES FROM OTHER LINEAGES

This work was performed in collaboration with Carlos G. Briseño, Vivek Durai, Jörn C. Albring, Malay Haldar, Ki-Wook Kim, Gwendalyn J. Randolph, Theresa L. Murphy, and Kenneth M. Murphy and is submitted for publication in the Journal of Experimental Medicine. Personal contributions included the initial conception of the project, the design and carrying out of experiments; data analysis; and writing of the paper.

Although cDCs represent a discrete lineage distinguishable in ontogeny and function from macrophages (Merad et al., 2013), no single transcriptomic or functional characteristic is sufficient to distinguish the classical, plasmacytoid, and monocyte-derived subsets of DCs taken as a whole from macrophage subsets (Hume et al., 2013). We sought to examine whether a macrophage reporter model could clarify the various origins of *Zbtb46*-expressing DCs observed *in vivo*. However, currently available model systems do not permit conditional gene deletion strictly within macrophage lineages (Abram et al., 2014). For example, LysM-Cre (Clausen et al., 1999) promotes significant deletion in macrophages and neutrophils, and F4/80-Cre (Schaller et al., 2002) deletes incompletely among macrophage populations (Abram et al., 2014). CD11c-Cre (Caton et al., 2007) deletes robustly in alveolar macrophages and in cDCs and pDCs, while *Cx3cr1*-Cre deletes in many subsets of macrophages and cDCs (Abram et al., 2014). Thus, we set out to design a new lineage-tracing model that would be more

faithfully restricted to macrophages in order to study the overlap between macrophage populations and *Zbtb46*-expressing DCs.

Results and Discussion

Generation of a Mafb–driven lineage-tracing model

Using principal component analysis to compare gene expression in macrophages and DCs (Figure 17A, B), we proposed that a reporter based on expression of the gene that encodes transcription factor MafB could distinguish macrophages from DCs (Miller et al., 2012; Satpathy et al., 2012b). In myeloid progenitors, MafB represses erythroid and DC fate (Bakri et al., 2005; Kelly et al., 2000). In resident macrophages, MafB and its parologue c-Maf repress a network of self-renewal genes and are transiently downregulated during cell proliferation (Soucie et al., 2016). Tumor-associated myeloid cells have been identified as macrophages rather than DCs partly on the basis of *Mafb* mRNA expression (Franklin et al., 2014).

We targeted C57BL6/N mouse embryonic stem cells to insert sequences encoding FLAG-tagged mCherry fluorescent protein and Cre recombinase into the endogenous *Mafb* locus. We used sequences encoding ‘self-cleaving’ 2A peptides (Ryan et al., 1991; Szymczak-Workman et al., 2012) to separate those exogenous protein-coding sequences from each other and from the endogenous single-exon *Mafb* coding sequence preserved upstream (Figure 17C). Our in-frame knock-in targeting strategy was informed by observations that protein synthesis rate and mRNA abundance together explain the vast majority of variation in protein abundance (Jovanovic et al., 2015; Li et al., 2014; Schwahnäusser et al., 2011). In using 2A peptides that yield almost stoichiometric protein co-expression (Szymczak-Workman et al., 2012), our aim

was to generate an allele that recapitulates the characteristics of WT *Mafb* in transcription and translation.

Our attention to faithful expression of MafB from the mutated allele was prompted by evidence that aberrant expression of that protein can severely decrease viability of the organism. The *kreisler* (*kr*) mutation is a radiation-induced chromosomal inversion that separates an intact *Mafb* transcriptional unit from putative distal enhancer elements (Cordes and Barsh, 1994). Mice homozygous for the *kr* mutation rarely survive to sexual maturity and show gross behavioural deficits due to abnormalities in hindbrain and inner ear development (Cordes and Barsh, 1994; Hertwig, 1942). By contrast, mice homozygous for our targeted allele (which we call MafB-mCherry-Cre) survived into adulthood and were reproductively competent. They showed behaviour indistinguishable from WT littermates, never manifesting the ‘circling’ or ‘dancing’ movement disorder observed in *kr/kr* mice (Hertwig, 1942). These observations suggest that regulation of the *Mafb* locus was minimally altered by the in-frame insertion of sequences encoding mCherry and Cre.

To generate lineage-tracing mice, we first crossed *Zbtb46*-GFP mice (Satpathy et al., 2012a) to R26-stop-YFP mice, which have a loxP-flanked stop sequence upstream of an enhanced yellow fluorescent protein (YFP) gene inserted into the constitutive and ubiquitous *Gt(ROSA)26Sor* locus (Srinivas et al., 2001); we then crossed either those progeny or R26-stop-YFP mice to MafB-mCherry-Cre mice.

Mafb–driven lineage tracing distinguishes monocytes and macrophages from other lineages

In the spleen of lineage-tracing mice, *Mafb*-mCherry was expressed abundantly in F4/80⁺ macrophages, and expression of the lineage-tracing marker YFP was found in nearly all F4/80⁺ macrophages but at background frequency among cDC subsets (Figure 18A). In the brain, *Mafb*-mCherry was detectable in microglia and YFP expression was found in nearly all such cells (Figure 18B). In the blood, *Mafb*-mCherry expression was detectable only faintly (data not shown); however, YFP expression was observed in ~10% of Ly-6C^{hi} monocytes and ~40% of Ly-6C^{lo} monocytes (Figure 18C). By contrast, we observed expression of the lineage-tracing marker YFP at a background frequency ranging from ~1% to ~6% in CD45[−] cells, B cells and neutrophils (Figure 18C).

We detected no interpretable differences in gene expression between YFP⁺ and YFP[−] Ly-6C^{lo} monocytes by microarray analysis (Figure 18D), suggesting that together they represent a single incompletely lineage-traced subset. We surmise that the short half-life (~20 h at steady state) of Ly-6C^{hi} monocytes (Ginhoux and Jung, 2014) accounts for the lack of extensive lineage-tracing activity. Although gene expression microarray data show some upregulation of *Mafb* transcript at the Ly-6C^{hi} monocyte stage (Gautier et al., 2012), the lineage-tracing marker YFP would be detectable at the same stage only if transcription and translation of Cre; Cre-mediated recombination; and transcription, translation, and maturation of YFP occur significantly within a day's span. By comparison, *Ccr2*-Cre-ER^{T2}–based lineage tracing marks nearly all Ly-6C^{hi} monocytes, but *Ccr2* expression is upregulated

prior to commitment to the monocyte–macrophage lineage at the MDP stage and lineage tracing is detectable in the CDP and its progeny (Croxford et al., 2015).

Spleen macrophages express *Mafb* mRNA more abundantly than do macrophages in nearly any other organ (Gautier et al., 2012). Thus, we assessed the frequency of YFP expression in other macrophage populations. We used surface markers to identify BM and alveolar macrophages, which express little or no *Mafb* mRNA (Gautier et al., 2012). However, in some tissues, characteristic macrophage surface markers such as F4/80 cannot unambiguously distinguish those cells from other populations (Randolph and Merad, 2013). In the BM, we found that cells with the highest abundance of F4/80 showed substantial lineage tracing (Figure 19A). In the lung, F4/80⁺ cells varied in Ly-6C expression; alveolar macrophages identified within the Ly-6C^{lo} fraction showed substantial lineage tracing, while a population of cells within the Ly-6C^{int} fraction expressing similar surface markers showed no lineage tracing (Figure 19B). Thus, MafB-mCherry-Cre–based lineage tracing can identify macrophages even where those cells express little or no *Mafb* mRNA. Furthermore, this system can help to distinguish such populations from other cells that are similar in expression of surface markers such as F4/80.

Small peritoneal macrophages (SPMs) have been found to exhibit some characteristics of DCs, including dendritic morphology and expression of markers such as DC-SIGN (Cain et al., 2013; Cassado et al., 2015). Although SPMs and DCs have been distinguished on the basis of M-CSFR or CD11c expression (Cain et al., 2013; Gautier et al., 2012), both populations are marked in lineage-tracing systems based on *Cx3cr1*-Cre or LysM-Cre (Cain et al., 2013). Using

MafB-mCherry-Cre–based lineage tracing in conjunction with the *Zbtb46*-GFP reporter allele, we found a population of M-CSFR⁺ cDCs that lacked expression of YFP (Figure 20A). After excluding those cells, large peritoneal macrophages (LPMs) and most SPMs expressed YFP (Figure 20A), and SPMs and DCs exhibited distinct morphologies (Figure 20B). By contrast, surface markers such as ICAM-2 (CD102) did not distinguish *Zbtb46*-GFP⁺ cells from SPMs (Figure 20C).

LCs are Zbtb46–expressing cells marked by Mafb–driven lineage tracing

In the epidermis, expression of epithelial cell adhesion molecule (EpCAM) is sufficient to distinguish LCs from cDCs (Henri et al., 2010). However, in the skin-draining LN, radioresistant LCs are greatly outnumbered by donor-derived cells within the EpCAM⁺ compartment after reconstitution of irradiated mice using heterologous BM (Henri et al., 2010). Therefore, we assessed whether dual macrophage and DC characteristics observed in LCs could be explained by population heterogeneity at steady state.

Using MafB-mCherry-Cre–based lineage tracing, we first examined LCs in the inguinal LN (Figure 21A, B). In that tissue, all EpCAM⁺ MHC-II⁺ cells were uniformly positive for expression of both *Zbtb46*-GFP and YFP, while EpCAM[–] *Zbtb46*-GFP⁺ DC populations did not show YFP expression above background frequency (Figure 21A). Conversely, we found that almost all *Zbtb46*-GFP⁺ YFP⁺ cells were positive for expression of EpCAM and MHC-II, while cells that did not express both *Zbtb46*-GFP and YFP also did not express EpCAM (Figure 21B). These observations suggest that *Mafb*–expressing cells are the sole source of EpCAM⁺ cells in the skin-draining LN at steady state.

We next examined LCs in the epidermis (Figure 21C, D). In that tissue, nearly all CD45⁺ MHC-II⁺ EpCAM⁺ CD24⁺ cells expressed abundant *Zbtb46*-GFP and YFP (Figure 21C). This observation was unexpected because a previous study has found that *Zbtb46* transcript is expressed at a similar abundance in skin LCs and splenic pDCs, much lower than that in cDCs (Miller et al., 2012; Satpathy et al., 2012b). Indeed, pDCs do not express detectable *Zbtb46*-GFP (Satpathy et al., 2012a). We then used anti-*Zbtb46* antibody to compare protein expression in *Zbtb46*-sufficient (*Zbtb46*^{+/+}) and *Zbtb46*-deficient (*Zbtb46*^{gfp/gfp}) epidermal LCs (Figure 21D). Consistent with our earlier observation, we found that epidermal LCs clearly expressed *Zbtb46* protein. Thus, LCs are monocyte-derived cells that express *Zbtb46* even at the tissue-resident stage.

Ly-6C⁺ monocyte-derived cells that infiltrate the lung are maturing macrophages

In the lung, administration of house dust mite (HDM) antigen induces an influx of cells that are distinguished from cDCs by expression of CD64, Ly-6C, and MAR-1 (Plantinga et al., 2013). There has been disagreement as to whether these cells should be considered moDCs (Plantinga et al., 2013) or simply macrophages (Schlitzer et al., 2013). Thus, we used MafB-mCherry-Cre-based lineage tracing to study the infiltrating population after exposure to HDM antigen (Figure 22A). In the lung of HDM antigen-treated mice, we found that CD45⁺ MHC-II⁺ CD11c⁺ CD11b⁺ CD64⁺ cells did not express *Zbtb46*-GFP (Figure 22B). Instead, we observed a continuum of Ly-6C expression in that population, with the Ly-6C^{hi} fraction expressing a lower abundance of YFP than the Ly-6C^{lo} fraction (Figure 22B). Since YFP expression is controlled by a constitutive and ubiquitous promoter, these results favour the

interpretation that infiltrating CD45⁺ MHC-II⁺ CD11c⁺ CD11b⁺ CD64⁺ cells are progressively adopting a macrophage identity.

Taken together, our results demonstrate that the MafB-mCherry-Cre model is suitable for driving gene deletion specifically in macrophages while sparing deletion in DCs or neutrophils. MafB is also expressed outside the hematopoietic system, where our model may find additional applications. In the mouse endocrine pancreas, for example, MafB is expressed in mature alpha cells but also required for beta cell maturation (Artner et al., 2007). In the kidney, MafB is required for podocyte foot process formation (Moriguchi et al., 2006). By using a lineage-tracing system based on MafB-mCherry-Cre, we found evidence that embryonic monocytes acquire Zbtb46 upon differentiation into LCs. By contrast, we found no evidence of similar cells in other organs either at steady state or in the lung under inflammatory conditions. Instead, cells elicited by HDM antigen could be resolved into either *Zbtb46*-expressing DCs or CD64⁺ macrophages. Although we cannot exclude the possibility that *Mafb*-expressing lineages can give rise to *Zbtb46*-expressing progeny under conditions not examined here, it appears that LCs may be unique in acquiring these distinctive characteristics of macrophages and DCs.

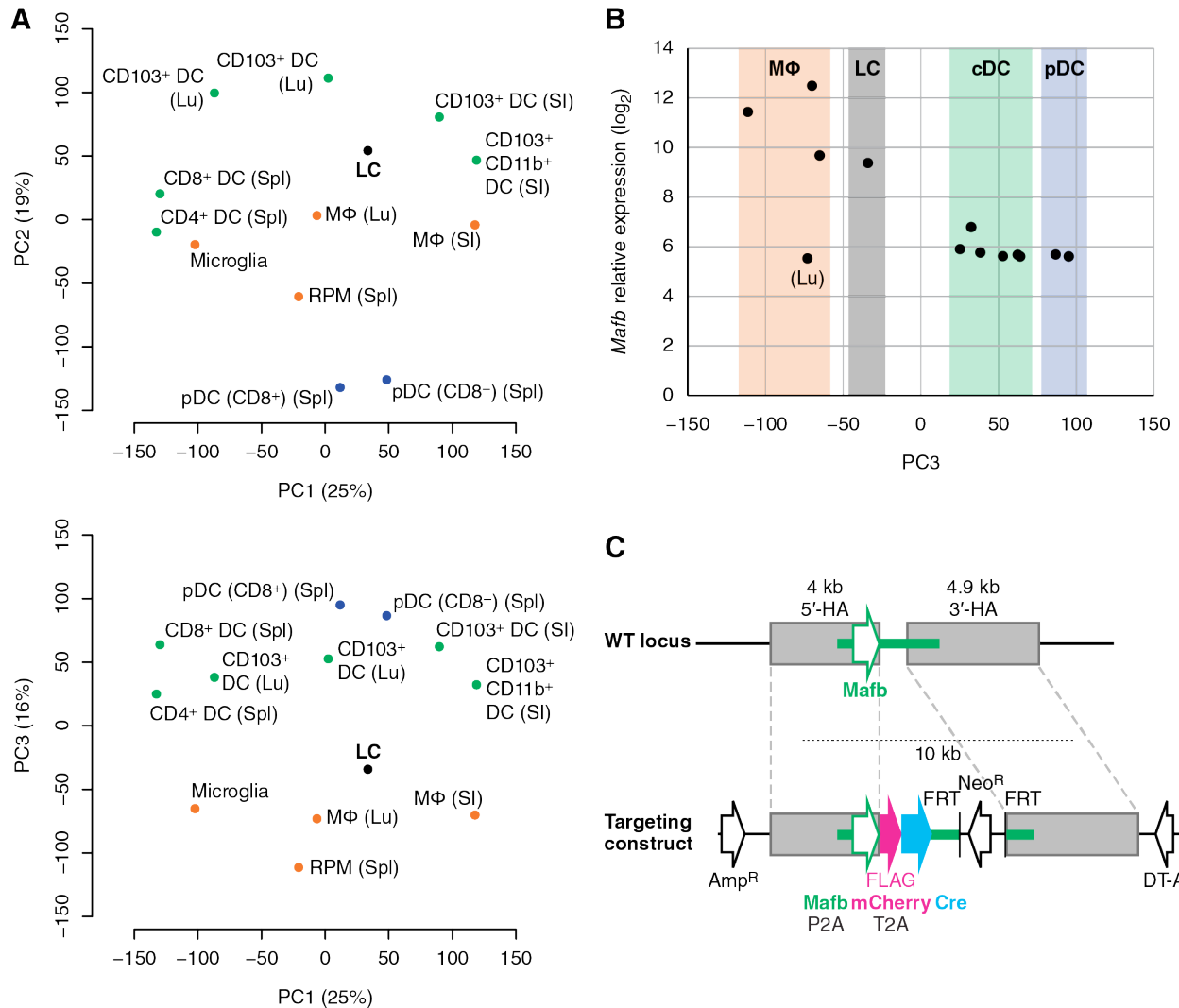


Figure 17: *Mafb* expression distinguishes macrophages from DCs

(A) Principal component analysis of gene expression microarray data for the indicated macrophage and DC subsets. Proportion of variance explained by each principal component is given in parentheses. Lu, lung; MΦ, macrophages; PC, principal component; RPM, red pulp macrophages; SI, small intestine; Spl, spleen. (B) *Mafb* relative expression (y -axis) plotted against PC3 score (x -axis) for macrophage and DC subsets analyzed in (A). (C) Targeting strategy to generate a MafB-mCherry-Cre knock-in mouse line. Arrows indicate orientation of coding sequences and green bars indicate untranslated regions. Amp^R, ampicillin resistance; DT-A, diphtheria toxin fragment A; FRT, flippase recognition target; HA, homology arm; Neo^R, neomycin resistance.

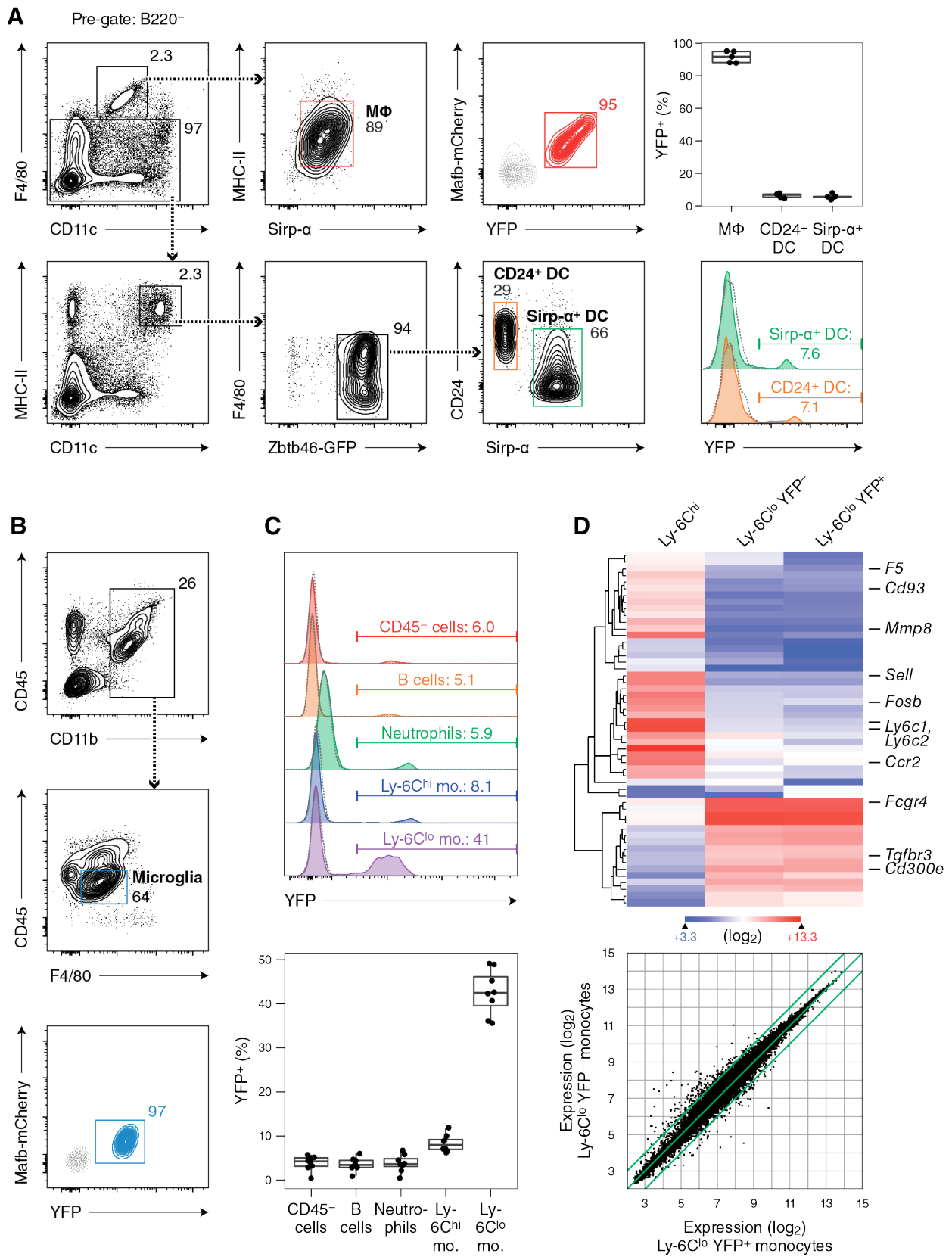


Figure 18: Monocyte progeny are marked by *Mafb*-driven lineage tracing

← *Continued from previous page*

(A) Macrophages in MafB-mCherry-Cre × R26-stop-YFP × *Zbtb46*-GFP mouse spleen, identified by surface markers as indicated, are displayed for expression of *Mafb*-mCherry and lineage-tracing marker YFP in a two-colour histogram, and cDC subsets are compared for expression of lineage-tracing marker YFP. Shown is one sample and a box plot representing first quartile, median, and third quartile frequencies (top right) ($n \geq 5$ animals over at least three independent experiments). (B) Microglia in MafB-mCherry-Cre × R26-stop-YFP mouse brain, identified by surface markers as indicated, are displayed for expression of *Mafb*-mCherry and lineage-tracing marker YFP in a two-colour histogram. Shown is one representative sample ($n \geq 3$ animals over at least two independent experiments). (C) Lineages in MafB-mCherry-Cre × R26-stop-YFP × *Zbtb46*-GFP mouse blood, identified by surface markers as indicated, are compared for expression of lineage-tracing marker YFP. Shown is one sample and a box plot representing first quartile, median, and third quartile frequencies ($n \geq 8$ animals over at least four independent experiments). Mo., monocytes. In all preceding panels, numbers indicate percentage of cells within the indicated gate and dotted grey lines show fluorescent signal measured in non-mCherry and non-YFP control samples. (D) Heat map showing relative expression in the indicated monocyte subsets for gene expression microarray probe sets differentially expressed in Ly-6C^{hi} and Ly-6C^{lo} monocytes (top) and scatterplot showing relative expression in YFP⁺ and YFP⁻ Ly-6C^{lo} monocytes for all probe sets excluding normalization controls (bottom). Shown are averages of two biological replicates, excluding one YFP⁻ Ly-6C^{lo} monocyte sample below quality control thresholds.

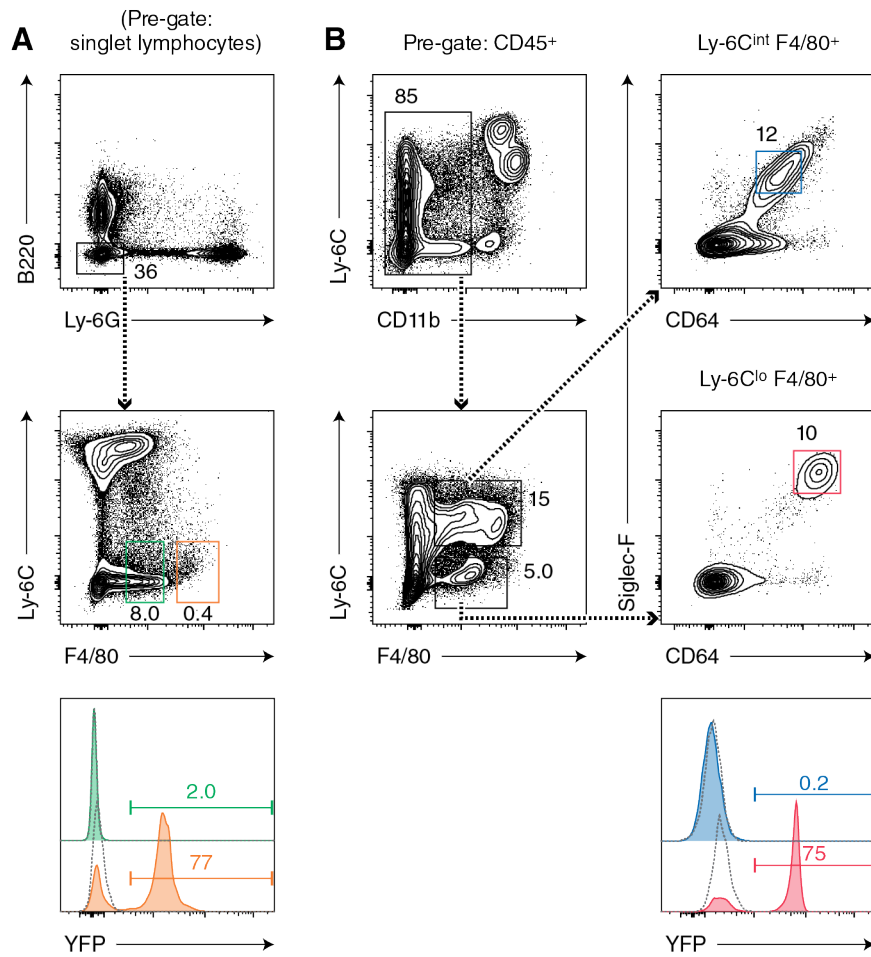


Figure 19: *Mafb*-driven lineage tracing distinguishes macrophages from populations of similar immunophenotype in the BM and lung

(A) Macrophages in *MafB-mCherry-Cre × R26-stop-YFP × Zbtb46-GFP* mouse BM, identified by surface markers as indicated (orange), are compared with $F4/80^+$ cells of similar immunophenotype (green) for expression of lineage-tracing marker YFP. Shown is one representative sample ($n \geq 4$ animals over at least two independent experiments). (B) Alveolar macrophages in *MafB-mCherry-Cre × R26-stop-YFP × Zbtb46-GFP* mouse lung, identified by surface markers as indicated (red), are compared with $F4/80^+$ Siglec-F^+ $CD64^+$ cells of similar immunophenotype (blue) for expression of lineage-tracing marker YFP. Shown is one representative sample ($n \geq 4$ animals over at least two independent experiments). In both panels, numbers indicate percentage of cells within the indicated gate and dotted grey lines show fluorescent signal measured in non-mCherry and non-YFP control samples.

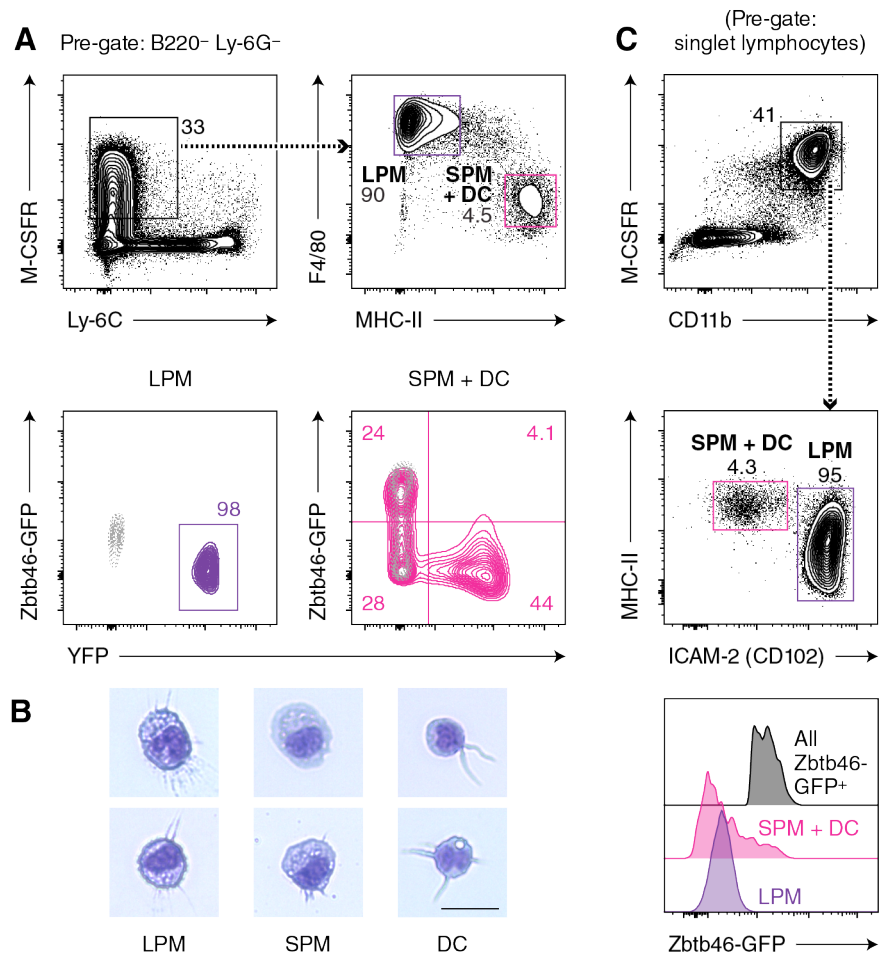


Figure 20: *Mafb*-driven lineage tracing distinguishes peritoneal macrophages from DCs

(A) *Mafb*-mCherry-Cre × R26-stop-YFP × *Zbtb46*-GFP large peritoneal macrophages (LPM, purple) and small peritoneal macrophages (SPM, magenta), identified in one scheme by surface markers including M-CSFR, are compared for expression of *Zbtb46*-GFP and lineage-tracing marker YFP in two-colour histograms. Shown is one representative sample ($n \geq 3$ animals over at least two independent experiments). Numbers indicate percentage of cells within the indicated gate and dotted grey lines show fluorescent signal measured in non-mCherry and non-YFP control samples. (B) Macrophages (*Zbtb46*-GFP⁻ Ly-6G⁻ CD11b⁺ *Mafb*-mCherry⁺ YFP⁺, which were uniformly M-CSFR⁺), distinguished as LPM (F4/80^{hi}) or SPM (F4/80^{lo}), and DCs (*Zbtb46*-GFP⁺ CD11c⁺) were sorted from the peritoneum of *Mafb*-mCherry-Cre × R26-stop-YFP × *Zbtb46*-GFP mice and concentrated by Cytospin for morphologic assessment by Wright–Giems staining. Shown are two representative cells for each population ($n = 2$ animals). Scale bar, 20 μ m. (E) LPM and SPM populations isolated from a *Zbtb46*-GFP mouse are identified in another scheme by surface markers as shown and compared for expression of *Zbtb46*-GFP ($n = 1$ animal). Numbers indicate percentage of cells within the indicated gate.

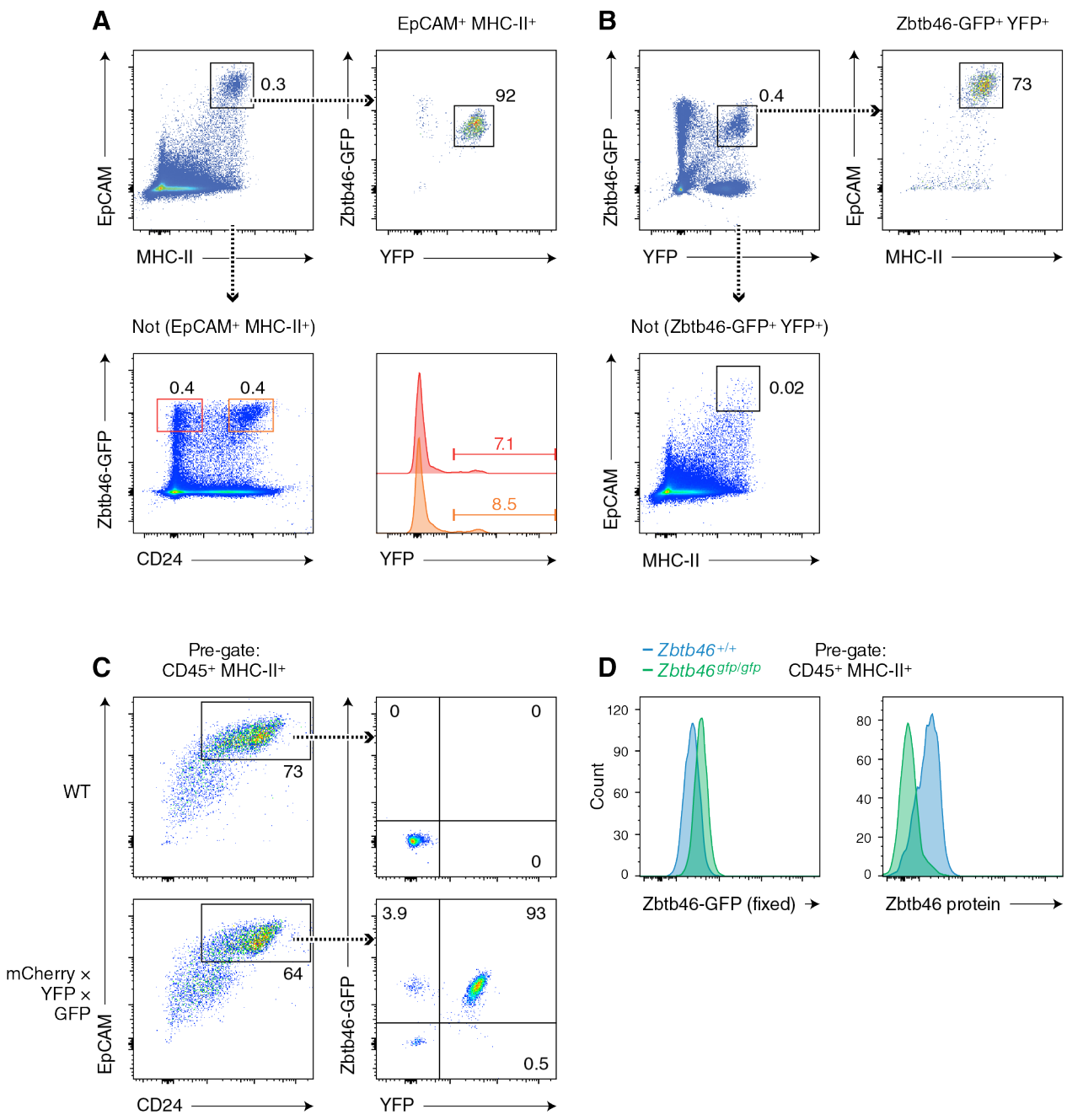


Figure 21: Steady state LCs are marked by *Mafb*-driven lineage tracing but express *Zbtb46*

(A) Migrated LCs in the inguinal LN of MafB-mCherry-Cre × R26-stop-YFP × *Zbtb46*-GFP mice are displayed for expression of *Zbtb46*-GFP and lineage-tracing marker YFP in a two-colour histogram (top) and dermal DC populations in the same tissue identified by *Zbtb46*-GFP and CD24 are displayed for expression of YFP (bottom). Shown is one representative sample ($n \geq 4$ animals over at least two independent experiments). (B) With the same samples as in (A), cells expressing both *Zbtb46*-GFP and YFP (top) or not expressing both fluorescent markers (bottom) are compared for expression of LC markers in a two-colour histogram.

Continued on next page →

← *Continued from previous page*

(C) LCs in the epidermis of WT or MafB-mCherry-Cre × R26-stop-YFP × *Zbtb46*-GFP (mCherry × YFP × GFP) mice are compared for expression of *Zbtb46*-GFP and lineage-tracing marker YFP in two-colour histograms. Shown is one representative sample per group ($n \geq 2$ animals per group over at least two independent experiments). In all preceding panels, numbers indicate percentage of cells within the indicated gate. **(D)** LCs in the epidermis of *Zbtb46*-sufficient (*Zbtb46*^{+/+}) or *Zbtb46*-deficient (*Zbtb46*^{gfp/gfp}) mice are compared for expression of *Zbtb46*-GFP and *Zbtb46* protein in one-colour histograms. Shown is one representative sample per group ($n \geq 3$ animals per group over at least two independent experiments).

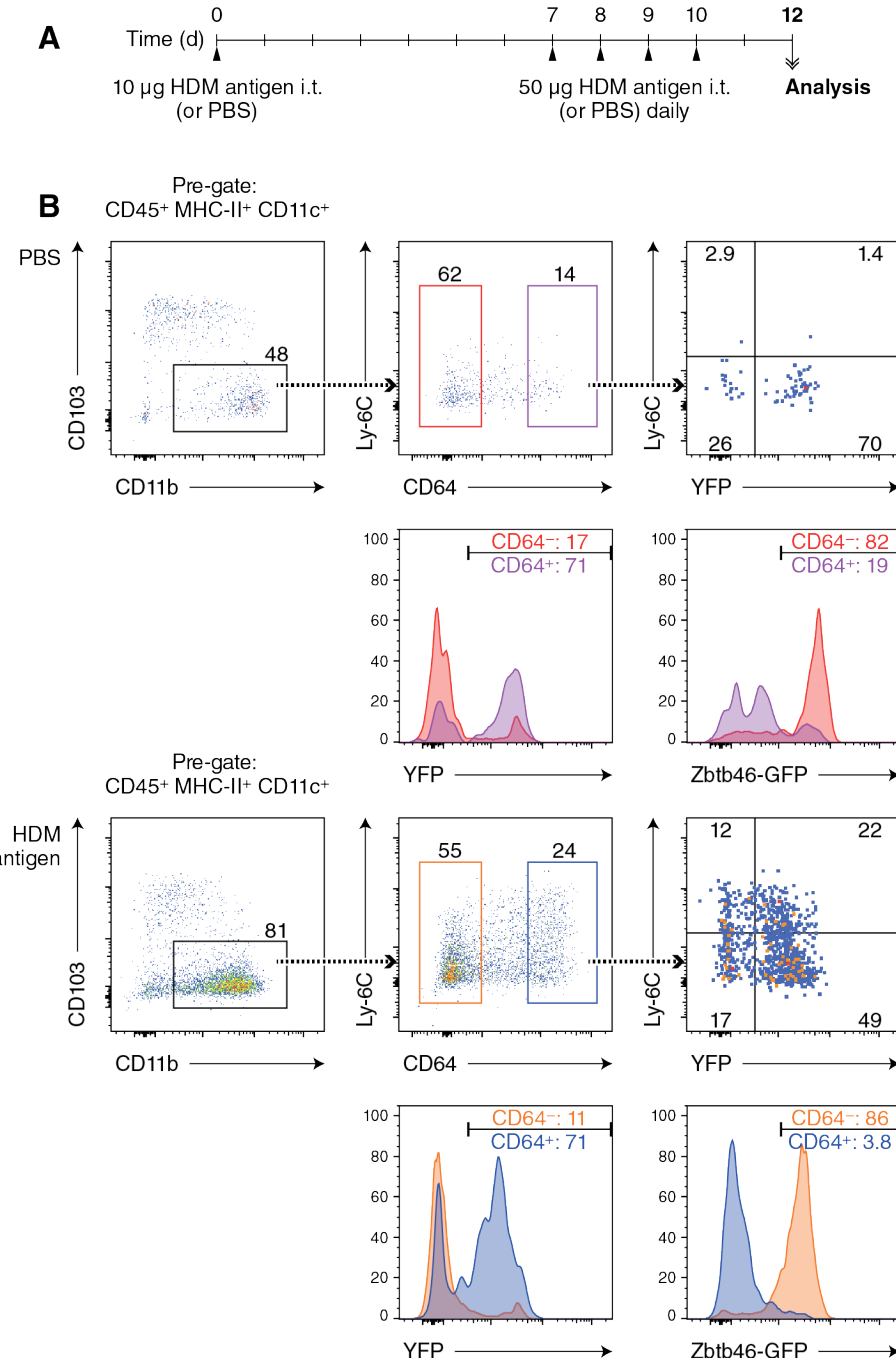


Figure 22: Ly-6C⁺ monocyte-derived cells mature in the inflamed lung but lack *Zbtb46*

(A) Experimental outline for intratracheal (i.t.) sensitization and challenge of MafB-mCherry-Cre × R26-stop-YFP × *Zbtb46*-GFP mice using HDM antigen. (B) Monocyte-derived cells and cDCs are compared for expression of Ly-6C, lineage-tracing marker YFP, and *Zbtb46*-GFP after treatment with vehicle (PBS) or HDM antigen following the schedule outlined in (A). Shown is one representative sample ($n \geq 4$ animals over at least two independent experiments). Numbers indicate percentage of cells within the indicated gate.

Methods

Mice

MafB-mCherry-Cre mice were maintained on the C57BL/6N background by interbreeding or by breeding to C57BL/6NJ mice (The Jackson Laboratory, Stock No. 000664). To remove the neomycin resistance cassette, mice were bred to R26-FLP knock-in (B6N.129S4-*Gt(ROSA)26Sor*^{tm1(FLP1)Dym}/J) mice (The Jackson Laboratory, Stock No. 016226), then interbred to remove the FLP-expressing allele.

Zbtb46-GFP (B6.129S6(C)-*Zbtb46*^{tm1.1Kmm}) mice were generated by breeding 129S-*Zbtb46*^{tm1Kmm} mice (Satpathy et al., 2012a) to B6.C-Tg(CMV-cre)1Cgn/J mice (The Jackson Laboratory, Stock No. 006054) to remove the neomycin resistance cassette. Offspring were bred to C57BL/6J mice for at least nine generations (removing the Cre-expressing transgene) and deposited at The Jackson Laboratory (Stock No. 027618). R26-stop-YFP (B6.129X1-*Gt(ROSA)26Sor*^{tm1(EYFP)Cos}/J) mice were purchased from The Jackson Laboratory (Stock No. 006148) and crossed to *Zbtb46*-GFP mice on the C57BL/6 background.

Experiments were performed using age-matched mice between 4 and 22 weeks of age. Mice were bred and maintained in a specific pathogen-free animal facility according to institutional guidelines and under protocols approved by the Animal Studies Committee of Washington University in St. Louis.

Generation of the MafB-mCherry-Cre targeted mutation

P2A-FLAG-mCherry, T2A-Cre, and mouse MafB coding sequences were ligated serially into the pMSCV T2A-GFP retroviral overexpression vector, which was modified from

the pMSCV IRES-GFP retroviral overexpression vector (Ranganath et al., 1998), to yield the pMSCV MafB-P2A-FLAG-mCherry-T2A-Cre retroviral overexpression vector. Primers used to amplify coding sequences by polymerase chain reaction (PCR) were as follows:

Figure 23: Primer sequences used for the generation of a MafB overexpression vector

Product	Primer sequence (5'→3')
P2A-FLAG-	attactcgagggcagcgggccacgaacttcagcctgctgaaggcaagcaggagat
mCherry coding sequence	gttgaagaaaaccccgccctgattacaaggatgacgatgacaagGTGAGCAAGG GCGAGGAG
T2A-Cre coding sequence	attatccggatcccttagaCTTGTACAGCTCGTCCATGC attatcttagaggatccggagagggcagaggaagtcttctaacatgcggtgacgtg gaggagaatcccgccctGTGCCAAGAAGAAGAGGAA
MafB coding sequence	attagaattcTCAGTCCCCATCCTCGAGCAG attaagatctcaccATGGCCGGAGCTGAGCAT attagtcgacCAGAAAGAACTCAGGAGAGGAG

Mafb 3'-untranslated region (UTR) sequence was amplified from 129S6 genomic DNA using the following primers: 5'-attagaattcttctgtgaGTCCTGGCGG-3' and 5'-attaatcgatGGGACTGCTTTTGACAAACTGTTGCCAGAGAATGTCCAAAC-3'. Both the amplified 3'-UTR fragment and pMSCV MafB-P2A-FLAG-mCherry-T2A-Cre retroviral overexpression vector were digested using *Eco*RI and *Cla*I, then ligated together. A MafB-P2A-FLAG-mCherry-T2A-Cre-UTR fragment was released from the resulting vector by restriction digest using *Sac*II, *Mlu*I, and Antarctic Phosphatase (New England Biolabs), and a fragment (~3 kb) containing *Mafb* 5'-UTR and upstream sequences was amplified from 129S6 genomic DNA and digested using *Mlu*I. The primers used to amplify the latter fragment were: 5'-attagatctGGGACAACTTGTATAGAAAAGTTGGAGTGTGGTGTCTCT-3' and 5'-attagatctGGGACAACTTGTATAGAAAAGTTGGAGTGTGGTGTCTCT-3' and 5'-attagatctGGGACAACTTGTATAGAAAAGTTGGAGTGTGGTGTCTCT-3'

CGTCTTCGTTCTCCAGGT-3'. The digested fragments were inserted into the pDONR (P4-P1R) plasmid (Invitrogen) by a modified BP recombination reaction in which incubation at room temperature was followed by addition of a supplemental buffer (10 mM MgCl₂, 1 mM ATP) and T4 DNA Ligase (New England Biolabs) and incubation at 16 °C for 5.5 h prior to addition of Proteinase K solution to terminate the reaction. That reaction generated pENTR MafB-P2A-FLAG-mCherry-T2A-Cre-UTR.

A loxP-flanked fragment containing a neomycin resistance gene under the control of the *Pgk1* promoter (*Pgk1*-Neo^R) was released by restriction digest from the pLNTK targeting vector (Gorman et al., 1996) and ligated into the pENTR lox-Puro vector (Iizumi et al., 2006) to yield pENTR lox-rNeo, as previously described (Satpathy et al., 2012a). Flippase recognition target (FRT) sites were introduced flanking the *Pgk1*-Neo^R cassette by site-directed mutagenesis using Pfu DNA Polymerase (Agilent) to yield pENTR lox-FRT-rNeo. Flanking loxP sites were removed in a two-step process. First, the loxP/FRT-flanked *Pgk1*-Neo^R cassette was replaced with a synthetic DNA fragment purchased from Integrated DNA Technologies to yield an intermediate pENTR plasmid. Second, the intermediate pENTR plasmid was digested using *Mfe*I-HF (New England Biolabs) and *Bam*HI, then ligated to a *Pgk1*-Neo^R fragment released from pENTR lox-FRT-rNeo using *Eco*RI and *Bam*HI. Orientation of the synthetic fragment in the intermediate pENTR plasmid determined orientation of the *Pgk1*-Neo^R fragment in the final product, yielding either pENTR FRT-Neo or pENTR FRT-rNeo. The sequence of the synthetic fragment was (5'→3'):

TACTACGCGGCCGCGAATTGAAAGTTCTATTCCGAAGTTCCTATTCTCTAGAAAGTATA
 GGAACATTCATTAAGGGTTCCGGATCTATAGATCATGAGTGGGAGGAATGAGCTGGCCCTT
 AATTTGGTTTGCTTAAATTATGATATCCAACATGAAACATTATCATAAAGCAAT
 AGTAAAGAGCCTTCAGTAAAGAGCAGGCATTATCTAATCCCACCCCACCCCCACCCCCG
 TAGCTCCAATCCTCCATTCAAAATGTAGGTACTCTGTTCTCACCCCTTAAACAAAGTA
 TGACAGGAAAAACTCCATTAGTGGACATCTTATTGTTAATAGATCATCAATTCT
 GCAGACTTACAGCGGATCCTAATTCAATTGGAAGTTCCTATTCCGAAGTTCCTATTCTC
 TAGAAAGTATAGGAACCTCGAATTGAAAGCGGCCATCAT

Homology arms (HAs) were amplified by PCR from C57BL/6 genomic DNA and the vector backbone was amplified from pDEST DTA-MLS (Iizumi et al., 2006) using Q5 High-Fidelity DNA Polymerase (New England Biolabs) and the following primers:

Figure 24: Primer sequences used for the generation of a *Mafb* targeting plasmid

Product	Primer sequence (5'→3')
5'-HA	ccatgattacgccaagctatCGGAGTGTGGTGTCTCTCT TGACCTTGTAGGCGTCTCTC
3'-HA	CATACACACACCCACGACTG aacgacggccagtgaattatCGGGACAAACAAAGATGTT
Vector backbone	CCACACTCCGatagcttggcgtaatcatgg GTTTGTCCC Gataattcactggccgtcggt

A synthetic DNA fragment was purchased from Integrated DNA Technologies incorporating partial mCherry coding sequence, partial *Mafb* 3'-UTR sequence, and restriction sites for subsequent use. The sequence of the synthetic fragment was (5'→3'):

GAGAGAGACGCCTACAAGGTCAAGTGCAGAAACTCGCCAACCTCGGCTTCAGGGAGGCG
GGCTCCACCAGCGACAGCCCCTCCTCTGAGTTCTTCTGGTCAGGGCAGCGGCC
ACGAACTTCAGCCTGCTGAAGCAAGCAGGAGATGTTGAAGAAAACCCGGCCCTGATTAC
AAGGATGACGATGACAAGGTGAGCAAGGGCGAGGAGGATAACATGGCCATCATCAAGGAG
TTCATGCGCTTCAAGGTGCACATGGAGGGCTCCGTGAACGCCACGAGTCGAGATCGAG
GGCGAGGGCGAGGGCCGCCCTACGAGGGCACCCAGACGCCAAGCTGAAGGTGACCAAG
GGTGGCCCCCTGCCCTCGCCTGGACATCCTGTCCCCTCAGTTCATGTACGGCTCCAAG
GCCTACGTGAAGCACCCGCCGACATCCCCGACTACTTGAAGCTGTCCTCCCCGAGGG
TTTAAATGGGAGCGCGTGTGAACCTCGAGGACGGCGCGTGGTGACCGTGACCCAGGAC
TCCTCCCTGCAGGACGGCGAGTCATCTACAAGGTGAAGCTGCGCGCACCAACTGATGT
GGCTCTCGCCCCCTCGCCTTCCACTTCAGTTAAGTTTGAGGGAAAGCGGC
CGCTAAGGGAGAGACAGATGCCGAGATCCACATCGTCAGGAGTGTGTCCTTATTATTG
TTGGGTCTTGGGGCAAATTGACATACACACACCCACGACTGCTCCT

The amplified HA fragments, amplified vector backbone fragment, and synthetic fragment were assembled using Gibson Assembly Master Mix (New England Biolabs) to yield the first intermediate targeting plasmid.

The first intermediate targeting plasmid was linearized using *NotI* and Antarctic Phosphatase (New England Biolabs), then used for ligation to a FRT–flanked *Pgk1*-Neo^R fragmented released from pENTR FRT-Neo or pENTR FRT-rNeo using *NotI* and *BsrGI* (having ensured that the pENTR vector backbone would not interfere with ligation by

digesting with *Nhe*I and *Af*II after digesting with *Not*I and *Bsr*GI). The ligation yielded the second intermediate targeting plasmid.

A fragment (~1 kb) containing a portion of the 3'-UTR sequence was amplified from pENTR MafB-P2A-FLAG-mCherry-T2A-Cre-UTR using the following primers: 5'-
gctcgaggatggggactgagaaCTGTGAGTCCTGGCGGGT-3' and 5'-*CTGAAGTGGGAAGGACGAGG-3'*. A fragment containing partial mCherry-T2A-Cre was released from pENTR MafB-P2A-FLAG-mCherry-T2A-Cre-UTR using *Sbf*I-HF and *Eco*RI-HF (New England Biolabs). The second intermediate targeting plasmid was linearized using *Csp*CI and assembled with the amplified 3'-UTR fragment and the released mCherry-T2A-Cre fragment using Gibson Assembly Master Mix (New England Biolabs) to yield the final targeting plasmid.

Linearized final targeting plasmid was electroporated into JM8.N4 mouse embryonic stem cells (C57BL/6N background, KOMP Repository). After selection with G418 (Calbiochem), targeted clones were individually picked, expanded, and screened by Southern blot analysis. First, homologous recombination was identified using *Bam*HI-digested genomic DNA and DIG-labelled 3'-probe amplified using the following primers: 5'-
GGCACCAAGGGAATCTAGAA-3' and 5'-*ATGCTCCAAGACAACGATGC-3'*. Next, homologous recombination was confirmed using *Swa*I-digested genomic DNA and DIG-labelled 5'-probe amplified using the following primers: 5'-*CGCCTCCTATGTGCCATAAA-3'* and 5'-
TTTCTCAAAGCAAGCCCTG-3'.

Targeted clones were injected into blastocysts and male chimeras were bred to female C57BL/6NJ mice (The Jackson Laboratory, Stock No. 000664). Confirmation of germline

transmission and determination of progeny genotype were carried out by PCR using the following primers: 5'-CGAGAAGACGCAGCTCATT-3' (common forward), 5'-GAATAGGGAGTCTGGGCCAG-3' (WT reverse), 5'-CTTGGTCACCTCAGCTTGG-3' (mutant reverse). The expected sizes of amplicons were: 424 bp (mutant) and 219 bp (WT).

Cell preparation

Cheek pouch (submandibular) blood samples were collected using BD Microtainer Tubes with EDTA after venipuncture using a 4-mm Golden Rod Animal Lancet (MEDIpoin) per manufacturer's instructions. Spleen samples were minced and digested in Iscove's modified Dulbecco's medium + 10% FCS (cIMDM) supplemented with 250 µg/ml collagenase B (Roche) and 30 U/ml DNase I (Sigma-Aldrich) for 30 min to 1 h at 37 °C with stirring; LN samples were digested in the same manner without mincing. Microglia were isolated from brain by density gradient centrifugation using Percoll (P4937, Sigma-Aldrich), modifying a previously described method (Lee and Tansey, 2013) by substituting Iscove's modified Dulbecco's medium for Dulbecco's Modified Eagle Medium: Nutrient Mixture F-12 (DMEM/F-12) and by additionally supplementing the dissociation medium with 1.7 mg/ml collagenase D (Roche) while omitting papain; briefly, brains were diced, dissociated in medium supplemented with Liberase TM (Roche), washed, filtered, and suspended in 37% Percoll; 70% Percoll was underlaid, 30% Percoll was overlaid, Hank's balanced salt solution (HBSS, Life Technologies) was overlaid, and samples were centrifuged before cells in the interface between 37% Percoll and 70% Percoll were recovered and washed. Peritoneum samples were harvested by injecting 10 ml PBS into the peritoneal cavity, agitating vigorously, then collecting the

injected fluid. BM samples were obtained by flushing the femur (or both the femur and the tibia) with MACS buffer (PBS + 0.5% BSA + 2 mM EDTA). Epidermis samples were prepared by splitting ears into dorsal and ventral halves, incubating atop RPMI-1640 medium + 1.25 U/ml Dispase (Roche) for 45 min to 1 h at 37 °C, then peeling and mincing epidermal sheets and digesting in 0.05% trypsin–EDTA solution (Gibco) for 40 min at 37 °C followed by repetitive pipetting. Lung samples were prepared after perfusion by injection of 5–10 ml PBS into the right ventricle; lung lobes were minced and digested in cIMDM supplemented with 2–4 mg/ml collagenase D and 30 U/ml DNase I for 1–2 h at 37 °C with stirring. Small intestinal lamina propria samples were prepared as follows: after removal of Peyer’s patches and fat, intestines were opened longitudinally, washed of fecal content, cut into pieces 1 cm in length, and incubated in HBSS + 15 mM HEPES + 5 mM EDTA at 37 °C for 40 min with shaking at 250 rpm; tissue suspensions were passed through a sieve and the tissue pieces remaining were washed twice in PBS, minced, and incubated in cIMDM supplemented with collagenase B, collagenase D, and DNase I for 90 min at 37 °C with stirring; cell suspensions were pelleted, suspended in 40% Percoll, overlaid on 70% Percoll and centrifuged for 20 min at 850×*g* before cells in the interface were recovered and washed in PBS.

To remove erythrocytes, samples were treated with ACK lysing buffer (0.15 M NH₄Cl + 10 mM KHCO₃ + 0.10 mM EDTA). Cells were filtered through 36-μm or 80-μm nylon mesh before resuspension in MACS buffer, and any cell counts were determined using a Vi-CELL Analyzer (Beckman Coulter).

Antibodies and flow cytometry

Samples were stained in MACS buffer at 4 °C in the presence of Fc Block (2.4G2, BD Biosciences). The following antibodies purchased from BD Biosciences, BioLegend, eBioscience, or Tonbo Biosciences were used to detect surface markers by flow cytometry: anti-CD3e (145-2C11) conjugated to biotin or FITC; anti-CD11b (M1/70) conjugated to eFluor 450, Pacific Blue, FITC, PE, PE-Cy7, Alexa Fluor (AF) 700, or APC-Cy7; anti-CD11c (N418) conjugated to biotin, PerCP-Cy5.5, AF647, or APC-Cy7; anti-CD11c (HL3) conjugated to Brilliant Ultraviolet 395; anti-CD19 (1D3) conjugated to biotin; anti-CD24 (M1/69) conjugated to PE, PE-Cy7, or AF647; anti-CD43 (S7) conjugated to APC; anti-CD45 (30-F11) conjugated to eVolve 605; anti-CD45.2 (104) conjugated to Brilliant Violet (BV) 605, PerCP-Cy5.5, APC, APC-Cy7, or APC-eFluor 780; anti-CD45R (B220; RA3-6B2) conjugated to eFluor 450, BV510, PE-Cy7, AF700, or APC-Cy7; anti-CD62L (MEL-14) conjugated to APC; anti-CD64 (X54-5/7.1) conjugated to AF647 or APC; anti-CD102 (3C4 (MIC2/4)) conjugated to AF647; anti-CD103 (M290) conjugated to BV421; anti-CD115 (M-CSFR; AFS98) conjugated to BV711, PerCP-eFluor 710, or PE; anti-CD117 (Kit; 2B8) conjugated to APC-eFluor 780; anti-CD135 (FLT3; A2F10) conjugated to APC; anti-CD170 (Siglec-F; E50-2440) conjugated to PE; anti-CD172a (Sirp- α ; P84) conjugated to PerCP-eFluor 710, PE-Cy7, or APC; anti-CD226 (10E5) conjugated to PE; anti-CD326 (EpCAM; G8.8) conjugated to APC; anti-Ly-6C (AL-21) conjugated to AF700 or APC; anti-Ly-6C (HK1.4) conjugated to APC-eFluor 780; anti-Ly-6G (1A8) conjugated to biotin, BV510, PerCP-Cy5.5, or PE; anti-NK1.1 (PK136) conjugated to eFluor 450; anti-F4/80 (BM8) conjugated to PE-Cy7 or APC-

eFluor 780; anti-TER-119 conjugated to eFluor 450; and anti-MHC-II (I-A/I-E; M5/114.15.2) conjugated to BV421, Pacific Blue, V500, or BV510. Streptavidin conjugated to eFluor 450 (eBioscience) or to BV510 (BD Biosciences) was also used for flow cytometry. To detect intracellular protein, samples were fixed, permeabilized, and washed using a Transcription Factor Buffer Set (BD Pharmingen). The following antibody from BD Pharmingen was used after fixation and permeabilization: anti-Zbtb46 (U4-1374) conjugated to PE. Cells were analysed using a FACSCanto II or FACSaria Fusion flow cytometer (BD) and data were analysed using FlowJo software (FlowJo, LLC). All gating strategies incorporated size and doublet discrimination based on forward and side scatter parameters.

Gene expression microarray analysis

RNA was isolated from cells using an RNAqueous-Micro Kit (Ambion) and target preparation was performed using the GeneChip WT Pico Kit (Affymetrix) for hybridization to Mouse Gene 1.0 ST Arrays (Affymetrix). Data were normalized and expression values were modelled using ArrayStar 5 software (DNASTAR).

For principal component analysis, data were pre-processed using ArrayStar 5 software with robust multiarray average summarization and quantile normalization. Replicates were grouped by sample, then mean log-transformed expression values from each replicate group were exported in table format, imported into R software (R Foundation for Statistical Computing), mean-centred by gene, root-mean-square-scaled by sample, transposed and subjected to principal component analysis computed by singular value decomposition without additional centring or scaling. Scores were plotted in R software.

Microscopy

Peritoneal macrophages and DCs were sorted using a FACS Aria Fusion flow cytometer (BD), concentrated by Cytospin, and stained with Wright–Giemsa stain using the Hema 3 System (Fisher Scientific). Bright-field images were captured at room temperature with a 40× objective lens using an EVOS FL Auto Imaging System (Invitrogen).

HDM antigen

HDM antigen (*Dermatophagoides pteronyssinus* extracts, Greer Laboratories) was dissolved in PBS. Mice were sensitized and challenged intratracheally as outlined in Figure 22A to induce allergic airway inflammation, and lung samples were prepared two days after final challenge.

REFERENCES

- Abram, C.L., G.L. Roberge, Y. Hu, and C.A. Lowell. 2014. Comparative analysis of the efficiency and specificity of myeloid-Cre deleting strains using ROSA-EYFP reporter mice. *Journal of Immunological Methods* 408:89-100.
- Akashi, K., D. Traver, T. Miyamoto, and I.L. Weissman. 2000. A clonogenic common myeloid progenitor that gives rise to all myeloid lineages. *Nature* 404:193-197.
- Alder, J.K., R.W. Georgantas, R.L. Hildreth, I.M. Kaplan, S. Morisot, X. Yu, M. McDevitt, and C.I. Civin. 2008. Kruppel-like factor 4 is essential for inflammatory monocyte differentiation in vivo. *Journal of Immunology* 180:5645-5652.
- Artner, I., B. Blanchi, J.C. Raum, M. Guo, T. Kaneko, S. Cordes, M. Sieweke, and R. Stein. 2007. MafB is required for islet beta cell maturation. *Proceedings of the National Academy of Sciences of the United States of America* 104:3853-3858.
- Artyomov, M.N., A. Munk, L. Gorvel, D. Korenfeld, M. Celli, T. Tung, and E. Klechevsky. 2015. Modular expression analysis reveals functional conservation between human Langerhans cells and mouse cross-priming dendritic cells. *Journal of Experimental Medicine* 212:743-757.
- Asselin-Paturel, C., A. Boonstra, M. Dalod, I. Durand, N. Yessaad, C. Dezutter-Dambuyant, A. Vicari, A. O'Garra, C. Biron, F. Brière, and G. Trinchieri. 2001. Mouse type I IFN-producing cells are immature APCs with plasmacytoid morphology. *Nature Immunology* 2:1144-1150.
- Auffray, C., D.K. Fogg, E. Narni-Mancinelli, B. Senechal, C. Trouillet, N. Saederup, J. Leemput, K. Bigot, L. Campisi, M. Abitbol, T. Molina, I. Charo, D.A. Hume, A. Cumano, G. Lauvau, and F. Geissmann. 2009. CX3CR1⁺ CD115⁺ CD135⁺ common macrophage/DC precursors and the role of CX3CR1 in their response to inflammation. *Journal of Experimental Medicine* 206:595-606.
- Bachem, A., E. Hartung, S. Guttler, A. Mora, X. Zhou, A. Hegemann, M. Plantinga, E. Mazzini, P. Stoitzner, S. Gurka, V. Henn, H.W. Mages, and R.A. Kroczeck. 2012. Expression of XCR1 characterizes the Batf3-dependent lineage of dendritic cells capable of antigen cross-presentation. *Frontiers in Immunology* 3:214.

- Bailey-Bucktrout, S.L., S.C. Caulkins, G. Goings, J.A.A. Fischer, A. Dziona, and S.D. Miller. 2008. Central nervous system plasmacytoid dendritic cells regulate the severity of relapsing experimental autoimmune encephalomyelitis. *Journal of Immunology* 180:6457-6461.
- Bajaña, S., K. Roach, S. Turner, J. Paul, and S. Kovats. 2012. IRF4 promotes cutaneous dendritic cell migration to lymph nodes during homeostasis and inflammation. *Journal of Immunology* 189:3368-3377.
- Bakri, Y., S. Sarrazin, U.P. Mayer, S. Tillmanns, C. Nerlov, A. Boned, and M.H. Sieweke. 2005. Balance of MafB and PU.1 specifies alternative macrophage or dendritic cell fate. *Blood* 105:2707-2716.
- Becker, A.M., D.G. Michael, A.T. Satpathy, R. Sciammas, H. Singh, and D. Bhattacharya. 2012. IRF-8 extinguishes neutrophil production and promotes dendritic cell lineage commitment in both myeloid and lymphoid mouse progenitors. *Blood* 119:2003-2012.
- Björck, P. 2001. Isolation and characterization of plasmacytoid dendritic cells from Flt3 ligand and granulocyte-macrophage colony-stimulating factor-treated mice. *Blood* 98:3520-3526.
- Blasius, A.L., M. Celli, J. Maldonado, T. Takai, and M. Colonna. 2006a. Siglec-H is an IPC-specific receptor that modulates type I IFN secretion through DAP12. *Blood* 107:2474-2476.
- Blasius, A.L., E. Giurisato, M. Celli, R.D. Schreiber, A.S. Shaw, and M. Colonna. 2006b. Bone marrow stromal cell antigen 2 is a specific marker of type I IFN-producing cells in the naive mouse, but a promiscuous cell surface antigen following IFN stimulation. *Journal of Immunology* 177:3260-3265.
- Blasius, A.L., P. Krebs, B.M. Sullivan, M.B. Oldstone, and D.L. Popkin. 2012. Slc15a4, a gene required for pDC sensing of TLR ligands, is required to control persistent viral infection. *PLOS Pathogens* 8:e1002915.
- Blasius, A.L., W. Vermi, A. Krug, F. Facchetti, M. Celli, and M. Colonna. 2004. A cell-surface molecule selectively expressed on murine natural interferon-producing cells that blocks secretion of interferon-alpha. *Blood* 103:4201-4206.

- Cain, D.W., E.G. O’Koren, M.J. Kan, M. Womble, G.D. Sempowski, K. Hopper, M.D. Gunn, and G. Kelsoe. 2013. Identification of a tissue-specific, C/EBP β -dependent pathway of differentiation for murine peritoneal macrophages. *Journal of Immunology* 191:4665-4675.
- Carotta, S., A. Dakic, A. D’Amico, S.H.M. Pang, K.T. Greig, S.L. Nutt, and L. Wu. 2010. The transcription factor PU.1 controls dendritic cell development and Flt3 cytokine receptor expression in a dose-dependent manner. *Immunity* 32:628-641.
- Cassado, A.d.A., M.R. D’Império Lima, and K.R. Bortoluci. 2015. Revisiting mouse peritoneal macrophages: heterogeneity, development, and function. *Frontiers in Immunology* 6:2.
- Caton, M.L., M.R. Smith-Raska, and B. Reizis. 2007. Notch–RBP-J signaling controls the homeostasis of CD8 $^{-}$ dendritic cells in the spleen. *Journal of Experimental Medicine* 204:1653-1664.
- Cella, M., D. Jarrossay, F. Facchetti, O. Alebardi, H. Nakajima, A. Lanzavecchia, and M. Colonna. 1999. Plasmacytoid monocytes migrate to inflamed lymph nodes and produce large amounts of type I interferon. *Nature Medicine* 5:919-923.
- Cervantes-Barragan, L., K.L. Lewis, S. Firner, V. Thiel, S. Hugues, W. Reith, B. Ludewig, and B. Reizis. 2012. Plasmacytoid dendritic cells control T-cell response to chronic viral infection. *Proceedings of the National Academy of Sciences of the United States of America* 109:3012-3017.
- Cervantes-Barragan, L., R. Züst, F. Weber, M. Spiegel, K.S. Lang, S. Akira, V. Thiel, and B. Ludewig. 2007. Control of coronavirus infection through plasmacytoid dendritic-cell-derived type I interferon. *Blood* 109:1131-1137.
- Chen, Y.-L., T.-T. Chen, L.-M. Pai, J. Wesoly, H.A.R. Bluysen, and C.-K. Lee. 2013. A type I IFN-Flt3 ligand axis augments plasmacytoid dendritic cell development from common lymphoid progenitors. *Journal of Experimental Medicine* 210:2515-2522.
- Chow, K.V., A.M. Lew, R.M. Sutherland, and Y. Zhan. 2016. Monocyte-derived dendritic cells promote Th polarization, whereas conventional dendritic cells promote Th proliferation. *Journal of Immunology* 196:624-636.
- Cisse, B., M.L. Caton, M. Lehner, T. Maeda, S. Scheu, R. Locksley, D. Holmberg, C. Zweier, N.S. den Hollander, S.G. Kant, W. Holter, A. Rauch, Y. Zhuang, and B. Reizis. 2008.

Transcription factor E2-2 is an essential and specific regulator of plasmacytoid dendritic cell development. *Cell* 135:37-48.

Clausen, B.E., C. Burkhardt, W. Reith, R. Renkawitz, and I. Forster. 1999. Conditional gene targeting in macrophages and granulocytes using LysMcre mice. *Transgenic Research* 8:265-277.

Comijn, J., G. Berx, P. Vermassen, K. Verschueren, L. van Grunsven, E. Bruyneel, M. Mareel, D. Huylebroeck, and F. Van Roy. 2001. The two-handed E box binding zinc finger protein SIP1 downregulates E-cadherin and induces invasion. *Molecular Cell* 7:1267-1278.

Cordes, S.P., and G.S. Barsh. 1994. The mouse segmentation gene kr encodes a novel basic domain-leucine zipper transcription factor. *Cell* 79:1025-1034.

Crowley, M., K. Inaba, M. Witmer-Pack, and R.M. Steinman. 1989. The cell surface of mouse dendritic cells: FACS analyses of dendritic cells from different tissues including thymus. *Cellular Immunology* 118:108-125.

Croxford, A.L., M. Lanzinger, F.J. Hartmann, B. Schreiner, F. Mair, P. Pelczar, B.E. Clausen, S. Jung, M. Greter, and B. Becher. 2015. The cytokine GM-CSF drives the inflammatory signature of CCR2⁺ monocytes and licenses autoimmunity. *Immunity* 43:502-514.

Crozat, K., S. Tamoutounour, T.-P. Vu Manh, E. Fossum, H. Luche, L. Ardouin, M. Guilliams, H. Azukizawa, B. Bogen, B. Malissen, S. Henri, and M. Dalod. 2011. Expression of XCR1 defines mouse lymphoid-tissue resident and migratory dendritic cells of the CD8α⁺ type. *Journal of Immunology* 187:4411-4415.

den Haan, J.M.M., S.M. Lehar, and M.J. Bevan. 2000. CD8⁺ but not CD8⁻ dendritic cells cross-prime cytotoxic T cells in vivo. *Journal of Experimental Medicine* 192:1685-1696.

Denning, T.L., Y.-c. Wang, S.R. Patel, I.R. Williams, and B. Pulendran. 2007. Lamina propria macrophages and dendritic cells differentially induce regulatory and interleukin 17-producing T cell responses. *Nature Immunology* 8:1086-1094.

Diao, J., E. Winter, C. Cantin, W. Chen, L. Xu, D. Kelvin, J. Phillips, and M.S. Cattral. 2006. In situ replication of immediate dendritic cell (DC) precursors contributes to conventional DC homeostasis in lymphoid tissue. *Journal of Immunology* 176:7196-7206.

- Dominguez, C.X., R.A. Amezquita, T. Guan, H.D. Marshall, N.S. Joshi, S.H. Kleinstein, and S.M. Kaech. 2015. The transcription factors ZEB2 and T-bet cooperate to program cytotoxic T cell terminal differentiation in response to LCMV viral infection. *Journal of Experimental Medicine* 212:2041-2056.
- Dudziak, D., A.O. Kamphorst, G.F. Heidkamp, V.R. Buchholz, C. Trumppheller, S. Yamazaki, C. Cheong, K. Liu, H.-W. Lee, C.G. Park, R.M. Steinman, and M.C. Nussenzweig. 2007. Differential antigen processing by dendritic cell subsets in vivo. *Science* 315:107-111.
- Edelson, B.T., T.R. Bradstreet, K. Hildner, J.A. Carrero, K.E. Frederick, W. KC, R. Belizaire, T. Aoshi, R.D. Schreiber, M.J. Miller, T.L. Murphy, E.R. Unanue, and K.M. Murphy. 2011a. CD8 α ⁺ dendritic cells are an obligate cellular entry point for productive infection by Listeria monocytogenes. *Immunity* 35:236-248.
- Edelson, B.T., T.R. Bradstreet, W. KC, K. Hildner, J.W. Herzog, J. Sim, J.H. Russell, T.L. Murphy, E.R. Unanue, and K.M. Murphy. 2011b. Batf3-dependent CD11b^{low/-} peripheral dendritic cells are GM-CSF-independent and are not required for Th cell priming after subcutaneous immunization. *PLOS ONE* 6:e25660.
- Edelson, B.T., W. KC, R. Juang, M. Kohyama, L.A. Benoit, P.A. Klekotka, C. Moon, J.C. Albring, W. Ise, D.G. Michael, D. Bhattacharya, T.S. Stappenbeck, M.J. Holtzman, S.-S.J. Sung, T.L. Murphy, K. Hildner, and K.M. Murphy. 2010. Peripheral CD103⁺ dendritic cells form a unified subset developmentally related to CD8 α ⁺ conventional dendritic cells. *Journal of Experimental Medicine* 207:823-836.
- Elpek, K.G., A. Bellemare-Pelletier, D. Malhotra, E.D. Reynoso, V. Lukacs-Kornek, R.H. DeKruyff, and S.J. Turley. 2011. Lymphoid organ-resident dendritic cells exhibit unique transcriptional fingerprints based on subset and site. *PLOS ONE* 6:e23921.
- Feinberg, M.W., A.K. Wara, Z. Cao, M.A. Lebedeva, F. Rosenbauer, H. Iwasaki, H. Hirai, J.P. Katz, R.L. Haspel, S. Gray, K. Akashi, J. Segre, K.H. Kaestner, D.G. Tenen, and M.K. Jain. 2007. The Kruppel-like factor KLF4 is a critical regulator of monocyte differentiation. *EMBO Journal* 26:4138-4148.
- Felker, P., K. Seré, Q. Lin, C. Becker, M. Hristov, T. Hieronymus, and M. Zenke. 2010. TGF- β 1 accelerates dendritic cell differentiation from common dendritic cell progenitors and directs subset specification toward conventional dendritic cells. *Journal of Immunology* 185:5326-5335.

- Fogg, D.K., C. Sibon, C. Miled, S. Jung, P. Aucouturier, D.R. Littman, A. Cumano, and F. Geissmann. 2006. A clonogenic bone marrow progenitor specific for macrophages and dendritic cells. *Science* 311:83-87.
- Franco, C.B., C.-C. Chen, M. Drukker, I.L. Weissman, and S.J. Galli. 2010. Distinguishing mast cell and granulocyte differentiation at the single-cell level. *Cell Stem Cell* 6:361-368.
- Franklin, R.A., W. Liao, A. Sarkar, M.V. Kim, M.R. Bivona, K. Liu, E.G. Pamer, and M.O. Li. 2014. The cellular and molecular origin of tumor-associated macrophages. *Science* 344:921-925.
- Gao, Y., S.A. Nish, R. Jiang, L. Hou, P. Licona-Limon, J.S. Weinstein, H. Zhao, and R. Medzhitov. 2013. Control of T helper 2 responses by transcription factor IRF4-dependent dendritic cells. *Immunity* 39:722-732.
- Gautier, E.L., T. Shay, J. Miller, M. Greter, C. Jakubzick, S. Ivanov, J. Helft, A. Chow, K.G. Elpek, S. Gordonov, A.R. Mazloom, A. Ma'ayan, W.-J. Chua, T.H. Hansen, S.J. Turley, M. Merad, G.J. Randolph, and Immunological Genome Consortium. 2012. Gene-expression profiles and transcriptional regulatory pathways that underlie the identity and diversity of mouse tissue macrophages. *Nature Immunology* 13:1118-1128.
- Ghosh, H.S., M. Ceribelli, I. Matos, A. Lazarovici, H.J. Bussemaker, A. Lasorella, S.W. Hiebert, K. Liu, L.M. Staudt, and B. Reizis. 2014. ETO family protein Mtg16 regulates the balance of dendritic cell subsets by repressing Id2. *Journal of Experimental Medicine* 211:1623-1635.
- Ghosh, H.S., B. Cisse, A. Bunin, K.L. Lewis, and B. Reizis. 2010. Continuous expression of the transcription factor E2-2 maintains the cell fate of mature plasmacytoid dendritic cells. *Immunity* 33:905-916.
- Ginhoux, F., M. Greter, M. Leboeuf, S. Nandi, P. See, S. Gokhan, M.F. Mehler, S.J. Conway, L.G. Ng, E.R. Stanley, I.M. Samokhvalov, and M. Merad. 2010. Fate mapping analysis reveals that adult microglia derive from primitive macrophages. *Science* 330:841-845.
- Ginhoux, F., and S. Jung. 2014. Monocytes and macrophages: developmental pathways and tissue homeostasis. *Nature Reviews Immunology* 14:392-404.
- Ginhoux, F., K. Liu, J. Helft, M. Bogunovic, M. Greter, D. Hashimoto, J. Price, N. Yin, J. Bromberg, S.A. Lira, E.R. Stanley, M. Nussenzweig, and M. Merad. 2009. The origin

and development of nonlymphoid tissue CD103⁺ DCs. *Journal of Experimental Medicine* 206:3115-3130.

Ginhoux, F., F. Tacke, V. Angeli, M. Bogunovic, M. Loubeau, X.-M. Dai, E.R. Stanley, G.J. Randolph, and M. Merad. 2006. Langerhans cells arise from monocytes in vivo. *Nature Immunology* 7:265-273.

Gorman, J.R., N. van der Stoep, R. Monroe, M. Cogne, L. Davidson, and F.W. Alt. 1996. The Igκ enhancer influences the ratio of Igκ versus Igλ B lymphocytes. *Immunity* 5:241-252.

Gosselin, D., V.M. Link, C.E. Romanoski, G.J. Fonseca, D.Z. Eichenfield, N.J. Spann, J.D. Stender, H.B. Chun, H. Garner, F. Geissmann, and C.K. Glass. 2014. Environment drives selection and function of enhancers controlling tissue-specific macrophage identities. *Cell* 159:1327-1340.

Grajales-Reyes, G.E., A. Iwata, J. Albring, X. Wu, R. Tussiwand, W. KC, N.M. Kretzer, C.G. Briseño, V. Durai, P. Bagadia, M. Haldar, J. Schönheit, F. Rosenbauer, T.L. Murphy, and K.M. Murphy. 2015. Batf3 maintains autoactivation of Irf8 for commitment of a CD8α⁺ conventional DC clonogenic progenitor. *Nature Immunology* 16:708-717.

Greter, M., J. Helft, A. Chow, D. Hashimoto, A. Mortha, J. Agudo-Cantero, M. Bogunovic, E.L. Gautier, J. Miller, M. Leboeuf, G. Lu, C. Aloman, B.D. Brown, J.W. Pollard, H. Xiong, G.J. Randolph, J.E. Chipuk, P.S. Frenette, and M. Merad. 2012a. GM-CSF controls nonlymphoid tissue dendritic cell homeostasis but is dispensable for the differentiation of inflammatory dendritic cells. *Immunity* 36:1031-1046.

Greter, M., I. Lelios, P. Pelczar, G. Hoeffel, J. Price, M. Leboeuf, T.M. Kundig, K. Frei, F. Ginhoux, M. Merad, and B. Becher. 2012b. Stroma-derived interleukin-34 controls the development and maintenance of langerhans cells and the maintenance of microglia. *Immunity* 37:1050-1060.

Guilliams, M., F. Ginhoux, C. Jakubzick, S.H. Naik, N. Onai, B.U. Schraml, E. Segura, R. Tussiwand, and S. Yona. 2014. Dendritic cells, monocytes and macrophages: a unified nomenclature based on ontogeny. *Nature Reviews Immunology* 14:571-578.

Hacker, C., R.D. Kirsch, X.-S. Ju, T. Hieronymus, T.C. Gust, C. Kuhl, T. Jorgas, S.M. Kurz, S. Rose-John, Y. Yokota, and M. Zenke. 2003. Transcriptional profiling identifies Id2 function in dendritic cell development. *Nature Immunology* 4:380-386.

Hall, J.C., and A. Rosen. 2010. Type I interferons: crucial participants in disease amplification in autoimmunity. *Nature Reviews Rheumatology* 6:40-49.

Hashimoto, D., A. Chow, C. Noizat, P. Teo, M.B. Beasley, M. Leboeuf, C.D. Becker, P. See, J. Price, D. Lucas, M. Greter, A. Mortha, S.W. Boyer, E.C. Forsberg, M. Tanaka, N. van Rooijen, A. Garcia-Sastre, E.R. Stanley, F. Ginhoux, P.S. Frenette, and M. Merad. 2013. Tissue-resident macrophages self-maintain locally throughout adult life with minimal contribution from circulating monocytes. *Immunity* 38:792-804.

Helft, J., J. Bottcher, P. Chakravarty, S. Zelenay, J. Huotari, B.U. Schraml, D. Goubau, and C. Reis e Sousa. 2015. GM-CSF mouse bone marrow cultures comprise a heterogeneous population of CD11c⁺MHCII⁺ macrophages and dendritic cells. *Immunity* 42:1197-1211.

Henri, S., L.F. Poulin, S. Tamoutounour, L. Ardouin, M. Guilliams, B. de Bovis, E. Devilard, C. Viret, H. Azukizawa, A. Kisselkell, and B. Malissen. 2010. CD207⁺ CD103⁺ dermal dendritic cells cross-present keratinocyte-derived antigens irrespective of the presence of Langerhans cells. *Journal of Experimental Medicine* 207:189-206.

Hertwig, P. 1942. Neue Mutationen und Koppelungsgruppen bei der Hausmaus. *Zeitschrift für Induktive Abstammungs- und Vererbungslehre* 80:220-246.

Hettinger, J., D.M. Richards, J. Hansson, M.M. Barra, A.-C. Joschko, J. Krijgsveld, and M. Feuerer. 2013. Origin of monocytes and macrophages in a committed progenitor. *Nature Immunology* 14:821-830.

Higashi, Y., M. Maruhashi, L. Nelles, T. Van de Putte, K. Verschueren, T. Miyoshi, A. Yoshimoto, H. Kondoh, and D. Huylebroeck. 2002. Generation of the floxed allele of the SIP1 (Smad-interacting protein 1) gene for Cre-mediated conditional knockout in the mouse. *Genesis* 32:82-84.

Hildner, K., B.T. Edelson, W.E. Purtha, M. Diamond, H. Matsushita, M. Kohyama, B. Calderon, B.U. Schraml, E.R. Unanue, M.S. Diamond, R.D. Schreiber, T.L. Murphy, and K.M. Murphy. 2008. Batf3 deficiency reveals a critical role for CD8α⁺ dendritic cells in cytotoxic T cell immunity. *Science* 322:1097-1100.

Hoeffel, G., Y. Wang, M. Greter, P. See, P. Teo, B. Malleret, M. Leboeuf, D. Low, G. Oller, F. Almeida, S.H.Y. Choy, M. Grisotto, L. Renia, S.J. Conway, E.R. Stanley, J.K.Y. Chan,

L.G. Ng, I.M. Samokhvalov, M. Merad, and F. Ginhoux. 2012. Adult Langerhans cells derive predominantly from embryonic fetal liver monocytes with a minor contribution of yolk sac-derived macrophages. *Journal of Experimental Medicine* 209:1167-1181.

Hume, D.A., N. Mabbott, S. Raza, and T.C. Freeman. 2013. Can DCs be distinguished from macrophages by molecular signatures? *Nature Immunology* 14:187-189.

Iizumi, S., Y. Nomura, S. So, K. Uegaki, K. Aoki, K.-i. Shibahara, N. Adachi, and H. Koyama. 2006. Simple one-week method to construct gene-targeting vectors: application to production of human knockout cell lines. *Biotechniques* 41:311-316.

Inaba, K., M. Inaba, N. Romani, H. Aya, M. Deguchi, S. Ikebara, S. Muramatsu, and R.M. Steinman. 1992. Generation of large numbers of dendritic cells from mouse bone marrow cultures supplemented with granulocyte/macrophage colony-stimulating factor. *Journal of Experimental Medicine* 176:1693-1702.

Ioannou, M., T. Alissafi, L. Boon, D. Boumpas, and P. Verginis. 2013. In vivo ablation of plasmacytoid dendritic cells inhibits autoimmunity through expansion of myeloid-derived suppressor cells. *Journal of Immunology* 190:2631-2640.

Isaksson, M., B. Ardesjö, L. Rönnblom, O. Kämpe, H. Lassmann, M.-L. Eloranta, and A. Lobell. 2009. Plasmacytoid DC promote priming of autoimmune Th17 cells and EAE. *European Journal of Immunology* 39:2925-2935.

Jackson, J.T., Y. Hu, R. Liu, F. Masson, A. D'Amico, S. Carotta, A. Xin, M.J. Camilleri, A.M. Mount, A. Kallies, L. Wu, G.K. Smyth, S.L. Nutt, and G.T. Belz. 2011. Id2 expression delineates differential checkpoints in the genetic program of CD8 α^+ and CD103 $^+$ dendritic cell lineages. *EMBO Journal* 30:2690-2704.

Jakubzick, C., E.L. Gautier, S.L. Gibbings, D.K. Sojka, A. Schlitzer, T.E. Johnson, S. Ivanov, Q. Duan, S. Bala, T. Condon, N. van Rooijen, J.R. Grainger, Y. Belkaid, A. Ma'ayan, D.W.H. Riches, W.M. Yokoyama, F. Ginhoux, P.M. Henson, and G.J. Randolph. 2013. Minimal differentiation of classical monocytes as they survey steady-state tissues and transport antigen to lymph nodes. *Immunity* 39:599-610.

Ji, M., H. Li, H.C. Suh, K.D. Klarmann, Y. Yokota, and J.R. Keller. 2008. Id2 intrinsically regulates lymphoid and erythroid development via interaction with different target proteins. *Blood* 112:1068-1077.

Jovanovic, M., M.S. Rooney, P. Mertins, D. Przybylski, N. Chevrier, R. Satija, E.H. Rodriguez, A.P. Fields, S. Schwartz, R. Raychowdhury, M.R. Mumbach, T. Eisenhaure, M. Rabani, D. Gennert, D. Lu, T. Delorey, J.S. Weissman, S.A. Carr, N. Hacohen, and A. Regev. 2015. Dynamic profiling of the protein life cycle in response to pathogens. *Science* 347:1259038.

Kamphorst, A.O., P. Guermonprez, D. Dudziak, and M.C. Nussenzweig. 2010. Route of antigen uptake differentially impacts presentation by dendritic cells and activated monocytes. *Journal of Immunology* 185:3426-3435.

Kashiwada, M., N.-L.L. Pham, L.L. Pewe, J.T. Harty, and P.B. Rothman. 2011. NFIL3/E4BP4 is a key transcription factor for CD8 α^+ dendritic cell development. *Blood* 117:6193-6197.

Kelly, L.M., U. Englmeier, I. Lafon, M.H. Sieweke, and T. Graf. 2000. MafB is an inducer of monocytic differentiation. *EMBO Journal* 19:1987-1997.

Kiel, M.J., O.H. Yilmaz, T. Iwashita, O.H. Yilmaz, C. Terhorst, and S.J. Morrison. 2005. SLAM family receptors distinguish hematopoietic stem and progenitor cells and reveal endothelial niches for stem cells. *Cell* 121:1109-1121.

Kingston, D., M.A. Schmid, N. Onai, A. Obata-Onai, D. Baumjohann, and M.G. Manz. 2009. The concerted action of GM-CSF and Flt3-ligand on in vivo dendritic cell homeostasis. *Blood* 114:835-843.

Kurotaki, D., N. Osato, A. Nishiyama, M. Yamamoto, T. Ban, H. Sato, J. Nakabayashi, M. Umehara, N. Miyake, N. Matsumoto, M. Nakazawa, K. Ozato, and T. Tamura. 2013. Essential role of the IRF8-KLF4 transcription factor cascade in murine monocyte differentiation. *Blood* 121:1839-1849.

Langlet, C., S. Tamoutounour, S. Henri, H. Luche, L. Arduin, C. Gregoire, B. Malissen, and M. Guilliams. 2012. CD64 expression distinguishes monocyte-derived and conventional dendritic cells and reveals their distinct role during intramuscular immunization. *Journal of Immunology* 188:1751-1760.

Laouar, Y., T. Welte, X.-Y. Fu, and R.A. Flavell. 2003. STAT3 is required for Flt3L-dependent dendritic cell differentiation. *Immunity* 19:903-912.

- Lavin, Y., D. Winter, R. Blecher-Gonen, E. David, H. Keren-Shaul, M. Merad, S. Jung, and I. Amit. 2014. Tissue-resident macrophage enhancer landscapes are shaped by the local microenvironment. *Cell* 159:1312-1326.
- Lechler, R.I., and J.R. Batchelor. 1982. Restoration of immunogenicity to passenger cell-depleted kidney allografts by the addition of donor strain dendritic cells. *Journal of Experimental Medicine* 155:31-41.
- Lee, J.-K., and M.G. Tansey. 2013. Microglia isolation from adult mouse brain. *Methods in Molecular Biology* 1041:17-23.
- Lewis, K.L., M.L. Caton, M. Bogunovic, M. Greter, L.T. Grajkowska, D. Ng, A. Klinakis, I.F. Charo, S. Jung, J.L. Gommerman, I.I. Ivanov, K. Liu, M. Merad, and B. Reizis. 2011. Notch2 receptor signaling controls functional differentiation of dendritic cells in the spleen and intestine. *Immunity* 35:780-791.
- Li, H.S., A. Gelbard, G.J. Martinez, E. Esashi, H. Zhang, H. Nguyen-Jackson, Y.-J. Liu, W.W. Overwijk, and S.S. Watowich. 2011. Cell-intrinsic role for IFN- α -STAT1 signals in regulating murine Peyer patch plasmacytoid dendritic cells and conditioning an inflammatory response. *Blood* 118:3879-3889.
- Li, J.J., P.J. Bickel, and M.D. Biggin. 2014. System wide analyses have underestimated protein abundances and the importance of transcription in mammals. *PeerJ* 2:e270.
- Liu, C.-J., E. Chang, J. Yu, C.S. Carlson, L. Prazak, X.-P. Yu, B. Ding, P. Lengyel, and P.E. Di Cesare. 2005. The interferon-inducible p204 protein acts as a transcriptional coactivator of Cbfa1 and enhances osteoblast differentiation. *Journal of Biological Chemistry* 280:2788-2796.
- Liu, K., G.D. Victora, T.A. Schwickert, P. Guermonprez, M.M. Meredith, K. Yao, F.-F. Chu, G.J. Randolph, A.Y. Rudensky, and M. Nussenzweig. 2009. In vivo analysis of dendritic cell development and homeostasis. *Science* 324:392-397.
- Liu, K., C. Waskow, X. Liu, K. Yao, J. Hoh, and M. Nussenzweig. 2007. Origin of dendritic cells in peripheral lymphoid organs of mice. *Nature Immunology* 8:578-583.
- Liu, P., J.R. Keller, M. Ortiz, L. Tessarollo, R.A. Rachel, T. Nakamura, N.A. Jenkins, and N.G. Copeland. 2003. Bcl11a is essential for normal lymphoid development. *Nature Immunology* 4:525-532.

- Lombardi, V., A.O. Speak, J. Kerzerho, N. Szely, and O. Akbari. 2012. CD8 α^+ β^- and CD8 α^+ β^+ plasmacytoid dendritic cells induce Foxp3 $^+$ regulatory T cells and prevent the induction of airway hyper-reactivity. *Mucosal Immunology* 5:432-443.
- Luan, Y., X.-P. Yu, N. Yang, S. Frenkel, L. Chen, and C.-j. Liu. 2008. p204 protein overcomes the inhibition of core binding factor α -1-mediated osteogenic differentiation by Id helix-loop-helix proteins. *Molecular Biology of the Cell* 19:2113-2126.
- Manfra, D.J., S.-C. Chen, K.K. Jensen, J.S. Fine, M.T. Wiekowski, and S.A. Lira. 2003. Conditional expression of murine Flt3 ligand leads to expansion of multiple dendritic cell subsets in peripheral blood and tissues of transgenic mice. *Journal of Immunology* 170:2843-2852.
- Maraskovsky, E., K. Brasel, M. Teepe, E.R. Roux, S.D. Lyman, K. Shortman, and H.J. McKenna. 1996. Dramatic increase in the numbers of functionally mature dendritic cells in Flt3 ligand-treated mice: multiple dendritic cell subpopulations identified. *Journal of Experimental Medicine* 184:1953-1962.
- Mashayekhi, M., M.M. Sandau, I.R. Dunay, E.M. Frickel, A. Khan, R.S. Goldszmid, A. Sher, H.L. Ploegh, T.L. Murphy, L.D. Sibley, and K.M. Murphy. 2011. CD8 α^+ dendritic cells are the critical source of interleukin-12 that controls acute infection by Toxoplasma gondii tachyzoites. *Immunity* 35:249-259.
- McKenna, H.J., K.L. Stocking, R.E. Miller, K. Brasel, T. De Smedt, E. Maraskovsky, C.R. Maliszewski, D.H. Lynch, J. Smith, B. Pulendran, E.R. Roux, M. Teepe, S.D. Lyman, and J.J. Peschon. 2000. Mice lacking flt3 ligand have deficient hematopoiesis affecting hematopoietic progenitor cells, dendritic cells, and natural killer cells. *Blood* 95:3489-3497.
- Merad, M., and M.G. Manz. 2009. Dendritic cell homeostasis. *Blood* 113:3418-3427.
- Merad, M., M.G. Manz, H. Karsunky, A. Wagers, W. Peters, I. Charo, I.L. Weissman, J.G. Cyster, and E.G. Engleman. 2002. Langerhans cells renew in the skin throughout life under steady-state conditions. *Nature Immunology* 3:1135-1141.
- Merad, M., P. Sathe, J. Helft, J. Miller, and A. Mortha. 2013. The dendritic cell lineage: ontogeny and function of dendritic cells and their subsets in the steady state and the inflamed setting. *Annual Review of Immunology* 31:563-604.

- Meredith, M.M., K. Liu, G. Darrasse-Jèze, A.O. Kamphorst, H.A. Schreiber, P. Guermonprez, J. Idoyaga, C. Cheong, K.-H. Yao, R.E. Niec, and M.C. Nussenzweig. 2012. Expression of the zinc finger transcription factor zDC (Zbtb46, Btbd4) defines the classical dendritic cell lineage. *Journal of Experimental Medicine* 209:1153-1165.
- Miller, J.C., B.D. Brown, T. Shay, E.L. Gautier, V. Jojic, A. Cohain, G. Pandey, M. Leboeuf, K.G. Elpek, J. Helft, D. Hashimoto, A. Chow, J. Price, M. Greter, M. Bogunovic, A. Bellemare-Pelletier, P.S. Frenette, G.J. Randolph, S.J. Turley, M. Merad, and Immunological Genome Consortium. 2012. Deciphering the transcriptional network of the dendritic cell lineage. *Nature Immunology* 13:888-899.
- Mollah, S.A., J.S. Dobrin, R.E. Feder, S.-W. Tse, I.G. Matos, C. Cheong, R.M. Steinman, and N. Anandasabapathy. 2014. Flt3L dependence helps define an uncharacterized subset of murine cutaneous dendritic cells. *Journal of Investigative Dermatology* 134:1265-1275.
- Moore, T.A., U. von Freeden-Jeffry, R. Murray, and A. Zlotnik. 1996. Inhibition of $\gamma\delta$ T cell development and early thymocyte maturation in IL-7 $-/-$ mice. *Journal of Immunology* 157:2366-2373.
- Moriguchi, T., M. Hamada, N. Morito, T. Terunuma, K. Hasegawa, C. Zhang, T. Yokomizo, R. Esaki, E. Kuroda, K. Yoh, T. Kudo, M. Nagata, D.R. Greaves, J.D. Engel, M. Yamamoto, and S. Takahashi. 2006. MafB is essential for renal development and F4/80 expression in macrophages. *Molecular and Cellular Biology* 26:5715-5727.
- Mosser, D.M., and J.P. Edwards. 2008. Exploring the full spectrum of macrophage activation. *Nature Reviews Immunology* 8:958-969.
- Murray, P.J., and T.A. Wynn. 2011. Protective and pathogenic functions of macrophage subsets. *Nature Reviews Immunology* 11:723-737.
- Naik, S.H., D. Metcalf, A. van Nieuwenhuijze, I. Wicks, L. Wu, M. O'Keeffe, and K. Shortman. 2006. Intrasplenic steady-state dendritic cell precursors that are distinct from monocytes. *Nature Immunology* 7:663-671.
- Naik, S.H., P. Sathe, H.-Y. Park, D. Metcalf, A.I. Proietto, A. Dakic, S. Carotta, M. O'Keeffe, M. Bahlo, A. Papenfuss, J.-Y. Kwak, L. Wu, and K. Shortman. 2007. Development of plasmacytoid and conventional dendritic cell subtypes from single precursor cells derived in vitro and in vivo. *Nature Immunology* 8:1217-1226.

- Nakamura, T., Y. Yamazaki, Y. Saiki, M. Moriyama, D.A. Largaespada, N.A. Jenkins, and N.G. Copeland. 2000. Evi9 encodes a novel zinc finger protein that physically interacts with BCL6, a known human B-cell proto-oncogene product. *Molecular and Cellular Biology* 20:3178-3186.
- Nakano, H., M. Yanagita, and M.D. Gunn. 2001. CD11c⁺B220⁺Gr-1⁺ cells in mouse lymph nodes and spleen display characteristics of plasmacytoid dendritic cells. *Journal of Experimental Medicine* 194:1171-1178.
- Neuenhahn, M., K.M. Kerksiek, M. Nauerth, M.H. Suhre, M. Schiemann, F.E. Gebhardt, C. Stemberger, K. Panthel, S. Schröder, T. Chakraborty, S. Jung, H. Hochrein, H. Rüssmann, T. Brocker, and D.H. Busch. 2006. CD8α⁺ dendritic cells are required for efficient entry of Listeria monocytogenes into the spleen. *Immunity* 25:619-630.
- Ogawa, M., Y. Matsuzaki, S. Nishikawa, S.-I. Hayashi, T. Kunisada, T. Sudo, T. Kina, H. Nakauchi, and S.-I. Nishikawa. 1991. Expression and function of c-kit in hemopoietic progenitor cells. *Journal of Experimental Medicine* 174:63-71.
- Omilusik, K.D., J.A. Best, B. Yu, S. Goossens, A. Weidemann, J.V. Nguyen, E. Seuntjens, A. Stryjewska, C. Zweier, R. Roychoudhuri, L. Gattinoni, L.M. Bird, Y. Higashi, H. Kondoh, D. Huylebroeck, J. Haigh, and A.W. Goldrath. 2015. Transcriptional repressor ZEB2 promotes terminal differentiation of CD8⁺ effector and memory T cell populations during infection. *Journal of Experimental Medicine* 212:2027-2039.
- Onai, N., K. Kurabayashi, M. Hosoi-Amaike, N. Toyama-Sorimachi, K. Matsushima, K. Inaba, and T. Ohteki. 2013. A clonogenic progenitor with prominent plasmacytoid dendritic cell developmental potential. *Immunity* 38:943-957.
- Onai, N., A. Obata-Onai, M.A. Schmid, T. Ohteki, D. Jarrossay, and M.G. Manz. 2007. Identification of clonogenic common Flt3⁺M-CSFR⁺ plasmacytoid and conventional dendritic cell progenitors in mouse bone marrow. *Nature Immunology* 8:1207-1216.
- Onai, N., A. Obata-Onai, R. Tussiwand, A. Lanzavecchia, and M.G. Manz. 2006. Activation of the Flt3 signal transduction cascade rescues and enhances type I interferon-producing and dendritic cell development. *Journal of Experimental Medicine* 203:227-238.
- Paul, F., Y.a. Arkin, A. Giladi, D.A. Jaitin, E. Kenigsberg, H. Keren-Shaul, D. Winter, D. Lara-Astiaso, M. Gury, A. Weiner, E. David, N. Cohen, F.K.B. Lauridsen, S. Haas, A.

Schlitzer, A. Mildner, F. Ginhoux, S. Jung, A. Trumpp, B.T. Porse, A. Tanay, and I. Amit. 2015. Transcriptional heterogeneity and lineage commitment in myeloid progenitors. *Cell* 163:1663-1677.

Pelayo, R., J. Hirose, J. Huang, K.P. Garrett, A. Delogu, M. Busslinger, and P.W. Kincade. 2005. Derivation of 2 categories of plasmacytoid dendritic cells in murine bone marrow. *Blood* 105:4407-4415.

Plantinga, M., M. Guilliams, M. Vanheerswynghels, K. Deswarte, F. Branco-Madeira, W. Toussaint, L. Vanhoutte, K. Neyt, N. Killeen, B. Malissen, H. Hammad, and B.N. Lambrecht. 2013. Conventional and monocyte-derived CD11b⁺ dendritic cells initiate and maintain T helper 2 cell-mediated immunity to house dust mite allergen. *Immunity* 38:322-335.

Pulford, K., A.H. Banham, L. Lyne, M. Jones, G.C. Ippolito, H. Liu, P.W. Tucker, G. Roncador, E. Lucas, S. Ashe, L. Stockwin, R. Walewska, L. Karran, R.D. Gascoyne, D.Y. Mason, and M.J. Dyer. 2006. The BCL11A_{XL} transcription factor: its distribution in normal and malignant tissues and use as a marker for plasmacytoid dendritic cells. *Leukemia* 20:1439-1441.

Randolph, G.J., and M. Merad. 2013. Reply to: "Can DCs be distinguished from macrophages by molecular signatures?". *Nature Immunology* 14:189-190.

Ranganath, S., W. Ouyang, D. Bhattacharya, W.C. Sha, A. Grupe, G. Peltz, and K.M. Murphy. 1998. GATA-3-dependent enhancer activity in IL-4 gene regulation. *Journal of Immunology* 161:3822-3826.

Reizis, B., A. Bunin, H.S. Ghosh, K.L. Lewis, and V. Sisirak. 2011a. Plasmacytoid dendritic cells: recent progress and open questions. *Annual Review of Immunology* 29:163-183.

Reizis, B., M. Colonna, G. Trinchieri, F. Barrat, and M. Gilliet. 2011b. Plasmacytoid dendritic cells: one-trick ponies or workhorses of the immune system? *Nature Reviews Immunology* 11:558-565.

Rivollier, A., J. He, A. Kole, V. Valatas, and B.L. Kelsall. 2012. Inflammation switches the differentiation program of Ly6C^{hi} monocytes from antiinflammatory macrophages to inflammatory dendritic cells in the colon. *Journal of Experimental Medicine* 209:139-155.

- Ryan, M.D., A.M. King, and G.P. Thomas. 1991. Cleavage of foot-and-mouth disease virus polyprotein is mediated by residues located within a 19 amino acid sequence. *Journal of General Virology* 72 (Pt 11):2727-2732.
- Sallusto, F., and A. Lanzavecchia. 1994. Efficient presentation of soluble antigen by cultured human dendritic cells is maintained by granulocyte/macrophage colony-stimulating factor plus interleukin 4 and downregulated by tumor necrosis factor alpha. *Journal of Experimental Medicine* 179:1109-1118.
- Sankaran, V.G., J. Xu, T. Ragoczy, G.C. Ippolito, C.R. Walkley, S.D. Maika, Y. Fujiwara, M. Ito, M. Groudine, M.A. Bender, P.W. Tucker, and S.H. Orkin. 2009. Developmental and species-divergent globin switching are driven by BCL11A. *Nature* 460:1093-1097.
- Sato, M., N. Hata, M. Asagiri, T. Nakaya, T. Taniguchi, and N. Tanaka. 1998. Positive feedback regulation of type I IFN genes by the IFN-inducible transcription factor IRF-7. *FEBS Letters* 441:106-110.
- Satpathy, A.T., C.G. Briseño, J.S. Lee, D. Ng, N.A. Manieri, W. KC, X. Wu, S.R. Thomas, W.-L. Lee, M. Turkoz, K.G. McDonald, M.M. Meredith, C. Song, C.J. Guidos, R.D. Newberry, W. Ouyang, T.L. Murphy, T.S. Stappenbeck, J.L. Gommerman, M.C. Nussenzweig, M. Colonna, R. Kopan, and K.M. Murphy. 2013. Notch2-dependent classical dendritic cells orchestrate intestinal immunity to attaching-and-effacing bacterial pathogens. *Nature Immunology* 14:937-948.
- Satpathy, A.T., W. KC, J.C. Albring, B.T. Edelson, N.M. Kretzer, D. Bhattacharya, T.L. Murphy, and K.M. Murphy. 2012a. Zbtb46 expression distinguishes classical dendritic cells and their committed progenitors from other immune lineages. *Journal of Experimental Medicine* 209:1135-1152.
- Satpathy, A.T., K.M. Murphy, and W. KC. 2011. Transcription factor networks in dendritic cell development. *Seminars in Immunology* 23:388-397.
- Satpathy, A.T., X. Wu, J.C. Albring, and K.M. Murphy. 2012b. Re(de)fining the dendritic cell lineage. *Nature Immunology* 13:1145-1154.
- Satterwhite, E., T. Sonoki, T.G. Willis, L. Harder, R. Nowak, E.L. Arriola, H. Liu, H.P. Price, S. Gesk, D. Steinemann, B. Schlegelberger, D.G. Oscier, R. Siebert, P.W. Tucker, and M.J.

Dyer. 2001. The BCL11 gene family: involvement of BCL11A in lymphoid malignancies. *Blood* 98:3413-3420.

Schaller, E., A.J. Macfarlane, R.A. Rupec, S. Gordon, A.J. McKnight, and K. Pfeffer. 2002. Inactivation of the F4/80 glycoprotein in the mouse germ line. *Molecular and Cellular Biology* 22:8035-8043.

Schiavoni, G., F. Mattei, P. Sestili, P. Borghi, M. Venditti, H.C. Morse, F. Belardelli, and L. Gabriele. 2002. ICSBP is essential for the development of mouse type I interferon-producing cells and for the generation and activation of CD8 α + dendritic cells. *Journal of Experimental Medicine* 196:1415-1425.

Schlitzer, A., N. McGovern, P. Teo, T. Zelante, K. Atarashi, D. Low, A.W.S. Ho, P. See, A. Shin, P.S. Wasan, G. Hoeffel, B. Malleret, A. Heiseke, S. Chew, L. Jardine, H.A. Purvis, C.M.U. Hilkens, J. Tam, M. Poidinger, E.R. Stanley, A.B. Krug, L. Renia, B. Sivasankar, L.G. Ng, M. Collin, P. Ricciardi-Castagnoli, K. Honda, M. Haniffa, and F. Ginhoux. 2013. IRF4 transcription factor-dependent CD11b $^+$ dendritic cells in human and mouse control mucosal IL-17 cytokine responses. *Immunity* 38:970-983.

Schlitzer, A., V. Sivakamasundari, J. Chen, H.R.B. Sumatoh, J. Schreuder, J. Lum, B. Malleret, S. Zhang, A. Larbi, F. Zolezzi, L. Renia, M. Poidinger, S. Naik, E.W. Newell, P. Robson, and F. Ginhoux. 2015. Identification of cDC1- and cDC2-committed DC progenitors reveals early lineage priming at the common DC progenitor stage in the bone marrow. *Nature Immunology* 16:718-728.

Schotte, R., M. Nagasawa, K. Weijer, H. Spits, and B. Blom. 2004. The ETS transcription factor Spi-B is required for human plasmacytoid dendritic cell development. *Journal of Experimental Medicine* 200:1503-1509.

Schraml, B.U., J. van Blijswijk, S. Zelenay, P.G. Whitney, A. Filby, S.E. Acton, N.C. Rogers, N. Moncaut, J.J. Carvajal, and C. Reis e Sousa. 2013. Genetic tracing via DNGR-1 expression history defines dendritic cells as a hematopoietic lineage. *Cell* 154:843-858.

Schulz, C., E. Gomez Perdiguero, L. Chorro, H. Szabo-Rogers, N. Cagnard, K. Kierdorf, M. Prinz, B. Wu, S.E.W. Jacobsen, J.W. Pollard, J. Frampton, K.J. Liu, and F. Geissmann. 2012. A lineage of myeloid cells independent of Myb and hematopoietic stem cells. *Science* 336:86-90.

- Schwanhäusser, B., D. Busse, N. Li, G. Dittmar, J. Schuchhardt, J. Wolf, W. Chen, and M. Selbach. 2011. Global quantification of mammalian gene expression control. *Nature* 473:337-342.
- Scott, C.L., B. Soen, L. Martens, N. Skrypek, W. Saelens, J. Taminau, G. Blancke, G. Van Isterdael, D. Huylebroeck, J. Haigh, Y. Saeys, M. Guilliams, B.N. Lambrecht, and G. Berx. 2016. The transcription factor Zeb2 regulates development of conventional and plasmacytoid DCs by repressing Id2. *Journal of Experimental Medicine* 213:897-911.
- Seillet, C., J.T. Jackson, K.A. Markey, H.J.M. Brady, G.R. Hill, K.P.A. Macdonald, S.L. Nutt, and G.T. Belz. 2013. CD8α+ DCs can be induced in the absence of transcription factors Id2, Nfil3, and Batf3. *Blood* 121:1574-1583.
- Seré, K., J.-H. Baek, J. Ober-Blöbaum, G. Müller-Newen, F. Tacke, Y. Yokota, M. Zenke, and T. Hieronymus. 2012. Two distinct types of Langerhans cells populate the skin during steady state and inflammation. *Immunity* 37:905-916.
- Siegal, F.P., N. Kadowaki, M. Shodell, P.A. Fitzgerald-Bocarsly, K. Shah, S. Ho, S. Antonenko, and Y.-J. Liu. 1999. The nature of the principal type 1 interferon-producing cells in human blood. *Science* 284:1835-1837.
- Silberberg-Sinakin, I., G.J. Thorbecke, R.L. Baer, S.A. Rosenthal, and V. Berezowsky. 1976. Antigen-bearing Langerhans cells in skin, dermal lymphatics and in lymph nodes. *Cellular Immunology* 25:137-151.
- Sitnicka, E., N. Buza-Vidas, H. Ahlenius, C.M. Cilio, C. Gekas, J.M. Nygren, R. Mansson, M. Cheng, C.T. Jensen, M. Svensson, K. Leandersson, W.W. Agace, M. Sigvardsson, and S.E.W. Jacobsen. 2007. Critical role of FLT3 ligand in IL-7 receptor independent T lymphopoiesis and regulation of lymphoid-primed multipotent progenitors. *Blood* 110:2955-2964.
- Soucie, E.L., Z. Weng, L. Geirsdottir, K. Molawi, J. Maurizio, R. Fenouil, N. Mossadegh-Keller, G. Gimenez, L. VanHille, M. Beniazza, J. Favret, C. Berruyer, P. Perrin, N. Hacohen, J.-C. Andrau, P. Ferrier, P. Dubreuil, A. Sidow, and M.H. Sieweke. 2016. Lineage-specific enhancers activate self-renewal genes in macrophages and embryonic stem cells. *Science* 351:aad5510.

- Spangrude, G.J., S. Heimfeld, and I.L. Weissman. 1988. Purification and characterization of mouse hematopoietic stem cells. *Science* 241:58-62.
- Spits, H., F. Couwenberg, A.Q. Bakker, K. Weijer, and C.H. Uittenbogaart. 2000. Id2 and Id3 inhibit development of CD34⁺ stem cells into predendritic cell (pre-DC)2 but not into pre-DC1: Evidence for a lymphoid origin of pre-DC2. *Journal of Experimental Medicine* 192:1775-1784.
- Srinivas, S., T. Watanabe, C.S. Lin, C.M. William, Y. Tanabe, T.M. Jessell, and F. Costantini. 2001. Cre reporter strains produced by targeted insertion of EYFP and ECFP into the ROSA26 locus. *BMC Developmental Biology* 1:4.
- Steinman, R.M. 2012. Decisions about dendritic cells: past, present, and future. *Annual Review of Immunology* 30:1-22.
- Steinman, R.M., and Z.A. Cohn. 1973. Identification of a novel cell type in peripheral lymphoid organs of mice. I. Morphology, quantitation, tissue distribution. *Journal of Experimental Medicine* 137:1142-1162.
- Steinman, R.M., and M.D. Witmer. 1978. Lymphoid dendritic cells are potent stimulators of the primary mixed leukocyte reaction in mice. *Proceedings of the National Academy of Sciences of the United States of America* 75:5132-5136.
- Sun, J., A. Ramos, B. Chapman, J.B. Johnnidis, L. Le, Y.-J. Ho, A. Klein, O. Hofmann, and F.D. Camargo. 2014. Clonal dynamics of native haematopoiesis. *Nature* 514:322-327.
- Suzuki, S., K. Honma, T. Matsuyama, K. Suzuki, K. Toriyama, I. Akitoyo, K. Yamamoto, T. Suematsu, M. Nakamura, K. Yui, and A. Kumatori. 2004. Critical roles of interferon regulatory factor 4 in CD11b^{high}CD8α⁻ dendritic cell development. *Proceedings of the National Academy of Sciences of the United States of America* 101:8981-8986.
- Swiecki, M., Y. Wang, W. Vermi, S. Gilfillan, R.D. Schreiber, and M. Colonna. 2011. Type I interferon negatively controls plasmacytoid dendritic cell numbers in vivo. *Journal of Experimental Medicine* 208:2367-2374.
- Szymczak-Workman, A.L., K.M. Vignali, and D.A.A. Vignali. 2012. Design and construction of 2A peptide-linked multicistronic vectors. *Cold Spring Harbor Protocols* 2012:199-204.

- Tamura, T., P. Tailor, K. Yamaoka, H.J. Kong, H. Tsujimura, J.J. O'Shea, H. Singh, and K. Ozato. 2005. IFN regulatory factor-4 and -8 govern dendritic cell subset development and their functional diversity. *Journal of Immunology* 174:2573-2581.
- Torti, N., S.M. Walton, K.M. Murphy, and A. Oxenius. 2011. Batf3 transcription factor-dependent DC subsets in murine CMV infection: differential impact on T-cell priming and memory inflation. *European Journal of Immunology* 41:2612-2618.
- Tsujimura, H., T. Tamura, and K. Ozato. 2003. IFN consensus sequence binding protein/IFN regulatory factor 8 drives the development of type I IFN-producing plasmacytoid dendritic cells. *Journal of Immunology* 170:1131-1135.
- Tussiwand, R., W.-L. Lee, T.L. Murphy, M. Mashayekhi, W. KC, J.C. Albring, A.T. Satpathy, J.A. Rotondo, B.T. Edelson, N.M. Kretzer, X. Wu, L.A. Weiss, E. Glasmacher, P. Li, W. Liao, M. Behnke, S.S.K. Lam, C.T. Aurthur, W.J. Leonard, H. Singh, C.L. Stallings, L.D. Sibley, R.D. Schreiber, and K.M. Murphy. 2012. Compensatory dendritic cell development mediated by BATF-IRF interactions. *Nature* 490:502-507.
- van de Laar, L., W. Saelens, S. De Prijck, L. Martens, C.L. Scott, G. Van Isterdael, E. Hoffmann, R. Beyaert, Y. Saeys, B.N. Lambrecht, and M. Guilliams. 2016. Yolk sac macrophages, fetal liver, and adult monocytes can colonize an empty niche and develop into functional tissue-resident macrophages. *Immunity* 44:755-768.
- Van de Putte, T., M. Maruhashi, A. Francis, L. Nelles, H. Kondoh, D. Huylebroeck, and Y. Higashi. 2003. Mice lacking Zfhx1b, the gene that codes for Smad-interacting protein-1, reveal a role for multiple neural crest cell defects in the etiology of Hirschsprung disease-mental retardation syndrome. *American Journal of Human Genetics* 72:465-470.
- van Helden, M.J., S. Goossens, C. Daussy, A.-L. Mathieu, F. Faure, A. Marçais, N. Vandamme, N. Farla, K. Mayol, S. Viel, S. Degouve, E. Debien, E. Seuntjens, A. Conidi, J. Chaix, P. Mangeot, S. de Bernard, L. Buffat, J.J. Haigh, D. Huylebroeck, B.N. Lambrecht, G. Berx, and T. Walzer. 2015. Terminal NK cell maturation is controlled by concerted actions of T-bet and Zeb2 and is essential for melanoma rejection. *Journal of Experimental Medicine* 212:2015-2025.
- Vandewalle, C., J. Comijn, B. De Craene, P. Vermassen, E. Bruyneel, H. Andersen, E. Tulchinsky, F. Van Roy, and G. Berx. 2005. SIP1/ZEB2 induces EMT by repressing genes of different epithelial cell-cell junctions. *Nucleic Acids Research* 33:6566-6578.

- Vandewalle, C., F. Van Roy, and G. Berx. 2009. The role of the ZEB family of transcription factors in development and disease. *Cellular and Molecular Life Sciences* 66:773-787.
- Verschueren, K., J.E. Remacle, C. Collart, H. Kraft, B.S. Baker, P. Tylzanowski, L. Nelles, G. Wuytens, M.T. Su, R. Bodmer, J.C. Smith, and D. Huylebroeck. 1999. SIP1, a novel zinc finger/homeodomain repressor, interacts with Smad proteins and binds to 5'-CACCT sequences in candidate target genes. *Journal of Biological Chemistry* 274:20489-20498.
- Villadangos, J.A., and L. Young. 2008. Antigen-presentation properties of plasmacytoid dendritic cells. *Immunity* 29:352-361.
- Vogt, T.K., A. Link, J. Perrin, D. Finke, and S.A. Luther. 2009. Novel function for interleukin-7 in dendritic cell development. *Blood* 113:3961-3968.
- Vremec, D., J. Pooley, H. Hochrein, L. Wu, and K. Shortman. 2000. CD4 and CD8 expression by dendritic cell subtypes in mouse thymus and spleen. *Journal of Immunology* 164:2978-2986.
- Vremec, D., and K. Shortman. 1997. Dendritic cell subtypes in mouse lymphoid organs: cross-correlation of surface markers, changes with incubation, and differences among thymus, spleen, and lymph nodes. *Journal of Immunology* 159:565-573.
- Vremec, D., M. Zorbas, R. Scollay, D.J. Saunders, C.F. Ardavin, L. Wu, and K. Shortman. 1992. The surface phenotype of dendritic cells purified from mouse thymus and spleen: investigation of the CD8 expression by a subpopulation of dendritic cells. *Journal of Experimental Medicine* 176:47-58.
- Wang, Y., K.J. Szretter, W. Vermi, S. Gilfillan, C. Rossini, M. Celli, A.D. Barrow, M.S. Diamond, and M. Colonna. 2012. IL-34 is a tissue-restricted ligand of CSF1R required for the development of Langerhans cells and microglia. *Nature Immunology* 13:753-760.
- Waskow, C., K. Liu, G. Darrasse-Jèze, P. Guermonprez, F. Ginhoux, M. Merad, T. Shengelia, K. Yao, and M. Nussenzweig. 2008. The receptor tyrosine kinase Flt3 is required for dendritic cell development in peripheral lymphoid tissues. *Nature Immunology* 9:676-683.
- Weng, Q., Y. Chen, H. Wang, X. Xu, B. Yang, Q. He, W. Shou, Y. Chen, Y. Higashi, V. van den Berghe, E. Seuntjens, S.G. Kernie, P. Bukshpun, E.H. Sherr, D. Huylebroeck, and Q.R.

- Lu. 2012. Dual-mode modulation of Smad signaling by Smad-interacting protein Sip1 is required for myelination in the central nervous system. *Neuron* 73:713-728.
- Wiktor-Jedrzejczak, W.W., A. Ahmed, C. Szczylik, and R.R. Skelly. 1982. Hematological characterization of congenital osteopetrosis in op/op mouse: Possible mechanism for abnormal macrophage differentiation. *Journal of Experimental Medicine* 156:1516-1527.
- Williams, J.W., M.Y. Tjota, B.S. Clay, B. Vander Lugt, H.S. Bandukwala, C.L. Hrusch, D.C. Decker, K.M. Blaine, B.R. Fixsen, H. Singh, R. Sciammas, and A.I. Sperling. 2013. Transcription factor IRF4 drives dendritic cells to promote Th2 differentiation. *Nature Communications* 4:2990.
- Wynn, T.A., A. Chawla, and J.W. Pollard. 2013. Macrophage biology in development, homeostasis and disease. *Nature* 496:445-455.
- Xu, J., V.G. Sankaran, M. Ni, T.F. Menne, R.V. Puram, W. Kim, and S.H. Orkin. 2010. Transcriptional silencing of γ -globin by BCL11A involves long-range interactions and cooperation with SOX6. *Genes & Development* 24:783-798.
- Yona, S., K.-W. Kim, Y. Wolf, A. Mildner, D. Varol, M. Breker, D. Strauss-Ayali, S. Viukov, M. Guilliams, A. Misharin, D.A. Hume, H. Perlman, B. Malissen, E. Zelzer, and S. Jung. 2013. Fate mapping reveals origins and dynamics of monocytes and tissue macrophages under homeostasis. *Immunity* 38:79-91.
- Yu, Y., J. Wang, W. Khaled, S. Burke, P. Li, X. Chen, W. Yang, N.A. Jenkins, N.G. Copeland, S. Zhang, and P. Liu. 2012. Bcl11a is essential for lymphoid development and negatively regulates p53. *Journal of Experimental Medicine* 209:2467-2483.
- Zelenay, S., A.M. Keller, P.G. Whitney, B.U. Schraml, S. Deddouche, N.C. Rogers, O. Schulz, D. Sancho, and C. Reis e Sousa. 2012. The dendritic cell receptor DNLR-1 controls endocytic handling of necrotic cell antigens to favor cross-priming of CTLs in virus-infected mice. *Journal of Clinical Investigation* 122:1615-1627.
- Zhang, J., A. Raper, N. Sugita, R. Hingorani, M. Salio, M.J. Palmowski, V. Cerundolo, and P.R. Crocker. 2006. Characterization of Siglec-H as a novel endocytic receptor expressed on murine plasmacytoid dendritic cell precursors. *Blood* 107:3600-3608.
- Zigmond, E., C. Varol, J. Farache, E. Elmaliyah, A.T. Satpathy, G. Friedlander, M. Mack, N. Shpigel, I.G. Boneca, K.M. Murphy, G. Shakhar, Z. Halpern, and S. Jung. 2012. Ly6C^{hi}

monocytes in the inflamed colon give rise to proinflammatory effector cells and migratory antigen-presenting cells. *Immunity* 37:1076-1090.

APPENDIX A: CODE LISTING

Given a *PATH* to a tab-delimited file containing gene expression values, with the first column containing probe set IDs and each subsequent column containing expression data from a sample, *my.pca* is a list with class *prcomp* containing the results of a principal component analysis by singular value decomposition.

Language: R

```
my.data.frame <- read.delim(PATH, row.names=1)
my.data.matrix <- as.matrix(my.data.frame)

# PCA by sample:
# center each gene (mean) without scaling
# scale each sample (root mean square) without centering
# transpose the matrix to PCA by sample instead of by gene

a <- scale(t(my.data.matrix), center=TRUE, scale=FALSE)
b <- scale(t(a), center=FALSE, scale=TRUE)
my.pca <- prcomp(t(b), center=FALSE)
```